INFORMATION TO USERS

This reproduction was made from a copy of a manuscript sent to us for publication and microfilming. While the most advanced technology has been used to photograph and reproduce this manuscript, the quality of the reproduction is heavily dependent upon the quality of the material submitted. Pages in any manuscript may have indistinct print. In all cases the best available copy has been filmed.

The following explanation of techniques is provided to help clarify notations which may appear on this reproduction.

1. Manuscripts may not always be complete. When it is not possible to obtain missing pages, a note appears to indicate this.

2. When copyrighted materials are removed from the manuscript, a note appears to indicate this.

3. Oversize materials (maps, drawings, and charts) are photographed by sectioning the original, beginning at the upper left hand corner and continuing from left to right in equal sections with small overlaps. Each oversize page is also filmed as one exposure and is available, for an additional charge, as a standard 35mm slide or in black and white paper format.*

4. Most photographs reproduce acceptably on positive microfilm or microfiche but lack clarity on xerographic copies made from the microfilm. For an additional charge, all photographs are available in black and white standard 35mm slide format.*

***For more information about black and white slides or enlarged paper reproductions, please contact the Dissertations Customer Services Department.**

Lawrence, Christopher John

INERTIAL INTERACTIONS OF PARTICLES AND BOUNDARIES IN VISCOUS FLOWS

City University of New York PH.D. 1986

PLEASE NOTE:

In all cases this material has been filmed in the best possible way from the available copy. Problems encountered with this document have been identified here with a check mark __✓__.

1. Glossy photographs or pages _____
2. Colored illustrations, paper or print _____
3. Photographs with dark background _____
4. Illustrations are poor copy _____
5. Pages with black marks, not original copy __✓__
6. Print shows through as there is text on both sides of page _____
7. Indistinct, broken or small print on several pages __✓__
8. Print exceeds margin requirements _____
9. Tightly bound copy with print lost in spine _____
10. Computer printout pages with indistinct print _____
11. Page(s) _____ lacking when material received, and not available from school or author.
12. Page(s) _____ seem to be missing in numbering only as text follows.
13. Two pages numbered _____. Text follows.
14. Curling and wrinkled pages _____
15. Dissertation contains pages with print at a slant, filmed as received __✓__
16. Other _____

_____

_____

University
Microfilms
International

INERTIAL INTERACTIONS OF PARTICLES AND BOUNDARIES IN VISCOUS FLOWS

by

CHRIS LAWRENCE

A dissertation submitted to the
Graduate Faculty in Engineering
in partial fulfillment of the requirements for the degree of
Doctor of Philosophy, The City University of New York.

1986

This manuscript has been read and accepted for the Graduate Faculty in Engineering in satisfaction of the dissertation requirement for the degree of Doctor of Philosophy.

3/6/86
Date

Sheldon Weinbaum
Chair of Examining Committee

March 7, 1986
Date

Paul Karmel
Executive Officer

Zeev Dagan
Peter Ganatos
Charles Maldarelli
Richard Skalak
Supervisory Committee

The City University of New York

Abstract

INERTIAL INTERACTIONS OF BODIES AND BOUNDARIES

IN VISCOUS FLOWS

by

Chris Lawrence

Adviser: Professor Sheldon Weinbaum

The first part of the dissertation examines the behavior of the time-dependent Stokes equations for flow around a nonspherical body. A new result is derived for the force on a body in oscillatory axisymmetric motion in terms of the far-field behaviour of the stream function. This general result is then applied to the unsteady motion of a spheroidal body in unbounded flow. Asymptotic solutions are presented for small or large frequency and for a perturbed sphere. The exact stream-function is found as a sum of Legendre and spheroidal wave functions and the complex force on the body is determined. Since the exact solution is complicated, an analytic approximation is proposed based on the asymptotic solutions for the force. The force contains four terms: the quasi-steady Stokes drag, the generalized Basset force, the added-mass force and a fourth term which has not previously been described. For a body in arbitrary motion the new force term transforms to a memory integral of all previous accelerations with a memory function which is less singular than the $t^{-\frac{1}{2}}$ of the Basset force.

The second part of the research relates to the solution of the full Navier-Stokes equations in the region beneath a flat-bottomed body which falls towards a parallel plane surface. The radial dependence of the stream-function separates and the flow is governed by three dimensionless parameters - a Reynolds number, an inertia parameter β and a forcing parameter γ. When the body approaches from "far away", a time-dependent Reynolds number is defined which decreases to zero as the motion progresses; the results for all Reynolds numbers are described by a single solution curve for each value of β. When $\beta = 0$, the large Re boundary layer solutions are new exact time-dependent similarity solutions of the full Navier-Stokes equations. When the body is dropped from rest, an integral momentum equation is used to describe the development of the boundary layers. The time-dependent gap height and radial velocity profiles are presented and the results are discussed in terms of the draining time, or the position of arrest when there is no applied force.

This work is dedicated to the members of my family who have made many sacrifices during its preparation.

I am grateful to the following organizations for their financial support which enabled me to perform this work:

The City University of New York

The City College of The City University of New York

The National Science Foundation

I am indebted to the members of my supervisory committee for their helpful and illuminating discussions and for their encouragement.

CONTENTS

TABLES

ILLUSTRATIONS

page

CHAPTER 5

CHAPTER 1. INTRODUCTION

1.1 THE PROBLEMS TO BE TACKLED

This is a study of the time-dependent motion of a particle moving in a real fluid near a plane wall or in an unbounded region. Axisymmetric flows are considered and inertial effects are to be included in both the linear and nonlinear regimes. The ultimate goal of the research is to generate a theoretical understanding of a class of problems dealing with the unsteady hydrodynamic interactions of a particle and a plane boundary at all Re wherein the flow of the intervening fluid remains laminar. The class of problems is important in many areas of fluid mechanics and has been extensively studied in the case of very low Reynolds numbers, when the governing equations are linear and quasi-steady, and in the lubrication limit where the Reynolds number based on gap height is small. In real flows, many of the interactions are nonlinear. In particular, for a particle moving perpendicularly to a wall, the geometry is inherently time-dependent with important mathematical consequences. It is for this reason that we will concentrate on such axisymmetric motions.

The work can be broadly divided into two parts. The first part deals with the solution of the governing equations in the linear, but time-dependent case. These

equations were originally formulated in studies of the motion of pendulums, and are of interest now because they are fundamental to the discussion of the mechanical nature of Brownian motion. On the large scale, Brownian motion is observed as a slow diffusion of small particles in a fluid; however the motion of an individual particle is highly erratic. The motion consists of a random vibration of very small amplitude which results in a net drift of the particle in three dimensions. This type of motion is well modelled by the linearized equations, since the Reynolds number is always small for small particles, but the local acceleration of the fluid may be important. The motion of small particles in turbulent flow has a similar random nature and this can also be modelled by the linearized equations under some circumstances.

The second and larger part of the work deals with the time-dependent motion of a body near a plane surface at arbitrary Reynolds number based on gap height. This very complicated problem is greatly simplified if the body is flat in the region of near contact. For such a simplified geometry, the governing equations can be solved analytically in a variety of cases and it will be possible to develop insight into the factors which are important in more general hydrodynamic collisions. Such collisions are important in studies of filtration and coagulation of particles and are not well understood in the general case.

The Navier-Stokes equations will be introduced in Chapter 2 and will be formulated in terms of the stream function for an axisymmetric coordinate system. A general form for the force on a body in terms of surface integrals of the stream function will then be derived. Special cases of this form will be described for steady Stokes flow and for potential flow and then a new specialized form will be derived for the force on a body in oscillatory motion. The latter form is analogous to the other special cases in that it gives the force in terms of the limiting behaviour of the stream function in the far field, as determined by a multipole expansion in spherical coordinates. This result will be used repeatedly in Chapter 3.

The time-dependent linearized equations of motion will be considered further in Chapter 3, where the force experienced by an oscillating spheroidal body will be calculated. Firstly, the equations will be formulated in terms of the natural coordinate system of the body, and the dimensionless parameters of the problem will be discussed. Before the most general problem is tackled, three special cases will be considered. For very low frequency, the motion differs only slightly from the quasi-steady solution; the stream function can be found by matching asymptotic expansions in the near and far fields. The force is calculated from the far-field stream function using the relation derived in Chapter 2, and the result is extended to

apply to a body of arbitrary shape. For very high frequency, on the other hand, the flow is effectively inviscid except in a thin boundary layer near the surface of the body. This boundary layer exhibits the same flow behaviour as the boundary layer on a flat plate which oscillates in its own plane. The correction to the force on the body may be found by calculating the dissipation of energy in the boundary layer and equating this energy to the work done by the body. The third special case occurs when the body is nearly spherical, in which case the stream function may be found as a series of spherical harmonics which satisfy a perturbed condition on a spherical boundary. The force can then be found using the relation derived in Chapter 2 and will be compared to the standard result for a sphere.

The stream function for the general problem will be found in terms of a double harmonic series of Legendre functions and spheroidal wave functions. The force is then determined by the coefficient of the term which is dominant in the far field. However, since the equation is not simply separable, this coefficient must be determined by solving an infinite system of linear algebraic equations. The results will be presented graphically, and it will be shown that there are four components of the force. Three of these are the classic forces associated with the well-known solution for a spherical body; the quasi-steady Stokes drag, the

Basset force and the added mass force. In the nonspherical case, the Basset force is defined as the term which is $\pi/4$ out of phase with the velocity and proportional to the square root of the frequency. Its amplitude is a function of aspect ratio which is expressed in terms of the high frequency behaviour. The fourth and new component is a much more complicated function of the aspect ratio and frequency, but curiously has a phase which is close to, though not exactly $\pi/4$.

The limiting results for high and low frequency will be used as the basis of a very accurate correlation for the force. The correlation contains the exact values of the steady Stokes drag, the Basset force and the added mass force, and a simple but accurate approximation for the fourth component, which reduces to zero for a spherical body. The oscillatory motion may be regarded as a Laplace transform of an arbitrary motion and, because of the simple nature of the correlation for the force, the transform may be inverted to find the force on a spheroidal body in arbitrary axial motion. The fourth term of the force, like the Basset force, transforms to a memory integral of previous accelerations. However, unlike the Basset force, the memory function is not singular at small times.

In Chapter 4, the case of a flat-bottomed body moving towards a wall will be considered, the Reynolds number being

arbitrary. For this geometry, the pressure on the underside of the body will be shown to have a simple parabolic radial dependence when the gap height is small compared to the disc radius. In this limit, the radial dependence is separable and an equation for the separated stream function will be derived which contains three parameters - the initial Reynolds number Re_0, a parameter β which represents the ratio of body inertia to fluid inertia, and a parameter γ which represents the relative importance of the external force on the body and the initial inertia of the fluid. Firstly, the limit of infinite Reynolds number will be considered and analytical solutions will be presented for an inviscid fluid when one of the parameters β or γ is zero. For real fluids, it will be shown that the important behaviour is contained in three problems. If the body comes from "far away", it may be driven principally by an external force or by the initial momentum. If the body is dropped from rest near the boundary, it must be driven by an external force; this problem will be considered in Chapter 5.

When the body comes from "far away", a time dependent Reynolds number Re(t) will be defined allowing the motion to be described by a single solution curve which depends only on β. Different initial conditions can be satisfied by using different portions of the curve. The solution for each consists of three parts - a boundary layer solution

for Re(t) > O(100), a numerical solution for O(1) < Re(t) < O(100) and a low Reynolds number solution. In the case where β is zero, the large Re(t) behavior will be described analytically by a new exact similarity solution of the Navier -Stokes equations. When the body is driven by an external force, this solution is simply a quasi-steady stagnation point boundary layer. However, when γ is zero, the similarity solution is fully time-dependent. Thus, the time-dependent two-dimensional flow field will be found in terms of a function of a single variable. In both problems, results for the time dependent radial velocity profile and gap height will be presented.

The case when the flat body is dropped from rest near the plane will be treated in Chapter 5, although only the problem with $\beta = 0$ will be considered, since the motion depends on the Reynolds number in a complex way. Three limiting problems will be treated; these are the limits of small Reynolds number, small time and large Reynolds number. Firstly, the classical problem of lubrication theory will be extended to the case of nonzero Reynolds number. Secondly, the small time solution will be developed to study the initial acceleration of the flow and to serve as a starting point for the solutions which follow. Thirdly, the large Re case will be considered;. In this problem, the boundary layer solution is not of similarity form, and there is no simplification of the governing equation at large Re. To

simplify the problem, an integral momentum equation will be used to describe the boundary layer development. The boundary layer will be represented as a double layer, with a different form for the velocity profile in each layer. The overall profile is determined by a single time-dependent shape parameter $\Lambda(t)$ and a constant k which gives the relative thicknesses of the two layers. An O.D.E. will be found for $\Lambda(t)$ and k will be chosen to give the correct initial behaviour in accordance with the short-time solution. Finally, the full numerical solution of the problem will be presented and compared to the three limiting solutions. The results will be discussed in terms of the three characteristic timescales of the problem which determine the time taken for the fluid to drain from the gap.

Some possible extensions of the current work will be proposed in Chapter 6. For the linearized equations, the problem of a spherical body moving towards a wall will be discussed and a procedure will be described to invert the Laplace transform in the problem with time-dependent geometry which is actually nonlinear. For the nonlinear equations with parallel wall geometry, a simple model of an elastic collision will be proposed. It will be shown that in the inviscid case, the model results in a fourth order set of O.D.E. which describes the motion of the system.

1.2 PREVIOUS WORK IN RELATED AREAS

There is a long history of interest in hydrodynamic collisions and the processes of coagulation and filtration of small particles. Most of the work in this area has been done for quasi-steady low Reynolds number flows. Stimson & Jeffrey (1926) and later Brenner (1961) gave a solution for the motion of a spherical partical towards a plane at zero Reynolds number. Their solution is singular wnen the sphere and plane are very close; the solution for the near-touching case was found by Cox & Brenner (1967), who also accounted for small inertial effects. The elastic deformation of the solid bodies can be important, and several authors have incorporated these effects (e.g. Christensen 1962). Davis , Serayssol & Hinch (1986) recently produced a solution for the collision of a sphere with a plane which includes the effects of body inertia and large elastic deformations, although no fluid inertial effects were included. In the absence of fluid inertia the body does not rebound, but exhibits an oscillation which is damped by viscosity.

The simplified model for collisions described herein will be valid for arbitrary Reynolds number and will lead to analytic and semi-analytic exact solutions of the governing equations. In this respect, the work may be compared to previous exact solutions of a similar nature, many of which were discussed by Schlichting (1979). Von Kármán (1921)

found the solution for the case of a semi-infinite fluid bounded by a single rotating disc. This was extended by Batchelor (1951) who found the solution for the flow between two rotating discs; his is the only previous exact solution of this kind to contain a characteristic length scale. Homann (1936) and Frössling (1940) found the solution for the flow near a steady axisymmetric stagnation point. Yang (1958) found a class of time-dependent similarity solutions for stagnation point flow and solutions of the same nature were found independently by Secomb (1978) and Uchida & Aoki (1977). All of the above solutions are of boundary layer type and are closely related to the solution for a flat body falling towards a plane surface which is essentially a superposition of two time-dependent stagnation point flows.

There is a dearth of experimental measurements of hydrodynamic collisions, although Adamczyk, Adamczyk & van de Ven (1983) found very good agreement with the results of Brenner (1961) for spherical particles falling towards a flat surface at very low Reynolds numbers.

The linearized Navier-Stokes equations were developed by Stokes (1851) who solved some problems related to the viscous damping of an oscillating pendulum. His work was extended by Basset (1888) to cover arbitrarily time-dependent motion, but subsequently little attention has been paid to the field. The basic results for a sphere were used

by a few authors and extended to find the force on a body in an arbitrary flow field (Mazur & Bedeaux 1974, Felderhof 1976a,b). It was only recently that the studies of Alder & Wainwright (1967,1970) led to the realization that Brownian motion of small particles is governed by the linearized equations, rather than the quasi-steady Stokes equations. Arminski & Weinbaum (1979) and Bedeaux & Mazur (1974) showed that the results for the diffusion coefficient obtained using Stokes' theorem for the drag on a sphere could in fact be extended to the more realistic time-dependent case. However certain results concerning the long time tail of the velocity autocorrelation function must be derived using the time-dependent equations (Bedeaux & Mazur 1974, Hocquart 1977b, Hocquart & Hinch 1983).

Until very recently, the only boundary geometries considered explicitly for the unsteady case were those discussed by Stokes (1851), i.e. the single sphere and single cylinder. Chen Wambsganss & Jendrzejczyk (1976) treated the case of an oscillating cylinder in a concentric rigid container, Lin (1986) used a multipole method to solve the problem for a small group of oscillating circular cylinders, and Leichtberg et al (1976) studied the relative motion of three coaxial spheres using a multipole method, but only accounted for interactions in the quasi-steady part of the motion. The only previous work to use a nonsimple curvilinear coordinate system is that of Hocquart (1976,

1977a) who studied the rotational oscillations of spheroids in Brownian motion in relation to the optical properties of suspensions.

Complex geometries are more commonly studied in the closely related cases of steady Stokes flow and potential flow, which are both governed by simpler linear equations. For Stokes flow, Brenner (1961) found the force on a sphere near a plane, Pell and Payne (1960) gave the result for a torus, and Happel & Brenner (1965) gave the results for spheroids; all these results are found by separation of variables in curvilinear coordinates. The analogous results for potential flow have been given by Jeffrey & Chen (1977), Miloh, Waisman & Weihs (1978) and Green (1833). Limiting cases of the geometry have been discussed by Miloh (1979), Small & Weihs (1975) and Weihs & Small (1975).

Recently, the boundary integral method and multipole collocation technique have been developed to deal with steady Stokes flow problems in more complex geometries. Ganatos, Weinbaum & Pfeffer (1980) applied the multipole method to the problem of a sphere moving perpendicular to one or two plane boundaries; a general discussion is given by Weinbaum (1981) and a detailed exposition of the technique has been given by Gluckman, Pfeffer & Weinbaum (1971). The boundary integral method was discussed by Hsu & Ganatos (1986) who applied it to the tumbling motion of an

axisymmetric body near a wall in Stokes flow. Kim (1985) has applied a nigh accuracy method of reflections technique to the sedimentation of a pair of spheroids.

CHAPTER 2. THEORETICAL FORMULATION IN TERMS OF THE STREAM FUNCTION

2.1 EQUATIONS OF MOTION

We begin with the Navier-Stokes equation for an incompressible fluid with density ρ and dynamic viscosity μ, and follow a similar path to that of Happel & Brenner (1965).

$$\nabla.\underset{\sim}{u} = 0, \qquad \rho(\underset{\sim}{u}_t + \underset{\sim}{u}.\nabla\underset{\sim}{u}) = -\nabla p + \mu\nabla^2\underset{\sim}{u} \tag{2.1}$$

Since all the problems to be treated involve axisymmetry, we introduce cylindrical polar coordinates:

$$\underset{\sim}{r} = (\varpi, \phi, z) = \varpi\,\underset{\sim}{i}_\varpi + z\,\underset{\sim}{i}_z \tag{2.2}$$

as shown in figure 2.1, choosing the z-axis for the axis of symmetry. The conditions of symmetry are:

(i) The body is axisymmetric (and simply connected), given by $\varpi = \varpi_0(z)$, say.

(ii) The velocity and angular velocity of the body are directed along the z-axis. $\underset{\sim}{U}(t) = W(t)\underset{\sim}{i}_z$, $\underset{\sim}{\Omega}(t) = \Omega\underset{\sim}{i}_z$. We only consider flows for which the azimuthal velocity is zero, so the body may not rotate: $\Omega = 0$.

(iii) Any external boundaries must be axisymmetric. In particular we will consider the case of a plane wall at $z = 0$.

(iv) Any ambient flow must be axisymmetric, i.e. $\frac{\partial \underset{\sim}{u}_\infty}{\partial \phi} = 0$. we will only consider flows for which $\underset{\sim}{u}_\infty = 0$.

In terms of the fluid velocity, $\underset{\sim}{u} = (u,0,w)$, the continuity equation becomes:

$$\frac{1}{\varpi}\frac{\partial}{\partial \varpi}(\varpi u) + \frac{\partial w}{\partial z} = 0 \qquad (2.3)$$

This leads us to define a stream function Ψ, so that

$$u = \frac{1}{\varpi}\Psi_z, \qquad w = -\frac{1}{\varpi}\Psi_\varpi \qquad (2.4)$$

A subscript is used to denote differentiation. A suitable definition for Ψ is:

$$\Psi(\underset{\sim}{r}) = \int_{\mathcal{C}} \varpi' \underset{\sim}{n}\cdot\underset{\sim}{u}(\underset{\sim}{r}')\,|d\underset{\sim}{r}'| \qquad (2.5)$$

where $\mathcal{C}$ is any contour joining the axis of symmetry to the point r in an azimuthal plane, and $\underset{\sim}{n}$ is the downward normal to $\mathcal{C}$ as shown in figure 2.1. Then the downward volume flow rate through any surface spanning the azimuthal circle defined by the point $\underset{\sim}{r}$ is Q, with

$$Q = 2\pi\Psi(\underset{\sim}{r}) \qquad (2.6)$$

By considering small displacements of the point $\underset{\sim}{r}$, it is easy to see that

$$\Psi_\varpi = -\varpi w \quad \text{and} \quad \Psi_z = \varpi u \qquad (2.7)$$

The continuity equation is identically satisfied by taking $u = -\nabla_\wedge(\underset{\sim}{i}_\phi \frac{1}{\varpi}\Psi) = \underset{\sim}{i}_\phi \wedge \frac{1}{\varpi}\nabla\Psi$. We take the curl of the momentum equation to eliminate the pressure and get the vorticity equation.

$$\omega_t - \nabla_\wedge(u_\wedge\omega) = -\nu\nabla_\wedge\nabla_\wedge\omega \qquad (2.8)$$

with kinematic viscosity ν and vorticity

$$\omega = \nabla_\wedge u = i_\phi \frac{1}{\varpi}E^2\Psi \qquad (2.9)$$

The generalized axisymmetric potential operator E^2 plays an important role in the sequel and is given by

$$E^2 = \varpi\frac{\partial}{\partial\varpi}\frac{1}{\varpi}\frac{\partial}{\partial\varpi} + \frac{\partial^2}{\partial z^2} = \nabla^2 - \frac{2}{\varpi}\frac{\partial}{\partial\varpi} \qquad (2.10)$$

with Laplacian $$\nabla^2 = \frac{1}{\varpi}\frac{\partial}{\partial\varpi}\varpi\frac{\partial}{\partial\varpi} + \frac{\partial^2}{\partial z^2} \qquad (2.11)$$

Equation (2.9) is substituted into (2.8) to give

$$\nu E^4\Psi - \varpi(\Psi_z\frac{\partial}{\partial\varpi} - \Psi_\varpi\frac{\partial}{\partial z})\frac{1}{\varpi^2}E^2\Psi - E^2\Psi_t = 0 \qquad (2.12)$$

which is the dynamic equation for the stream function. This form is much more convenient than the original set of equations (2.1). We started with four equations for the four dependent variables p and $\underset{\sim}{u}$ in terms of four independent variables $\underset{\sim}{r}$ and t; these have been reduced to a single equation for Ψ in terms of three variables ϖ, z and t. The class of motions we are considering is clearly much smaller than the general class.

Once Ψ is known, we can recover the two velocity components from (2.4) and the pressure can be found by a relatively simple integration of the momentum equation.

$$\nabla p = \mu \nabla^2 \underset{\sim}{u} - \rho(\underset{\sim}{u}_t + \underset{\sim}{u}.\nabla \underset{\sim}{u}) \tag{2.13}$$

in which $$\nabla^2 \underset{\sim}{u} = \underset{\sim}{i}_\phi \wedge \frac{1}{\varpi} \nabla (E^2 \Psi) \tag{2.14}$$

$$\underset{\sim}{u}_t = \underset{\sim}{i}_\phi \wedge \frac{1}{\varpi} \nabla \Psi_t \tag{2.15}$$

and $$\underset{\sim}{u}.\nabla \underset{\sim}{u} = \nabla(\tfrac{1}{2}\underset{\sim}{u}^2) - \underset{\sim}{u} \wedge \underset{\sim}{\omega} = \tfrac{1}{2}\nabla(\tfrac{1}{\varpi}\nabla\Psi)^2 - \tfrac{1}{\varpi^2}(E^2\Psi)\nabla\Psi \tag{2.16}$$

So $$\nabla p = \mu \underset{\sim}{i}_\phi \wedge \tfrac{1}{\varpi}\nabla(E^2\Psi) - \rho \underset{\sim}{i}_\phi \wedge \tfrac{1}{\varpi}\nabla\Psi_t + \rho\tfrac{1}{\varpi^2}(E^2\Psi)\nabla\Psi - \tfrac{1}{2}\rho\nabla(\tfrac{1}{\varpi}\nabla\Psi)^2 \tag{2.17}$$

The boundary conditions for the problem are that there is no disturbance at infinity and that the fluid sticks to the moving body and the plane. In addition there is a regularity condition on the axis of symmetry and we may specify the arbitrary constant in Ψ using (2.5).

Put $$r^2 = \varpi^2 + z^2 \tag{2.18}$$

then as $r \to \infty$: $\frac{1}{r}\Psi \to 0$, $p \to 0$ (2.19)

on $\varpi = 0$: $\Psi = 0$, $\Psi_\varpi = 0$ (2.20)

on $\varpi = \varpi_0(z)$: $\Psi = -\tfrac{1}{2}\varpi^2 W$, $\Psi_n = -\varpi W \varpi_n$ (2.21)

on $z = 0$: $\Psi = 0$, $\Psi_z = 0$ (2.22)

In the above, $\underset{\sim}{n}$ is the outward normal to the body.

2.2 THE FORCE ON A BODY

In some cases, the applied force on the body $\mathcal{F}_A(t)\underset{\sim}{i}_z$ may be specified rather than the velocity $W(t)\underset{\sim}{i}_z$. Then it is necessary to find the relationship between the two. Even when W(t) is specified, it is of major interest to find the hydrodynamic force on the body $\mathcal{F}_H(t)\underset{\sim}{i}_z$. The equation of motion for a body of mass m is:

$$\mathcal{F}_A + \mathcal{F}_H = mW_t \tag{2.23}$$

The hydrodynamic force $\mathcal{F}_H$ is determined from the integral

$$\mathcal{F}_H = \iint_{\mathcal{B}} \underset{\sim}{i}_z \cdot \underset{\approx}{\sigma} \cdot \underset{\sim}{n}\, dA = 2\pi \int_\Gamma \varpi\, \underset{\sim}{i}_z \cdot \underset{\approx}{\sigma} \cdot \underset{\sim}{n}\, ds \tag{2.24}$$

in terms of the stress tensor $\underset{\approx}{\sigma}$ and local intrinsic surface coordinates (n, s, ϕ). Γ is the curve in the ϖ-z plane which generates the body surface $\mathcal{B}$.

Now,
$$\underset{\sim}{i}_z \cdot \underset{\approx}{\sigma} = \sigma_{\varpi z}\underset{\sim}{i}_\varpi + \sigma_{zz}\underset{\sim}{i}_z \tag{2.25a}$$

$$= \mu(u_z + w_\varpi)\underset{\sim}{i}_\varpi + (-p + 2\mu w_z)\underset{\sim}{i}_z \tag{2.25b}$$

$$= \mu\left(\tfrac{1}{\varpi}\Psi_{zz} - \tfrac{\partial}{\partial\varpi}\tfrac{1}{\varpi}\Psi_\varpi\right)\underset{\sim}{i}_\varpi - (p + 2\mu\Psi_{\varpi z})\underset{\sim}{i}_z \tag{2.25c}$$

we put
$$\underset{\sim}{n} = \varpi_n \underset{\sim}{i}_\varpi + z_n \underset{\sim}{i}_z \tag{2.26}$$

and note that
$$z_n = \varpi_s \quad \text{and} \quad z_s = -\varpi_n \tag{2.27}$$

Then
$$\underset{\sim}{i}_z \cdot \underset{\approx}{\sigma} \cdot \underset{\sim}{n} = \mu\varpi_n\left(\tfrac{1}{\varpi}\Psi_{zz} - \tfrac{\partial}{\partial\varpi}\tfrac{1}{\varpi}\Psi_{\varpi}\right) - 2\mu z_n \tfrac{1}{\varpi}\Psi_{\varpi z} - pz_n \tag{2.28}$$

The integral (2.24) is split into three parts

$$\mathcal{F}_H = 2\pi(I_1 + I_2 + I_3) \tag{2.29}$$

with $$I_1 = \mu\int_\Gamma \varpi_n(\Psi_{zz} - \varpi\frac{\partial}{\partial\varpi}\frac{1}{\varpi}\Psi_\varpi)ds = -\mu\int_\Gamma \varpi_n(E^2\Psi - 2\Psi_{zz})ds \quad (2.30)$$

and $$I_2 = -2\mu\int_\Gamma \varpi(z_n\frac{1}{\varpi}\Psi_{\varpi z})ds = -2\mu\int_\Gamma \varpi_s\Psi_{\varpi z}ds \quad (2.31a)$$

$$= -2\mu\int_\Gamma(\frac{\partial}{\partial s}\Psi_z - z_s\Psi_{zz})ds \quad (2.31b)$$

$$= -2\mu[\Psi_z]_{TOP}^{BOTTOM} - 2\pi\int_\Gamma \varpi_n\Psi_{zz}ds \quad (2.31c)$$

But $\Psi_z = 0$ on the poles of the body, so

$$I_2 = -2\mu\int_\Gamma \varpi_n\Psi_{zz}ds \quad (2.32)$$

Thirdly, $$I_3 = -\int_\Gamma \varpi p z_n ds = -\int_\Gamma \varpi p\varpi_s ds \quad (2.33a)$$

$$= -\int_\Gamma(\frac{1}{2}\frac{\partial}{\partial s}(p\varpi^2) - \frac{1}{2}\varpi^2 p_s)ds \quad (2.33b)$$

$$= -[\frac{1}{2}p\varpi^2]_{TOP}^{BOTTOM} + \int_\Gamma\frac{1}{2}\varpi^2 p_s ds \quad (2.33c)$$

Now $p\varpi^2 = 0$ on top and bottom, so

$$I_3 = \frac{1}{2}\int_\Gamma \varpi^2 p_s ds \quad (2.34)$$

We sum (2.30), (2.32) and (2.34) to get the total force

$$\mathcal{F}_H = \pi\int_\Gamma \varpi^2 p_s ds - 2\mu\pi\int_\Gamma \varpi_n E^2\Psi ds \quad (2.35)$$

Equation (2.17) gives the pressure gradient

$$p_s = \nabla p\cdot i_s = \frac{\mu}{\varpi}\frac{\partial}{\partial n}(E^2\Psi) - \rho\frac{1}{\varpi}\frac{\partial}{\partial n}\Psi_t + \rho\frac{1}{\varpi^2}(E^2\Psi)\Psi_s - \frac{1}{2}\rho\frac{\partial}{\partial s}(\frac{1}{\varpi}\nabla\Psi)^2 \quad (2.36)$$

This is inserted in (2.35) to give

$$\mathcal{F}_H = \pi\mu\int_\Gamma \varpi^3\frac{\partial}{\partial n}(\frac{1}{\varpi^2}E^2\Psi)ds - \rho\pi\int_\Gamma \varpi\Psi_{tn}ds + \rho\pi\int_\Gamma E^2\Psi\Psi_s ds - \rho\frac{\pi}{2}\int_\Gamma \varpi^2\frac{\partial}{\partial s}(\frac{1}{\varpi}\nabla\Psi)^2 ds \quad (2.37)$$

The boundary conditions on the body (2.21) enable us to simplify (2.37) as follows

$$\left(\frac{1}{\varpi}\nabla\Psi\right)^2 = \omega^2 = W^2, \quad \text{so} \quad \frac{\partial}{\partial s}\left(\frac{1}{\varpi}\nabla\Psi\right)^2 = 0 \tag{2.38}$$

Also $$\Psi_n = -\varpi W \varpi_n = \varpi W z_s \tag{2.39}$$

so $$\int_\Gamma \varpi \Psi_{tn} ds = \int_\Gamma \varpi^2 W_t z_s ds = W_t \int_\Gamma \varpi_0^2(z) dz \tag{2.40}$$

Thus $$\pi \int_\Gamma \varpi \Psi_{tn} ds = -W_t V \tag{2.41}$$

where V is the volume of the body.

And, $$\Psi_s = -\varpi W \varpi_s \quad \text{on } \Gamma \tag{2.42}$$

so $$\int_\Gamma E^2 \Psi \Psi_s ds = -W \int_\Gamma \varpi \varpi_s E^2 \Psi ds = W \int_\Gamma \frac{1}{2}\varpi^2 \frac{\partial}{\partial s}(E^2\Psi) ds \tag{2.43}$$

Finally, we have a simplified form of the hydrodynamic force of the body,

$$\mathcal{F}_H = \pi\mu \int_\Gamma \varpi^3 \frac{\partial}{\partial n}\left(\frac{1}{\varpi^2}E^2\Psi\right) ds + \rho W_t V + \pi\rho W \int_\Gamma \frac{1}{2}\varpi^2 \frac{\partial}{\partial s}(E^2\Psi) ds \tag{2.44}$$

This equation is used to determine the relationship between $\mathcal{F}_H$ and W once Ψ is known.

Equation (2.44) is valid for all axisymmetric flows of a viscous incompressible fluid. The first term is simply an integration of the viscous stresses over the surface and the other two terms are derived from the pressure. The second term represents the inertia of the displaced volume of fluid; it appears because the solution of the equations

(2.12), (2.20), (2.21), (2.22) inside the body is just a rigid body motion. The third term in (2.44) is nonlinear and difficult to interpret in general; however, for motions with fore-and-aft symmetry, the term is zero because $\frac{\partial}{\partial s}(E^2\Psi)$ changes sign at the equator. For linearized flow, the third term is negligible; for steady flow the second term is zero, so for steady Stokes flow only the first term is needed.

If the fluid is assumed to be inviscid, (2.44) no longer applies because the no-slip condition (2.21) was used in deriving it. For potential flow, $E^2\Psi = 0$ and (2.37) becomes:

$$\mathcal{T}_4 = -\pi\rho\int_\Gamma \varpi \Psi_t n_s ds - \tfrac{1}{2}\pi\rho\int_\Gamma \varpi^2 \frac{\partial}{\partial s}\left(\frac{1}{\varpi}\nabla\Psi\right)^2 ds \qquad (2.45)$$

As before, the nonlinear term is zero for flows with equatorial symmetry; in fact, it is always zero as we now prove. For potential flow, the time-dependence is separable,

$$\Psi(x,t) = W(t)\psi(x) \qquad (2.46)$$

Then the equation and boundary conditions reduce to:

$$E^2\psi = 0 \qquad (2.47)$$

$$\text{on } \varpi = \varpi_0(z): \quad \psi = -\tfrac{1}{2}\varpi^2 \qquad (2.48a)$$

$$\text{on } \varpi = 0: \quad \psi = 0 \qquad (2.48b)$$

$$\text{as } r \to \infty: \quad \psi/r^2 \to 0 \qquad (2.49)$$

Equation (2.45) becomes

$$\mathcal{F}_H = -\rho\pi W_t \int_\Gamma \varpi \psi_n \, ds - \tfrac{1}{2}\pi\rho W^2 \int_\Gamma \varpi^2 \frac{\partial}{\partial s}\left(\frac{1}{\varpi}\nabla\psi\right)^2 ds \qquad (2.50)$$

Now for steady flow, D'Alembert's paradox tells us that $\mathcal{F}_H = 0$.

Therefore $$\int_\Gamma \varpi^2 \frac{\partial}{\partial s}\left(\frac{1}{\varpi}\nabla\psi\right)^2 = 0 \qquad (2.51)$$

Statement (2.51) is independent of W(t), so it holds equally for unsteady flow. Thus,

$$\mathcal{F}_H = -\pi\rho \int_\Gamma \varpi \Psi_{tn} \, ds \qquad (2.52)$$

The integral in (2.52) is equivalent to the second term in (2.44) and gives the added mass of the body

$$m_a = \pi\rho \int_\Gamma \varpi \psi_n \, ds \qquad (2.53)$$

Equation (2.53) can also be derived by considering the kinetic energy of the flow field, and is equivalent to Taylor's (1928) theorem which gives the virtual mass in terms of the velocity potential in the far field, and may be written as:

$$m_a = 4\pi a_1 - V \qquad (2.54)$$

in which $$a_1 = \lim_{r\to\infty} \frac{\varphi r^2}{Wz}, \qquad (2.55)$$

V is the volume of the body, φ is the velocity potential and W is the velocity of the body in the z-direction.

Equation (2.55) is analogous to the result of Payne & Pell (1960) for steady Stokes flow. They found the Stokes drag on a body in steady axisymmetric motion to be

$$F_s = 8\pi \lim_{r\to\infty} \frac{r\psi}{\varpi^2} \tag{2.56}$$

Both results (2.54) and (2.56) are found by integrating the equations of motion over the flow field and using known solutions in spherical coordinates to represent the flow in the far field. This approach will be applied to the unsteady linearized equations in the next section.

2.3 RESULTS FOR LINEARIZED EQUATIONS

We introduce dimensionless variables $\underset{\sim}{u}^* = \underset{\sim}{u}/U$, $\underset{\sim}{r}^* = \underset{\sim}{r}/L$, $p^* = p/P$ and $t^* = t/T$ in which U, L, P, and T are typical scales for their respective variables for a particular problem. The Navier-Stokes equations (2.1) then take the form:

$$\nabla^*\cdot\underset{\sim}{u}^* = 0, \quad [Re][St]\underset{\sim}{u}^*_{t^*} + [Re]\underset{\sim}{u}^*\cdot\nabla^*\underset{\sim}{u}^* = -\left[\frac{PL}{\mu U}\right]\nabla^* p^* + \nabla^{*2}\underset{\sim}{u}^* \tag{2.57}$$

with Reynolds number $$Re = \frac{UL}{\nu} \tag{2.58}$$

and Strouhal number $$St = \frac{L}{UT} \tag{2.59}$$

It is convenient to choose $P = \mu U/L$, a viscous pressure scale, and to introduce a new dimensionless parameter,

$$|\lambda^2| = [Re][St] = \frac{L^2}{\nu T} \tag{2.60}$$

which is the ratio of the viscous diffusion time to the natural timescale of the problem. Then we have:

$$\nabla \cdot \underset{\sim}{u} = 0, \quad [|\lambda^2|]\, \underset{\sim}{u}_t + [Re]\, \underset{\sim}{u} \cdot \nabla \underset{\sim}{u} = -\nabla p + \nabla^2 \underset{\sim}{u} \tag{2.61}$$

in which the asterisks have been dropped.

In the case where Re is small, but St is large, it may happen that the convective inertia of the fluid is negligible, but the local inertia is not. Formally, we let $Re \to 0$ and $St \to \infty$, so that $|\lambda^2|$ remains O(1). Then the momentum equation becomes linear.

$$|\lambda^2|\, \underset{\sim}{u}_t = -\nabla p + \nabla^2 \underset{\sim}{u} \tag{2.62}$$

If we consider a body oscillating periodically with small amplitude in either bounded or unbounded fluid which is otherwise at rest, the boundary condition on the body surface $\mathcal{B}(t)$ is (in dimensional form)

$$\text{on } \mathcal{B}(t): \quad \underset{\sim}{u} = \underset{\sim}{U}(t) \tag{2.63}$$

The boundary moves with time, making the condition nonlinear. However, for small displacements from the average position $\mathcal{B}_0$, we can expand the condition in a Taylor series about $\mathcal{B}_0$. For a point $\underset{\sim}{r}$ on $\mathcal{B}(t)$ and the corresponding point $\underset{\sim}{r}_0$ on $\mathcal{B}_0$ we have

$$\underset{\sim}{u}(r) = \underset{\sim}{u}(r_0) + (r - r_0) \cdot \nabla \underset{\sim}{u}(r_1) \tag{2.64}$$

where $\underset{\sim}{r}_1$ is some point on the line connecting $\underset{\sim}{r}$ and $\underset{\sim}{r}_0$. So we have a new condition in terms of $\underset{\sim}{\delta} = \underset{\sim}{r} - \underset{\sim}{r}_0$,

$$\underset{\sim}{u}(\underset{\sim}{r}_0) = \underset{\sim}{U}(t) - \underset{\sim}{\delta} \cdot \nabla \underset{\sim}{u}(\underset{\sim}{r}_1) \tag{2.65}$$

Now we define $\underset{\sim}{\delta}^* = \delta / UT$ to get a dimensionless form,

$$\underset{\sim}{u}^*(\underset{\sim}{r}_0^*) = \underset{\sim}{U}^*(t^*) - [St]^{-1} \underset{\sim}{\delta}^* \cdot \nabla^* \underset{\sim}{u}^*(\underset{\sim}{r}_1^*) \tag{2.66}$$

Then in the limit as $Re \to 0$ and $St \to \infty$, the correction term in the Taylor expansion is negligible and we have the linearized boundary condition

$$\text{on } \mathcal{B}_0: \quad \underset{\sim}{u} = \underset{\sim}{U}(t) \tag{2.67}$$

It is as though the body were fixed at $\mathcal{B}_0$. The above procedure can be circumvented to deal with the case when the body motion is not periodic, but results in a net displacement, provided that the displacement does not change the gross geometry of the problem. In the latter case, the boundary condition remains nonlinear and an alternative approach must be used if the problem is to be simplified.

If the geometry remains self-similar, we can transform to a coordinate system fixed in the body. This changes the boundary conditions on the body and at infinity and introduces an acceleration term into the momentum equation since the frame of reference is not Galilean. However, if we define a new variable $\underset{\sim}{u}' = \underset{\sim}{u} - \underset{\sim}{U}$, then $\underset{\sim}{u}'$ is governed by the same equations and conditions as applied in the

stationary frame of reference, except that the boundary is fixed. Thus, even though the body may move substantially, the solution is valid in the instantaneous frame of reference fixed in the body.

For an axisymmetric problem the stream function is introduced and the equations become:

$$E^4\Psi - |\lambda^2| E^2\Psi_t = 0 \tag{2.68}$$

$$\text{as } r \to \infty: \quad \Psi/r^2 \to 0 \tag{2.69}$$

$$\text{on } \varpi = 0: \quad \Psi = 0, \ \Psi_{\varpi} = 0 \tag{2.70}$$

$$\text{on } \varpi = \varpi_0(z): \quad \Psi = -\tfrac{1}{2}\varpi^2 W, \ \Psi_n = -\varpi W \varpi_n \tag{2.71}$$

$$\text{on } z = 0: \quad \Psi = 0, \ \Psi_z = 0 \tag{2.72}$$

As a final simplification, we consider the case when the dimensional velocity is

$$W(t) = U e^{-i\omega t} \tag{2.73}$$

Then

$$\Psi(r,t) = \psi(\varpi,z) e^{-i\omega t} \tag{2.74}$$

This is formally equivalent to taking a Laplace or Fourier transform of the problem with respect to time. We introduce a new, complex parameter

$$\lambda^2 = -i|\lambda^2| = -i\frac{\omega L^2}{\nu}, \qquad \lambda = \sqrt{-i}\,|\lambda| = \frac{1-i}{\sqrt{2}}|\lambda| \tag{2.75}$$

so that (2.68) and (2.71) become:

$$E^4 \psi - \lambda^2 E^2 \psi = 0 \qquad (2.76)$$

and $$\text{on } \varpi = \varpi_0(z): \quad \psi = -\tfrac{1}{2}\varpi^2, \quad \psi_n = -\varpi \varpi_n \qquad (2.77)$$

The other conditions (2.69), (2.70) and (2.72) are unaltered.

The differential equation (2.76) has a solution made up of a potential part and a diffusive part,

$$\psi = \psi^P + \psi^D \qquad (2.78)$$

with $$E^2 \psi^P = 0 \qquad \text{and} \qquad (E^2 - \lambda^2)\psi^D = 0 \qquad (2.79)$$

The inhomogeneous part of the solution has been combined with ψ^P. We are left with a simple linear problem of second order, which can be solved by separation of variables whenever the boundary $\varpi_0(z)$ is of suitable form. In other cases, a more sophisticated procedure such as the boundary integral method or multipole collocation technique may be used.

Basset (1888) has given the general solution of (2.79) subject to (2.69) in terms of spherical coordinates (r, θ), with $\zeta = \cos\theta$.

$$\psi^P = \sum_{n=0}^{\infty} A_n r^{-n+1} S_n(\zeta) \qquad (2.80)$$

$$\psi^D = \sum_{n=0}^{\infty} B_n R_n^{(-)}(r) S_n(\zeta) \qquad (2.81)$$

The $R_n^{(-)}(r)$ are polynomials in $(1/r)$ with an exponential multiplier

$$R_n^{(-)}(r) = r^n \left(\frac{1}{r}\frac{d}{dr}\right)^{n-1} \frac{1}{r} e^{-\lambda r} \qquad (2.82)$$

The $S_n(\zeta)$ are Gegenbauer functions of degree $-\frac{1}{2}$ which are defined in terms of Legendre polynomials by

$$S_0(\zeta) = 1, \quad S_1(\zeta) = -\zeta, \quad S_2 = \tfrac{1}{2}(1-\zeta^2) \tag{2.83}$$

$$S_n(\zeta) = \frac{1}{2n-1}\left(P_{n-2}(\zeta) - P_n(\zeta)\right), \quad n \geq 2 \tag{2.84}$$

and we shall use the property,

$$\int_{-1}^{1} S_n(\zeta)\, d\zeta = 2\,\delta_{n0} + \tfrac{2}{3}\,\delta_{n2} \tag{2.85}$$

In the case of a spherical body, only the second harmonic is required and the boundary conditions (2.77) are applied at $r = 1$ to give Stokes' (1851) result,

$$\psi = -\tfrac{1}{2}\sin^2\theta\left[\left(1+\tfrac{3}{\lambda}+\tfrac{3}{\lambda^2}\right)\tfrac{1}{r} - \tfrac{3}{\lambda}\left(1+\tfrac{1}{\lambda r}\right)e^{-\lambda(r-1)}\right] \tag{2.86}$$

The linearized version of the force on the body (2.44) with the time-dependence separated is

$$F = \pi\mu\int_{\Gamma}\varpi^2\frac{\partial}{\partial n}\left(\frac{1}{\varpi^2}E^2\psi\right)ds - \rho i\omega W V \tag{2.87}$$

Or in dimensionless form with force-scale μUL,

$$F = \pi\int_{\Gamma}\varpi^2\frac{\partial}{\partial n}\left(\frac{1}{\varpi^2}E^2\psi\right)ds + \lambda^2 V \tag{2.88}$$

However, we can find a much more convenient form as will be shown below.

The velocity is given by:

$$\underset{\sim}{u} = -\nabla_\wedge\left(i_\phi\,\psi/\varpi\right) \tag{2.89}$$

Then (2.76) or (2.62) can be replaced by,

$$\nabla \cdot \underset{\sim}{\sigma} = -\lambda^2 \nabla_\Lambda (\underset{\sim}{i}_\phi \psi/\varpi) \tag{2.90}$$

Equation (2.90) is integrated over the domain $\mathcal{D}$ bounded by $\mathcal{B}$ and a large concentric sphere $\mathcal{B}'$ of radius R. The volume integrals are changed to surface integrals using Stokes' theorem and we retain only the z-component of the vector equation.

$$\iint_{\mathcal{B}} \underset{\sim}{i}_z \cdot \underset{\sim}{\sigma} \cdot \underset{\sim}{n}\, dS + \iint_{\mathcal{B}'} \underset{\sim}{i}_z \cdot \underset{\sim}{\sigma} \cdot \underset{\sim}{n}\, dS$$

$$+ \iint_{\mathcal{B}} \underset{\sim}{i}_z \cdot \underset{\sim}{n} \wedge \underset{\sim}{i}_\phi \lambda^2 (\psi/\varpi) dS + \iint_{\mathcal{B}'} \underset{\sim}{i}_z \cdot \underset{\sim}{n} \wedge \underset{\sim}{i}_\phi \lambda^2 (\psi/\varpi) dS = 0 \tag{2.91}$$

Here $\underset{\sim}{n}$ is the local <u>outward</u> unit normal to the domain .

The first integral of (2.91) is simply the force exerted by the body on the fluid, -F, and the others may be evaluated individually. We follow the method of Happel & Brenner (1965) to put the second integral of (2.91) in the form

$$\iint_{\mathcal{B}'} \underset{\sim}{i}_z \cdot \underset{\sim}{\sigma} \cdot \underset{\sim}{n}\, dS = \pi \int_\Gamma \varpi^3 \frac{\partial}{\partial n} (E^2 \psi/\varpi^2) ds - \pi \int_\Gamma \lambda^2 \varpi \frac{\partial \psi}{\partial n} ds \tag{2.92}$$

in which s is the coordinate along the generating arc of , λ is defined by (2.75) and E^2 is the differential operator

$$E^2 = \frac{\partial^2}{\partial r^2} + \frac{1-\zeta^2}{r^2} \frac{\partial^2}{\partial \zeta^2} \tag{2.93}$$

We now use Basset's (1888) solution (2.80) and (2.81) at the spherical boundary $\mathcal{B}'$. If there are no sources, then A_0 is

zero. The $R_n^{(-)}(r)$ are exponentially small at large r, so we may neglect them in (2.92) if R is large enough. This leaves

$$\iint_{\mathcal{B}'} i_z \cdot \underset{\sim}{\xi} \cdot \underset{\sim}{n}\, dS = -\pi\lambda^2 \int_{\Pi_\infty} \frac{\partial \psi^P}{\partial \bar{z}}\, ds \qquad (2.94)$$

Finally, we use the property of the S_n, (2.85) to get:

$$\iint_{\mathcal{B}'} i_z \cdot \underset{\sim}{\xi} \cdot \underset{\sim}{n}\, dS = \tfrac{2}{3}\pi\lambda^2 A_2 \qquad (2.95)$$

which is independent of R. The third integral in (2.91) is evaluated using the condition (2.71) on $\mathcal{B}$. It takes the value $\lambda^2 V$ with V the dimensionless volume of the body. The fourth integral in (2.91) is evaluated in a similar way to the second and has the value $\frac{4}{3}\pi\lambda^2 A_2$.

The values for the four integrals are combined to give an expression for the force on the body,

$$F = \lambda^2 (2\pi A_2 + V) \qquad (2.96)$$

The term $\lambda^2 V$ is simply the inertial resistance of the displaced fluid. A_2 depends on and the geometry of the body in a complex way. From (2.80) and (2.81), we may express A_2 in the form:

$$A_2 = \lim_{r\to\infty} \frac{2r^3\psi}{\varpi^2} \qquad (2.97)$$

to give

$$F = \lambda^2 V + \lim_{r\to\infty} 4\pi\lambda^2 \frac{r^3}{\varpi^2}\psi \qquad (2.98)$$

Equation (2.98) is exactly equivalent to Taylor's theorem (2.54) for potential flow, since the far field is purely inviscid. It does not reduce directly to Payne & Pell's formula for steady Stokes flow (2.56) since in that limit λ^2 is zero. However, if (2.80), (2.81), (2.82) and (2.98) are combined and the limit is taken, equation (2.56) can be recovered.

The result (2.98) provides a rapid way of determining the force once the stream function is known. It saves the labour of determining the stress and integrating over the surface of the body. For example, if we apply (2.98) to the stream function (2.86) for an oscillating sphere, we get Stokes' (1851) result for the force,

$$F = -6\pi (1 + \lambda + \tfrac{1}{9}\lambda^2) \qquad (2.99)$$

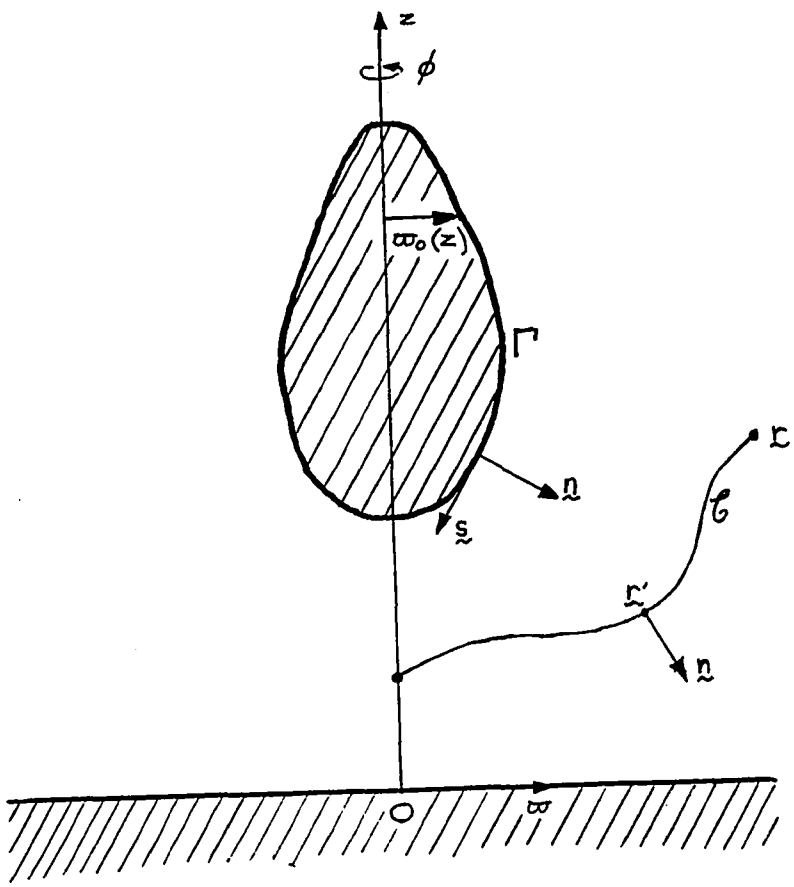

Figure 2.1. Geometry for an axisymmetric body. $\mathcal{C}$ is the contour of integration used in (2.5)

CHAPTER 3. THE FORCE ON AN OSCILLATING SPHEROID

3.1 INTRODUCTION

As discussed in Chapter 2, the linearized Navier-Stokes equations were first postulated by Stokes (1850) who was able to solve them for the oscillatory motion of spherical and cylindrical pendulums. In particular, he found the hydrodynamic force on the oscillating sphere to be:

$$\mathcal{F}_H = \mathrm{Re}\left\{ -6\pi\mu U a \left(1+\lambda+\tfrac{1}{9}\lambda^2\right) e^{-i\omega t} \right\} \qquad (3.1)$$

in which μ is the fluid viscosity, U and a are the peak velocity and radius of the sphere and λ is a dimensionless parameter given by

$$\lambda^2 = -i\,\frac{a^2\omega}{\nu} \qquad (3.2)$$

The frequency of oscillation is ω and ν is the kinematic viscosity of the fluid. Basset (1888) integrated equation (3.1) to obtain the force on a sphere in an arbitrary time-dependent motion with velocity W(t) in the form of a memory integral.

$$\mathcal{F}_H = -6\pi\mu a W + 6\pi(\mu a)^{1/2}(\rho a^3)^{1/2}\frac{1}{\sqrt{\pi}}\int_0^t \frac{dW}{d\tau}(t-\tau)^{-1/2}d\tau - \tfrac{2}{3}\pi\rho a^3\frac{dW}{dt} \qquad (3.3)$$

A simple derivation of this result is given by Landau & Lifschitz (1959), who treat the problem in terms of Laplace

transforms. Stokes formula (3.1) contains three terms and is a simple quadratic function of $\omega^{1/2}$. The first term is in anti-phase with W and is equal to the so-called steady Stokes drag. The third term, which is proportional to ω, is $\pi/2$ out of phase with W and is the nondissipative added mass force. The middle term, which has a phase lag of $\pi/4$ compared to the first, is proportional to $\omega^{\frac{1}{2}}$ and is the so-called Basset force. This term describes the growth of the time-dependent boundary layer at the body surface and the displacement effect of the viscous layer on the inviscid pressure field in a rapidly changing flow, or the effect of the far field for a nearly steady flow

It is interesting to note that if the force on the sphere were calculated as an asymptotic series for small ω starting with the steady Stokes equations and including small inertial effects, the series would terminate after three terms and yield equation (3.1). Similarly, if an asymptotic series is developed for large ω, starting with potential flow and including boundary layer effects (c.f. Batchelor 1967), equation (3.1) is again obtained wherein the damping force on the oscillating sphere can be identified as the part of (3.1) which is in phase with the velocity. Thus, for a sphere at least, the Basset force on an isolated body at all frequencies can be obtained by considering the first order correction to the Stokes drag, or the first order boundary layer correction to the virtual mass in small amplitude motion.

Now for any body shape, we can obtain the small ω behaviour from the quasi-steady Stokes equations and the large ω behaviour from the potential flow equations. The question which then arises is: "Can we derive the middle term, i.e. the Basset force for an arbitrary body, as a first order correction to the Stokes drag or the virtual mass?", or equivalently: "Is the hydrodynamic force on an oscillating body of arbitrary shape a quadratic function of λ with coefficients depending only on the body shape?" This possibility is suggested by the fact that the coefficients of both the steady term in phase with the velocity and the added mass term depend only on the geometry. If the answer to these questions is yes, then we have a very quick method for obtaining the hydrodynamic force on a variety of body shapes for which the Stokes drag and virtual mass are already known. Unfortunately, the answer is no; it is shown below that the force is not quadratic in λ, and that a fourth term must be added to the equation. The functional form and phase of this force depend on the body geometry; however, for aspect ratios not too different from unity, it is quite small.

Since Basset's work, the linearized equations were seldom studied until interest in the equations was re-awakened when Alder & Wainwright (1967, 1970) showed that Brownian motion of small particles is governed by the time-dependent Stokes equations rather than the quasi-steady

equations. Subsequently, Bedeaux & Mazur (1974) and Arminski & Weinbaum (1979) showed that the results obtained using quasi-steady assumptions were in fact valid for the diffusivity tensor, although they confirmed the important new results of Alder & Wainwright regarding the long-time tail of the velocity autocorrelation. A few other authors extended the results for the spherical geometry to cover more general flows (Mazur & Bedeaux 1974, Felderhof 1976a,b). Leichtberg et al (1976) studied the relative motion of groups of spheres using a multipole method, but were only able to account for interactions in the quasi-steady part of the motion. A similar method was used by Lin (1986) for a group of vibrating cylinders; since the geometry is stationary, he was able to include all the interactions.

Basset's (1888) result is also applicable to the random motion of small solid particles in a turbulent fluid, provided certain conditions are satisfied. Tchen (1947) pioneered this application of the result (3.3) and used it to find an analytical form for the turbulent diffusivity of the particles.

All the work mentioned above has related to the basic spherical or cylindrical geometry and so is based on the solutions of Stokes (1850) and Basset (1888). To the author's knowledge, the only work which deals with more

complex shapes explicitly is that of Hocquart (1976,1977a,b), who has found solutions for the case of a spheroid rotating about its axis or an equator. Subsequently, Hocquart & Hinch (1983) gave a general result for the long time behaviour of an arbitrary centrally symmetric body in terms of the far field of the flow. The purpose of the last four papers was to investigate Brownian motion, so they have concentrated on the low frequency range of oscillations. Aoi (1955a,b) tackled the mathematically similar problem of Oseen flow past a spheroid, which apart from the work of Hocquart (1976,1977a) is the only work in fluid mechanics that requires the use of the spheroidal wave functions (Flammer 1957). This work was also directed towards the calculation of small inertial corrections. Lawrence & Weinbaum (1986) have given a simple relation for the force on an oscillating axisymmetric body in terms of the stream function in the far field and applied it to a nearly spherical spheroid. (See sections 2.3, 3.3(c).) However, the coordinate system used is spherical, so the solutions of Basset can be utilized. In the present chapter, the result will be applied to an arbitrary spheroid and so the use of spheroidal wave functions will be required. The frequency will be arbitrary, so the problem is more general than those of Hocquart and that of Aoi.

In the next section, the equations of motion will be formulated in terms of the stream function in spheroidal

coordinates. There are two dimensionless parameters in the problem which may be chosen in different ways, depending on the circumstances. The results will be presented in terms of the physically significant parameters which are the aspect ratio b/a and the frequency parameter $|\lambda| = a\sqrt{\omega/\nu}$. For most applications, aspect ratios between 0.1 and 10 may be considered. The three limiting cases $b/a = 0, 1, \infty$ correspond to the disc, sphere and infinite cylinder respectively, but are relatively unimportant; an oscillating disc sheds nonlinear vortices at all but the lowest frequencies, whilst the sphere and cylinder can be treated more effectively in their natural coordinate systems (Stokes 1851, Batchelor 1954). The frequency parameter, $|\lambda|$, may be quite large (of order 10 or 100 for a pendulum), but is generally small for microscopic particles.

Some asymptotic results are derived in section 3.3 and these give a good indication of the general solution. Firstly, results for small and large frequencies will be obtained, and then a result for a perturbed sphere. The small frequency result can be extended to include bodies of arbitrary shape after the fashion of Hocquart & Hinch (1983). The complete solution will be obtained in section 3.4 and the results are presented in section 3.5. Many of the calculations are involved and so will be included in the Appendix.

Useful results are obtained in the parameter ranges $0.1 < b/a < 10$, $0.1 < |\lambda| < 10$. These indicate that the force is made up of four contributions - the Stokes drag, the added mass force , the Basset force and a fourth term which depends on aspect ratio and frequency in a complicated way. The first two of these are very familiar, but the third has not been well understood and the fourth has never been discussed. Finally a correlation is proposed, based on the asymptotic results of section 3.3 with parameters abstracted from the general results of section 3.4. The correlation is accurate in the range $0.1 < b/a < 10$ for all frequencies and reduces to Stokes' result for a sphere. The result may be regarded as a Laplace transform which, in special cases, may be inverted to give the force on a spheroid in arbitrary motion along its axis.

3.2 FORMULATION IN SPHEROIDAL COORDINATES

We consider the spheroid generated by rotating the ellipse $\omega^2/a^2 + z^2/b^2 = 1$ about the z-axis as shown in figure 3.1. For the time being, we will restrict consideration to an oblate spheroid, with $b < a$, although it will prove to be simple to extend the results to the prolate case (see part (d) of this section). We introduce conjugate coordinates of revolution (ξ, η) with $x = \sinh\xi$ and $y = \cos\eta$ defined by

$$z = d\,xy\,, \qquad \varpi = d(1+x^2)^{\frac{1}{2}}(1-y^2)^{\frac{1}{2}} \tag{3.4}$$

where $d = (a^2 - b^2)^{1/2}$ is the radius of the focal circle. The surface of the spheroid is now the coordinate surface $x = x_0$ with

$$a^2 = d^2(1+x_0^2) \quad \text{and} \quad b^2 = d^2 x_0^2 \tag{3.5}$$

and the flow domain is the region

$$x_0 \le x \le \infty, \qquad -1 \le y \le 1 \tag{3.6}$$

The spheroid is a solid body which executes oscillations along its axis of symmetry with velocity $U \cos\omega t \, \underset{\sim}{i}_z$. If the velocity of the fluid is so small that its square may be neglected, the equations of motion are the linearized Navier-Stokes equations, otherwise known as the unsteady Stokes equations.

$$\nabla \cdot \underset{\sim}{u} = 0, \qquad \rho \underset{\sim}{u}_t = -\nabla p + \mu \nabla^2 \underset{\sim}{u} \tag{3.7}$$

We take the curl of the momentum equation to eliminate the pressure and introduce the stream function Ψ defined in cylindrical coordinates by

$$\underset{\sim}{u} \cdot \underset{\sim}{i}_\varpi = \frac{1}{\varpi} \Psi_z, \qquad \underset{\sim}{u} \cdot \underset{\sim}{i}_z = -\frac{1}{\varpi} \Psi_\varpi \tag{3.8}$$

Then we have the vorticity equation:

$$E^4 \Psi - \frac{1}{\nu} E^2 \Psi_t = 0 \tag{3.9}$$

where E^2 is the generalized axisymmetric potential operator given by

$$E^2 = \varpi h^2\left[\frac{\partial}{\partial\xi}\left(\frac{1}{\varpi}\frac{\partial}{\partial\xi}\right) + \frac{\partial}{\partial\eta}\left(\frac{1}{\varpi}\frac{\partial}{\partial\eta}\right)\right] \tag{3.10}$$

For oblate spheroidal coordinates,

$$h = \frac{1}{d(\cosh^2\xi - \sin^2\eta)^{\frac{1}{2}}} = \frac{1}{d(x^2+y^2)^{\frac{1}{2}}} \tag{3.11}$$

so E^2 reduces to

$$E^2 = \frac{1}{d^2(x^2+y^2)}\left[(1+x^2)\frac{\partial^2}{\partial x^2} + (1-y^2)\frac{\partial^2}{\partial y^2}\right] \tag{3.12}$$

The limiting conditions on the velocity are:

on the body $\quad \underset{\sim}{u} = U\cos\omega t\, \underset{\sim}{i}_z$ (3.13)

at infinity $\quad \underset{\sim}{u} \longrightarrow 0$ (3.14)

The rate of decay of $\underset{\sim}{u}$ must be so fast that there are no source or circulation fields at infinity. Therefore we need

$$r^2\underset{\sim}{u} \longrightarrow 0 \quad \text{as} \quad r \longrightarrow \infty \tag{3.15}$$

where $r^2 = \varpi^2 + z^2$ is the spherical radius. We also require that there are no singularities in the flow field. (This precludes the limit $x_0 = 0$ in which the body is a disc.) The flow is periodic in time, so we may take the stream function to be of the form $\Psi(\varpi, z, t) = \mathrm{Re}\{\psi(\varpi, z)e^{-i\omega t}\}$ where ψ may be complex. Then we have:

$$E^4\psi + i\frac{\omega}{\nu}E^2\psi = 0 \tag{3.16}$$

$$\text{on } x = x_0: \quad \psi = -\tfrac{1}{2}\varpi^2 U = -\tfrac{1}{2}d^2U(1+x_0^2)(1-y^2) \tag{3.17}$$

$$\psi_x = -\varpi\varpi_x U = -d^2U(1-y^2)x_0 \tag{3.18}$$

$$\text{as } x \to \infty: \quad \psi \to 0 \tag{3.19}$$

$$\text{on } y = \pm 1: \quad \psi = 0, \quad \psi_y \text{ is Finite} \tag{3.20}$$

There is also symmetry about the plane y = 0, so we have $\psi(y) = \psi(-y)$ and $\psi_y = 0$ on y = 0. It is worthy of note that these equations are valid in the coordinate system which is fixed in the body. This accelerated frame of reference has no effect other than the inclusion in the force of a buoyancy term which represents the acceleration of the displaced volume of fluid.

We are ultimately interested in the force on the body which is of the form $\mathcal{F}_H = \mathrm{Re}\{Fe^{-i\omega t}\}$. The complex amplitude F is given by (2.98) to be

$$F = -\rho i\omega\left[UV + 4\pi \lim_{r\to\infty} \frac{r^2}{\varpi^2}\psi\right] \tag{3.21}$$

where $V = \frac{4}{3}\pi a^2 b$ is the volume of the body.

To facilitate the solution, we introduce dimensionless quantities with velocity-scale U, length-scale d, and force-scale μUd as follows:

$$\psi^* = \psi/d^2U, \quad (E^2)^* = d^2E^2, \quad F^* = F/\mu Ud, \quad V^* = V/d^3 = \tfrac{4}{3}\pi x_0(1+x_0^2) \tag{3.22}$$

The asterisks will be ignored and the governing equations simplify to:

$$E^4\psi - c^2E^2\psi = 0, \quad \text{with} \quad c^2 = -i\frac{\omega d^2}{\nu}, \ \mathrm{Re}\{c\}>0. \tag{3.23}$$

$$\text{on } x = x_0: \quad \psi = -\tfrac{1}{2}(1+x_0^2)(1-y^2), \quad \psi_x = -x_0(1-y^2) \tag{3.24}$$

$$F = c^2\left[V + 4\pi \lim_{r\to\infty} \frac{r^3}{\varpi^2}\psi\right] \tag{3.25}$$

Conditions (3.19) and (3.20) are unchanged.

The above is a linear boundary value problem with two parameters x_o and $|c|$. It is more usual to use the parameters: aspect ratio b/a, frequency parameter $|\lambda| = a\sqrt{\omega/\nu}$, as well as to use the dimensionless force $F_a^* = F/6\pi\mu U\, a$. However, this would unnecessarily complicate the equations. After the results are obtained, it is simple to convert them to the above form by using length-scale a instead of d in (3.22).

3.3 ANALYTIC SOLUTIONS FOUND VIA SMALL PERTURBATIONS

The solution to equations (3.23), etc. is very complex in the general case and will be treated in section 3.4. Valuable insights can first be obtained by examining certain limiting cases which will also be useful for checking the full calculations. Three cases will be considered: (a) low frequency $|c| \ll 1$, (b) high frequency $|c| \gg 1$, (c) nearly spherical body $x_o \gg 1$.

(a) low frequency

At very low frequencies, the flow becomes quasi-steady and so the solution to zero-order is that for steady flow past a spheroid first given by Sampson (1890) and discussed by Happel & Brenner (1965). (Here we use the dimensionless quantities of section 3.2.)

$$\psi_0 = (1-y^2)\left\{-\tfrac{1}{2}C_1 x + \tfrac{1}{2}C_2\left[x - (x^2+1)\cot^{-1}x\right] + C_3(x^2+1)\right\} \quad (3.26)$$

with $C_1 = \dfrac{2}{x_0 - (x_0^2-1)\cot^{-1}x_0}$, $C_2 = \dfrac{-(x_0^2-1)}{x_0-(x_0^2-1)\cot^{-1}x_0}$, $C_3 = 0$ (3.27)

and $$F_0 = -4\pi C_1 = \frac{-8\pi}{x_0 - (x_0^2-1)\cot^{-1}x_0} \quad (3.28)$$

For slightly larger frequencies, we expect that the stream function and the force F may be represented as asymptotic power series in c, and we will attempt to find the first-order correction. We set

$$\psi \sim \psi_0 + c\psi_1 + c^2\psi_2 \quad (3.29)$$

Then the equations of motion become:

$$E^4\psi_0 = 0, \quad E^4\psi_1 = 0, \quad E^4\psi_2 = E^2\psi_0 \quad (3.30)$$

on $x = x_0$: $\psi_0 = -\tfrac{1}{2}(1-y^2)(1+x_0^2)$, $\psi_1 = 0$, $\psi_2 = 0$ (3.31)

$$\psi_{0x} = -x_0(1-y^2), \quad \psi_{1x} = 0, \quad \psi_{2x} = 0 \quad (3.32)$$

We may not impose the conditions at infinity since for large x, $E^2 \sim 1/x^2$ may be as small as c^2 and the nature of the

equation will change. We see at once that ψ_1 must be of the same general form as ψ_0, while ψ_2 may be considerably more complicated. So we have:

$$\psi_1 = (1-y^2)\left\{-\tfrac{1}{2}\hat{C}_1 x + \tfrac{1}{2}\hat{C}_2\left[x - (x^2+1)\cot^{-1}x\right] + \hat{C}_3(x^2+1)\right\} \quad (3.33)$$

In this case $\hat{C}_3$ will not be zero, in fact it is directly responsible for the first correction to F. The conditions on the body give:

$$-\tfrac{1}{2}\hat{C}_1 + \tfrac{1}{2}\hat{C}_2\left[x_0 - (x_0^2+1)\cot^{-1}x_0\right] + \hat{C}_3(x_0^2+1) = 0 \quad (3.34)$$

$$-\tfrac{1}{2}\hat{C}_1 + \tfrac{1}{2}\hat{C}_2\left[2 - 2x_0\cot^{-1}x_0\right] + \hat{C}_3\, 2x_0 = 0 \quad (3.35)$$

We need an outer condition to determine the constants $\hat{C}_i$, so we must consider the outer region of the flow more carefully. We define an "outer" variable R = cx and re-cast the problem in terms of R.

Then $$E^2 = c^2\mathcal{E}_0^2 + c^4\mathcal{E}_2^2 + O(c^4) \quad (3.36)$$

with $$\mathcal{E}_0^2 = \frac{\partial^2}{\partial R^2} + \frac{1-y^2}{R^2}\frac{\partial^2}{\partial y^2} \quad (3.37)$$

$$\mathcal{E}_2^2 = \frac{1-y^2}{R^4}\left[R^2\frac{\partial^2}{\partial R^2} + y^2\frac{\partial^2}{\partial y^2}\right] \quad (3.38)$$

From (3.25) and (3.28), we see that the dominant term in the far field of ψ is likely to be of order 1/c, so we pose an expansion for ψ to be valid at fixed R as $c \to 0$.

$$\psi \sim \frac{1}{c}\tilde{\psi}_0 + \tilde{\psi}_1 + c\tilde{\psi}_2 \quad (3.39)$$

Then we have the following equations of motion:

$$(\mathcal{E}_0^4 - \mathcal{E}_0^2)\tilde{\psi}_0 = 0, \quad \tilde{\psi}_0 \to 0 \text{ as } R \to \infty \tag{3.40}$$

$$(\mathcal{E}_0^4 - \mathcal{E}_0^2)\tilde{\psi}_1 = 0, \quad \tilde{\psi}_1 \to 0 \text{ as } R \to \infty \tag{3.41}$$

$$(\mathcal{E}_0^4 - \mathcal{E}_0^2)\tilde{\psi}_2 = (\mathcal{E}_0^2\mathcal{E}_2^2 + \mathcal{E}_2^2\mathcal{E}_0^2 - \mathcal{E}_2^2)\tilde{\psi}_0, \quad \tilde{\psi}_2 \to 0 \text{ as } R \to \infty \tag{3.42}$$

The forcing for $\tilde{\psi}_0$ and $\tilde{\psi}_1$ is provided by ψ_0 and ψ_1, so we can expect the simple $(1-y^2)$ angular dependence. Again, the $\tilde{\psi}_2$ term will be considerably more complicated.

Now $\mathcal{E}_0^2$ is simply the spherical form of E^2, with R the spherical radius and $y = \cos\theta$, so the solutions for $\tilde{\psi}_0$ and $\tilde{\psi}_1$ are simply Stokes' (1851) solution for the region outside a sphere.

$$\tilde{\psi}_0 = (1-y^2)\left[A_1\frac{1}{R} + A_2 e^{-R}\left(1+\frac{1}{R}\right)\right] \tag{3.43}$$

$$\tilde{\psi}_1 = (1-y^2)\left[\hat{A}_1\frac{1}{R} + \hat{A}_2 e^{-R}\left(1+\frac{1}{R}\right)\right] \tag{3.44}$$

The coefficients $\hat{C}_1$, $\hat{C}_2$, $\hat{C}_3$, A_1, A_2, $\hat{A}_1$, $\hat{A}_2$ are to be found by matching the expansions. To do this, we define the intermediate variable $\chi = c^\alpha x = c^{\alpha-1}R$ with $0 < \alpha < 1$, and re-write each expansion in terms of χ. The outer expansion (3.39) gives

$$\psi \sim (1-y^2)\left\{\frac{1}{c}\left[A_1 c^{\alpha-1}\frac{1}{\chi} + A_2 c^{\alpha-1}\frac{1}{\chi}(1+c^{1-\alpha}\chi)(1-c^{1-\alpha}\chi+\tfrac{1}{2}c^{2-2\alpha}\chi^2-\tfrac{1}{6}c^{3-3\alpha}\chi^3+\ldots)\right]\right.$$
$$\left. + \left[\hat{A}_1 c^{\alpha-1}\frac{1}{\chi} + \hat{A}_2 c^{\alpha-1}\frac{1}{\chi}(1+c^{1-\alpha}\chi)(1-c^{1-\alpha}\chi+\tfrac{1}{2}c^{2-2\alpha}\chi^2+\ldots)\right] + O(c)\right\} \tag{3.45}$$

The inner expansion (3.29) gives:

$$\psi \sim (1-y^2)\{ [-\tfrac{1}{2}C_1 c^{-\alpha}\chi + \tfrac{1}{2}C_2(c^{-\alpha}\chi - (c^{-2\alpha}\chi^2+1)(\tfrac{c^\alpha}{\chi} - \tfrac{c^{3\alpha}}{\chi^3}+\cdots))]$$

$$+c[-\tfrac{1}{2}\hat{C}_1 c^{-\alpha}\chi + \tfrac{1}{2}\hat{C}_2(c^{-\alpha}\chi - (c^{-2\alpha}\chi^2+1)(\tfrac{c^\alpha}{\chi}-\cdots))] + O(c^2)\} \quad (3.46)$$

The two expansions (3.45), (3.46) must have identical functions of χ as coefficients for each power of c up to those which have been neglected. Thus we find the following equations.

$$A_2 = C_1, \quad A_1 = -C, \quad \hat{A}_2 = \hat{C}_1, \quad \hat{A}_1 = -\hat{C}_1 \quad (3.47)$$

$$\hat{C}_3 = \tfrac{1}{3}A_2 = \tfrac{1}{3}C_1 \quad (3.48)$$

Equation (3.48) is substituted into (3.34) and (3.35) to obtain $\hat{C}_1$ and $\hat{C}_2$.

$$\hat{C}_2 = \tfrac{2}{3}C_1 C_2 \quad (3.49)$$

$$\hat{C}_1 = \tfrac{2}{3}C_1^2 \quad (3.50)$$

Thus, in the inner region, for $x < O(c^{-1})$

$$\psi \sim (1-y^2)\{(1+\tfrac{2}{3}cC_1)[-\tfrac{1}{2}C_1 x + \tfrac{1}{2}C_2(x-(x^2+1)\cot^{-1}x)] + \tfrac{1}{3}cC_1(x^2+1) + O(c^2) \quad (3.51)$$

In the outer region, for $x \geq O(c^{-1})$

$$\psi \sim -\tfrac{1}{c}(1-y^2)\{(C_1+\tfrac{2}{3}cC_1^2)[\tfrac{1}{cx} - e^{-cx}(1+\tfrac{1}{cx})] + O(c^2)\} \quad (3.52)$$

From (3.25) we find the force to be

$$F = F_0 + cF_1 + O(c^2) \quad (3.53)$$

with $$F_0 = -4\pi C_1 \quad \text{and} \quad F_1 = -\tfrac{8}{3}\pi C_1^2 = -\frac{F_0^2}{6\pi} \quad (3.54)$$

The relationship between F_0 and F_1 can be carried over to more general body shapes (c.f. Hocquart & Hinch 1983). For an arbitrary body whose (symmetric) resistance tensor for steady flow is $6\pi\mu a\underset{\approx}{A}$, the force generated by slow oscillations will be:

$$\underset{\sim}{F} = -6\pi\mu a\,\underset{\sim}{U}\cdot\left(\underset{\approx}{A} + \lambda\underset{\approx}{A}\cdot\underset{\approx}{A} + O(\lambda^2)\right) \qquad (3.55)$$

(b) high frequency

When the frequency of oscillation is very high, the flow field will be almost inviscid and the potential flow solution will be valid everywhere except in a thin boundary layer on the surface of the body. In order to calculate the perturbed stream function, one must compute the boundary layer velocities and the displacement effect on the external pressure field via matched asymptotic expansions, in a similar way to part (a) above. However, Batchelor (1967) gives a simple method for obtaining the in-phase part of the force, i.e. the damping force, from the dissipation in the boundary layer.

It is clear that the force on the body may be represented in the asymptotic (dimensional) form:

$$F \sim \lambda^2\left(F_2 + \lambda^{-1}F_1\right) \qquad (3.56)$$

where F_2 is proportional to the added mass and $\lambda^2 = -\frac{i\omega a^2}{\nu}$ is the frequency parameter. It is also true that the mathematical problems which determine F_2 and F_1 are entirely real, so that F_2 and F_1, are also real as in (a) above. The damping force is, therefore, simply $|\lambda| F_1 / \sqrt{2}$ and we can determine F_1 from the same calculation.

Batchelor (1967) gives the in-phase part of the force to be $F_R \cos \omega t$ with

$$\tfrac{1}{2} U F_R = \frac{\mu}{2\delta} \int_{body} U_s^2 \, dA, \qquad \delta = \left(\frac{2\nu}{\omega}\right)^{1/2} \ll a \tag{3.57}$$

In equation (3.57), U_s is the velocity of the fluid at the surface of a spheroid which is stationary in uniform potential flow at infinity. Batchelor (1967) also gives the stream function for a spheroid moving through stationary inviscid fluid to be:

$$\psi = \frac{\frac{1}{2} U a^2 (a^2-b^2) \sin^2 \eta}{b(a^2-b^2)^{1/2} - a^2 \cos^{-1} \frac{b}{a}} \left(\sinh \xi - \cosh^2 \xi \coth^{-1} \sinh \xi \right) \tag{3.58}$$

To change (3.58) to the case of the stationary spheroid, we simply subtract a uniform stream, which is a term

$$\tfrac{1}{2} U (a^2-b^2) \sin^2 \eta \sinh^2 \xi \tag{3.59}$$

The velocity components are $\underset{\sim}{u} \cdot \underset{\sim}{i}_\xi = h \psi_\eta / \varpi$, $\underset{\sim}{u} \cdot \underset{\sim}{i}_\eta = -h \psi_\xi / \varpi$, with h given by (3.11), and the elemental area dA is given by:

$$dA = 2\pi \varpi \frac{1}{h} d\eta \tag{3.60}$$

So
$$F_R = \frac{2\pi\mu}{U} \left(\frac{\omega}{2\nu}\right)^{1/2} \int_0^\pi \frac{h}{\varpi} \psi_\xi^2 \, d\eta \tag{3.61}$$

Now (3.58), (3.59) and (3.61) are combined and (ξ,η) are replaced by (x,y) as follows:

$$\psi = \frac{\frac{1}{2}U a^2 d^2}{bd - a^2\cot^{-1}x_0}\left[x - (1+x^2)\cot^{-1}x\right] - \frac{1}{2}U d^2(1+x^2)(1-y^2) \qquad (3.62)$$

$$\int_0^{\pi} \cdots d\eta = \int_{-1}^{1} \cdots \frac{dy}{(1-y^2)^{1/2}} \qquad (3.63)$$

$$\psi_\xi = (1+x^2)^{1/2}\psi_x = (1+x^2)^{1/2}\left\{\frac{\frac{1}{2}Ua^2d^2}{bd - a^2\cot^{-1}x_0}(2 - 2x\cot^{-1}x) - U d^2 x\right\}(1-y^2) \qquad (3.64)$$

So

$$F_R = \frac{2\pi\mu}{U}\left(\frac{\omega}{2\nu}\right)^{1/2}(1+x_0^2)\left[\frac{U a^2d^2}{bd - a^2\cot^{-1}x_0}(1 - x_0\cot^{-1}x_0) - Ud^2x_0\right]^2 \frac{1}{d^2}\int_{-1}^{1}(1-y^2)^2\frac{(x_0^2+y^2)^{\frac{1}{2}}}{(1+x_0^2)^{1/2}(1-y^2)^{1/4}(1-y^2)^{1/2}}\frac{dy}{(1-y^2)^{1/2}} \qquad (3.65)$$

$$= 2\pi\mu U a^2\left(\frac{\omega}{2\nu}\right)^{1/2}(1+x_0^2)\left[\frac{ad}{bd - a^2\cot^{-1}x_0}(1 - x_0\cot^{-1}x_0) - \frac{d}{a}x_0\right]^2 \int_{-1}^{1}\frac{(1-y^2)}{(x_0^2+y^2)^{1/2}}\,dy \qquad (3.66)$$

The integral in (3.66) is evaluated with the help of Gradshteyn & Ryzhik (1980) to give:

$$\int_{-1}^{1}\frac{(1-y^2)dy}{(x_0^2+y^2)^{1/2}} = (2+x_0^2)\coth^{-1}(1+x_0^2)^{\frac{1}{2}} = (2+x_0^2)\sinh^{-1}\left(\frac{1}{x_0}\right) \qquad (3.67)$$

So $$F_R = 2\pi\mu U a^2\left(\frac{\omega}{2\nu}\right)^{1/2}(1+x_0^2)^{1/2}\left[\frac{(1+x_0^2)^{1/4}(1 - x_0\cot^{-1}x_0)}{x_0 - (1+x_0^2)\cot^{-1}x_0} - \frac{x_0}{(1+x_0^2)^{1/2}}\right]^2 \times$$

$$\times\left[(2+x_0^2)\sinh^{-1}\left(\frac{1}{x_0}\right) - (1+x_0^2)^{1/2}\right] \qquad (3.68)$$

and $$F_1 = -\frac{\sqrt{2}}{|\lambda|}F_R \qquad (3.69)$$

We can find the added mass force on an oblate spheroid from Green (1833) to be:

$$\lambda^2 F_2 = -\frac{4}{3}\pi\frac{a}{b}\frac{(1+x_0^2)(1 - x_0\cot^{-1}x_0)}{(1+x_0^2)x_0\cot^{-1}x_0 - x_0^2}Upa^2 \qquad (3.70)$$

Clearly the first order correction F_1 given by (3.68) and (3.69) is not the same as that obtained for low frequencies (3.54) in part (a).

(c) nearly spherical body

For a spherical body, we have the classical result (3.1) of Stokes (1851) from which the time-dependence is separated to give

$$F = -6\pi\mu Ua\,(1+\lambda+\tfrac{1}{9}\lambda^2). \qquad (3.71)$$

This indicates that the F_1 terms for low and high frequency as calculated in parts (a) and (b) of this section must be equal when the body is spherical. It is interesting to see now the behaviour deviates when the body is not quite spherical. In part (c) we will use b for the characteristic length scale, since this simplifies the algebra a little.

We consider a spheroid with semi-minor axis $a = b(1+\epsilon)$ and use spherical coordinates (r,θ) with $\zeta = \cos\theta$. Then the surface of the body is given by

$$r = r_0(\zeta) = 1 + \epsilon 2 S_2(\zeta) + \epsilon^2 3(S_2^2(\zeta) - S_2(\zeta)) + O(\epsilon^3) \qquad (3.72)$$

where $S_n(\zeta)$ is the Gegenbauer Polynomial of order n. Since $\epsilon \ll 1$, it is convenient to move the boundary conditions from $r = r_0$ to $r = 1$ by expanding ψ and ψ_r in Taylor series about $r = 1$ and retaining terms up to $O(\epsilon^3)$. We also write ψ as a power series in ϵ,

$$\psi(r,\zeta;\epsilon) = \psi_0(r,\zeta) + \epsilon\psi_1(r,\zeta) + \epsilon^2\psi_2(r,\zeta) + O(\epsilon^3) \tag{3.73}$$

Then we have a set of boundary value problems for the ψ_i.

$$E^2(E^2-\lambda^2)\psi_i = 0, \qquad i = 0,1,2 \tag{3.74}$$

$$\text{as } r \to \infty: \qquad \psi_i \to 0, \quad i = 0,1,2 \tag{3.75}$$

The boundary conditions on r = 1 are:

$$\psi_0 = -S_2(\zeta), \qquad \psi_{0r} = -2S_2(\zeta) \tag{3.76}$$

$$\psi_1 = 0, \qquad \psi_{1r} = -2S_2(\zeta)\psi_{0rr} \tag{3.77}$$

$$\psi_2 = 4S_2^3(\zeta) + 2S_2^2(\zeta)\psi_{0rr} \tag{3.78}$$

$$\psi_{2r} = -2S_2(\zeta)\psi_{1rr} - [6S_2^2 - 3S_2]\psi_{0rr} - 2S_2^3\psi_{0rrr} - 12S_2^3 + 6S_2^2 \tag{3.79}$$

These equations can be simplified using the recurrence relation for $m \geq 2$

$$S_m S_2 = -\frac{(m-2)(m-3)}{2(2m-1)(2m-3)}S_{m-2} + \frac{m(m-1)}{(2m+1)(2m-3)}S_m - \frac{(m+1)(m+2)}{2(2m-1)(2m+1)}S_{m+2} \tag{3.80}$$

Then suitable forms for the ψ_i are:

$$\psi_i(r,\zeta) = \sum_{n=0}^{i} S_{2(n+1)}(\zeta) f_{2(n+1)}^{(i)}(r) \tag{3.81}$$

The functions $f_{2n}^{(i)}(r)$ come from Basset's (1888) work, equations (2.80) (2.81) and may be written:

$$f_2^{(i)}(r) = A_2^{(i)}\frac{1}{r} + B_2^{(i)}e^{-\lambda(r-1)}\left(1+\frac{1}{\lambda r}\right), \quad i = 0,1,2 \tag{3.82}$$

$$f_4^{(i)}(r) = A_4^{(i)}\frac{1}{r^3} + B_4^{(i)}e^{-\lambda(r-1)}\left(1+\frac{6}{\lambda r}+\frac{15}{\lambda^2 r^2}+\frac{15}{\lambda^3 r^3}\right) \tag{3.83}$$

The functions $f_4^{(2)}$ and $f_6^{(2)}$ make no contribution to the force up to order ϵ^2, and we shall not need them. The boundary conditions (3.76)-(3.79) simplify to:

$$\text{on } r=1: \quad f_2^{(0)} = -1, \quad f_{2r}^{(0)} = -2 \tag{3.84}$$

$$f_2^{(1)} = 0, \quad f_{2r}^{(1)} = -\frac{4}{5}\left(f_{2rr}^{(0)} + 2\right) \tag{3.85}$$

$$f_4^{(1)} = 0, \quad f_{4r}^{(1)} = \frac{4}{5}\left(f_{2rr}^{(0)} + 2\right) \tag{3.86}$$

$$f_2^{(2)} = \frac{12}{35}\left(f_{2rr}^{(0)} + 2\right) \tag{3.87}$$

$$f_{2r}^{(2)} = -\frac{4}{5}f_{2rr}^{(1)} + \frac{2}{25}f_{4rr}^{(1)} + \frac{6}{35}\left(f_{2rr}^{(0)} + 2\right) - \frac{12}{35}f_{2rrr}^{(0)} \tag{3.88}$$

Equations (3.84)-(3.88) are used to obtain the coefficients $A_2^{(i)}$ as follows:

$$A_2^{(0)} = -\left(1 + \frac{3}{\lambda} + \frac{3}{\lambda^2}\right) \tag{3.89}$$

$$A_2^{(1)} = -\frac{12}{5}\left(1 + \frac{1}{\lambda}\right)^2 \tag{3.90}$$

$$A_2^{(2)} = -\frac{6}{175}\left(53 + \frac{58}{\lambda} + \frac{1}{\lambda^2}\right) - \frac{24}{175}\,\frac{1}{3+3\lambda+\lambda^2} \tag{3.91}$$

The force on the spheroid is given by (3.21) in which

$$\lim_{r\to\infty} \frac{r^3\psi}{\varpi^2} = \frac{1}{2}A_2 = \frac{1}{2}\sum_0^2 A_2^{(i)}\epsilon^i \tag{3.92}$$

and

$$V = \frac{4}{3}\pi\left(1+\epsilon^2\right) \tag{3.93}$$

So we have

$$F = -6\pi\left[\left(1+\lambda+\tfrac{1}{9}\lambda^2\right) + \epsilon\tfrac{4}{5}\left(1+2\lambda+\tfrac{4}{9}\lambda^2\right) + \epsilon^2\tfrac{2}{175}\left(1+58\lambda+\tfrac{302}{9}\lambda^2 + \frac{4\lambda^2\epsilon^2}{3+3\lambda+\lambda^2}\right)\right] \tag{3.94}$$

$$= -6\pi\left[\left(1+\tfrac{4}{5}\epsilon+\tfrac{2}{175}\epsilon^2\right) + \lambda\left(1+\tfrac{8}{5}\epsilon+\tfrac{116}{175}\epsilon^2\right) + \tfrac{1}{9}\lambda^2\left(1+\tfrac{16}{15}\epsilon+\tfrac{604}{175}\epsilon^2\right) + \tfrac{8}{175}\frac{\lambda^2\epsilon^2}{3+3\lambda+\lambda^2}\right] \tag{3.95}$$

The final term of (3.94) and (3.95) is $O(1)$ when λ is large and $O(\lambda^2)$ when λ is small. Hence the equality of the first order corrections F_1 of parts (a) and (b) persists until $O(\epsilon^3)$. The nonquadratic term $\frac{8}{175}\frac{\lambda^2\epsilon^2}{3+3\lambda+\lambda^2}$ is always very small and is unimportant for practical purposes. However, it will be seen that for a general spheroid the term becomes more important.

3.4 FULL SOLUTION IN SPHEROIDAL HARMONICS

The governing equation (3.23) may be factored to give:

$$E^2(E^2-c^2)\psi = 0 \qquad (3.96)$$

This in turn has a solution made up of two parts:

$$\psi = \psi^P + \psi^D \qquad (3.97)$$

The first part ψ^P is a potential function and must satisfy the equation

$$E^2\,\psi^P = 0 \qquad (3.98)$$

The second part ψ^D is a diffusive function and satisfies

$$(E^2-c^2)\,\psi^D = 0 \qquad (3.99)$$

The inhomogeneous terms generated may be absorbed in ψ^P. It is simpler to treat the two components separately as far as is possible and combine them at the end.

(a) solution for ψ^p

The governing equation (3.98) is linear and there are several homogeneous boundary conditions, so this is an eigenvalue problem and we expect the solution to be a superposition of harmonics of the form $X^p(x)Y^p(y)$. The differential equation separates to give:

$$(1-y^2)\,Y^{p\prime\prime} + k^2 Y^p = 0 \qquad (3.100)$$

$$(1+x^2)\,X^{p\prime\prime} - k^2 X^p = 0 \qquad (3.101)$$

We have chosen the separation constant k^2 to be positive in the y-direction so as to get wave-like solutions there. We impose homogeneous boundary conditions:

$$\text{on } y = \pm 1 : \quad Y^p = 0, \quad Y^{p\prime} \text{ is finite} \qquad (3.102)$$

although these can only be applied rigorously to the sum of ψ^p and ψ^b. The conditions (3.102) are not necessary; however, they are certainly sufficient to satisfy the correct conditions (3.20), assuming that the uniqueness theorem for steady Stokes flow may be extended to cover the time-dependent case. The functions X^p and Y^p may be written as Gegenbauer functions as in Sampson (1891), but it is more convenient to write them in terms of Legendre functions. We set $Y^p = (1-y^2)^{\frac{1}{2}}\, I^p(y)$, then:

$$I^{p\prime\prime}(1-y^2) - 2yI^{p\prime} + \left(k^2 - \frac{1}{1-y^2}\right) I^p = 0 \qquad (3.103)$$

Equation (3.103) is Legendre's equation of order 1 and degree n with $k_n^2 = n(n+1)$. The regular solutions are Legendre polynomials $P_n^1(y)$, so we have eigensolutions:

$$Y_n^p = (1-y^2)^{1/2} P_n^1(y), \qquad K_n^2 = n(n+1), \quad n=1,2,3,... \tag{3.104}$$

To find the solutions for X^p, we introduce $\chi = ix$, then:

$$(1-\chi^2)X^{p\prime\prime} + k^2 X^p = 0, \quad X^p \to 0 \text{ as } \chi \to i\infty \tag{3.105}$$

Equation (3.105) is the same as (3.100) for Y, but we now require the solution to decay at infinity. Magnus, Oberhettinger & Soni (1966) give the behaviour of Legendre functions for large argument. In particular

$$\text{as } \chi \to \infty, \quad Q_n^1(\chi) \sim \frac{-(n+1)!}{\chi^{n+1}(2n+1)!!} \tag{3.106}$$

Thus for $n \geq 1$,

$$(1-\chi^2)^{1/2} Q_n^1(\chi) \longrightarrow 0 \text{ as } \chi \to \infty \tag{3.107}$$

So we have solutions for the X_n^p for $n \geq 1$:

$$X_n^p = (1-\chi^2)^{1/2} Q_n^1(\chi) = (1+x^2)^{1/2} Q_n^1(ix) \tag{3.108}$$

The general solution for ψ^p which satisfies the homogeneous boundary conditions is thus:

$$\psi^p = (1-y^2)^{1/2}(1+x^2)^{1/2} \sum_{n=1}^{\infty}{}' A_n P_n^1(y) Q_n^1(ix) \tag{3.109}$$

We may enforce fore-and-aft symmetry by setting $A_n = 0$ for even values of n, since for these values P_n^1 is an odd function. Then we have

$$\psi^a = (1-y^2)^{1/2}(1+x^2)^{1/2} \sum_{n=1}^{\infty}{}' A_n P_n^1(y)\, Q_n^1(ix) \qquad (3.110)$$

Here Σ' indicates that only alternate values of n are included in the sum.

(b) solution for ψ^b

Equation (3.99) can be written in the form:

$$(1+x^2)\psi^b_{xx} + (1-y^2)\psi^b_{yy} - c^2(x^2+y^2)\psi^b = 0 \qquad (3.111)$$

This is separable in the form $X^b(x)Y^b(y)$ and yields the following ordinary differential equations.

$$(1+x^2)X^{b\prime\prime} - (\lambda + c^2x^2)X^b = 0 \qquad (3.112)$$

$$(1-y^2)Y^{b\prime\prime} + (\lambda - c^2y^2)Y^b = 0, \quad Re\{\lambda\} > 0 \qquad (3.113)$$

The eigenfunctions Y_n^b and eigenvalues λ_n are quite different from those in part (a), but the solution is found in the same way (Stratton et al 1941). We let $Y^b = (1-y^2)^{1/2}\mathcal{Y}^b$, then

$$(1-y^2)\mathcal{Y}^{b\prime\prime} - 2y\mathcal{Y}^{b\prime} + \left[\lambda - c^2y^2 - \frac{1}{1-y^2}\right]\mathcal{Y}^b = 0 \qquad (3.114)$$

Equation (3.114) is the spheroidal wave equation. The solutions which are regular at the poles are given in Flammer (1957) to be the <u>prolate</u> angle spheroidal wave functions of the first kind of order 1 and degree n.

$$Y_n^D = S_{1n}(c,y) \qquad n=1,2,3 \tag{3.115}$$

The S_{1n} are defined in terms of series of Legendre polynomials

$$S_{1n}(c,y) = \sum_{r=0,1}^{\infty}{}' d_r^{1n}(c) P_{1+r}^1(y) \tag{3.116}$$

In equation (3.116), the sum starts at zero if n is odd and at one if n is even. Since S_{1n} has the same parity as P_n^1, we will only require the functions for which n is odd. The $d_r^{1n}(c)$ and $\lambda_{1n}(c)$ are determined by a complicated procedure which is described in the Appendix. So we have our eigenfunctions,

$$Y_n^D = (1-y^2)^{1/2} S_{1n}(c,y) \qquad n=1,3,5,\ldots \tag{3.117}$$

The X_n^D are found by introducing $\chi = ix$, when (3.112) becomes identical to (3.113). Thus X^D can also be written in terms of spheroidal wave functions. The radial functions are proportional to the angle functions and Flammer (1957) gives the behaviour for large arguments. In particular,

$$\text{as } c\chi \to \infty, \quad R_{1n}^{(3)}(c,\chi) \longrightarrow \frac{1}{c\chi} e^{i[c\chi - \frac{1}{2}(n+1)\pi]} \tag{3.118}$$

Thus X_n^D can be written in terms of the radial spheroidal wave functions of the third kind.

$$X_n^D = (1-\chi^2)^{1/2} R_{1n}^{(3)}(c,\chi) = (1+x^2)^{1/2} R_{1n}^{(3)}(c,ix) \tag{3.119}$$

Finally, we may write the general solution for ψ^D which satisfies the homogeneous conditions as:

$$\psi^D = (1-y^2)^{1/2}(1+x^2)^{1/2} \sum_{n=1}^{\infty}{}' B_n S_{1n}(c,y) R_{1n}^{(2)}(c,ix) \qquad (3.120)$$

(c) inhomogeneous conditions

Before we apply the inhomogeneous conditions (3.24), we must sum the two components of the solution from (a) and (b). The stream function is

$$\psi = (1-y^2)^{1/2}(1+x^2)^{1/2} \sum_{n=1}^{\infty}{}' \left[A_n P_n^1(y) Q_n^1(ix) + B_n S_{1n}(c,y) R_{1n}^{(3)}(c,ix) \right] \qquad (3.121)$$

This satisfies the requirements of symmetry, evanescence at infinity and regularity at the poles. The coefficients A_n and B_n are to be determined from (3.24) which gives:

$$\sum_{n=1}^{\infty}{}' \left[A_n P_n^1(y) Q_n^1(ix_0) + B_n S_{1n}(c,y) R_{1n}^{(3)}(c,ix_0) \right] = -\tfrac{1}{2}(1+x_0^2)^{1/2}(1-y^2)^{1/2} \qquad (3.122)$$

$$\sum_{n=1}^{\infty}{}' \left[A_n P_n^1(y) D Q_n^1(ix_0) + B_n S_{1n}(c,y) D R_{1n}^{(3)}(c,ix_0) \right] = -x_0(1-y^2)^{1/2} \qquad (3.123)$$

The differential operator D is defined by:

$$D f(\chi) = \frac{d}{d\chi}(\chi^2-1)^{1/2} f(\chi) \qquad (3.124)$$

so

$$D f(ix) = \frac{d}{dx}(x^2+1)^{1/2} f(ix) \qquad (3.125)$$

At this point, it is convenient to note some of the properties of the functions $P_n^1(y)$ and $S_{1n}(c,y)$. Abramowitz & Stegun (1965) give the definitions:

$$P_n'(y) = -(1-y^2)^{1/2}\frac{d}{dy}P_n(y) \tag{3.126}$$

$$P_1(y) = y, \quad P_2(y) = \tfrac{1}{2}(3y^2-1), \text{ etc.} \tag{3.127}$$

So we can determine

$$P_1'(y) = -(1-y^2)^{1/2}, \quad P_2'(y) = -3y(1-y^2)^{1/2}, \text{ etc.} \tag{3.128}$$

The orthogonality relation

$$\int_{-1}^{1} P_m'(y)P_n'(y)dy = \delta_{mn}\frac{2n(n+1)}{2n+1} \tag{3.129}$$

is used to determine for n odd

$$\int_{-1}^{1} P_m'(y)S_{in}(c,y)dy = \sum_{r=0}^{\infty}{}' d_r^{in}(c)\int_{-1}^{1} P_m'(y)P_{1+r}'(y)dy \tag{3.130}$$

$$= d_{m-1}^{in}(c)\frac{2m(m+1)}{2m+1} \tag{3.131}$$

and finally,

$$\int_{-1}^{1} P_m'(y)(1-y^2)^{1/2} = -\int_{-1}^{1} P_m'(y)P_1'(y)dy = -\frac{4}{3}\delta_{m1} \tag{3.132}$$

Now we multiply (3.122), (3.123) by $P_m'(y)$ and integrate from $y = -1$ to $y = 1$, making use of the orthogonality relations (3.129)-(3.132). this gives:

$$A_m Q_m'(ix_0)\frac{2m(m+1)}{2m+1} + \sum_{n=1}^{\infty}{}' B_n R_{1n}^{(3)}(c,ix_0)d_{m-1}^{in}(c)\frac{2m(m+1)}{2m+1} = \frac{2}{3}(1+x_0^2)^{1/2}\delta_{1m} \tag{3.133}$$

$$A_m DQ_m'(ix_0)\frac{2m(m+1)}{2m+1} + \sum_{n=1}^{\infty}{}' B_n DR_{1n}^{(3)}(c,ix_0)d_{m-1}^{in}(c)\frac{2m(m+1)}{2m+1} = \frac{4}{3}x_0\delta_{1m} \tag{3.134}$$

We define $\bar{B}_n = B_n R_{1n}^{(3)}(c,ix_0)$ and rearrange equations (3.133), (3.134) to get:

$$A_m + \sum_{n=1}^{\infty}{}' \bar{B}_n d_{m-1}^{in}(c) / Q_m'(ix_0) = \delta_{1m}\left[\tfrac{1}{2}(1+x_0^2)^{1/2}/Q_m'(ix_0)\right] \tag{3.135}$$

$$A_m + \sum_{n=1}^{\infty}{}' \bar{B}_n d^{1n}_{m-1}(c) \frac{DR^{(3)}_{1n}(c,ix_0)}{R^{(3)}_{1n}(c,ix_0)\, DQ'_m(ix_0)} = \delta_{1m}\left[x_0 / DQ'_m(ix_0)\right] \qquad (3.136)$$

Equations (3.135), (3.136) represent a pair of coupled infinite systems of linear equations for the coefficients A_n and $\bar{B}_n$. They are to be solved by truncation and matrix inversion as explained in the Appendix. The force is found from (3.25), so we need to find $\lim_{r\to\infty} \frac{r^2}{\varpi^2}\psi$. Equation (3.118) indicates that the terms of ψ^D decay exponentially in the far field, whereas (3.106) and (3.110) yield the dominant term,

$$\psi \sim (1-y^2)^{1/2}(1+x^2)^{1/2} A_1 P'_1(y) Q'_1(ix) \qquad (3.137)$$

$$\sim -(1-y^2)\tfrac{2}{3} A_1 x^{-1} \qquad (3.138)$$

Thus $$\lim_{r\to\infty} \frac{r^3}{\varpi^2}\psi = \lim_{r\to\infty} \frac{x^3}{x^2(1-y^2)}\psi = -\tfrac{2}{3}A_1 \qquad (3.139)$$

Finally we have

$$F = \tfrac{4}{3}\pi c^2 \left[x_0(1+x_0^2) - 2A_1\right] \qquad (3.140)$$

Thus the force on the spheroid depends only on the first coefficient A_1. However, the value of A_1 depends on all the coefficients whose values must be found by solving (3.135), (3.136) simultaneously as described in the Appendix.

(d) prolate spheroid

The prolate spheroid is a simple extension of the oblate spheroid and can be organized so as to generate exactly the same equations and the same result for the force. The geometry is as shown in figure 3.1(b), with $b > a$ and $e^2 = b^2 - a^2$. The coordinate transformation is slightly different in this case.

$$z = e\bar{x}y, \quad \varpi = e(\bar{x}^2-1)^{1/2}(1-y^2)^{1/2} \tag{3.141}$$

$$h = \frac{1}{e}\frac{1}{(\bar{x}^2-y^2)^{1/2}} \tag{3.142}$$

The surface coordinate is $\bar{x}_o = b/e$, with $a/e = (\bar{x}_o^2-1)^{1/2}$.

The above quantities can be made the same as for an oblate spheroid by using imaginary values of d and x. Let $e = -id$ and $\bar{x} = ix$, then:

$$z = dxy, \quad \varpi = d(x^2+1)^{1/2}(1-y^2)^{1/2} \tag{3.143}$$

$$h = \frac{1}{d(x^2+y^2)^{1/2}} \tag{3.144}$$

And the surface coordinate is $x_o = b/d$, with $a/d = (x_o^2+1)^{1/2}$. Equations (3.143)) and (3.144) are exactly the same as (3.4) and (3.11). Thus the problem reduces to that for an oblate spheroid provided we allow $d = (a^2-b^2)^{1/2}$ to become imaginary and $x_o = b/d$ to be negative imaginary. The parameter c will have the same definition as before, viz $c^2 = -id^2\omega/\nu$, but c will now have phase $+\pi/4$. Some care must be taken in

determining the sign of square roots like $(1+x_0^2)^{\frac{1}{2}}$, but otherwise, the extension presents no difficulty. The results of sections 3.3(a),(b),(c) and section 3.4 all carry over to the prolate case.

3.5 RESULTS AND DISCUSSION

Several different length scales have been used in the preceding sections, so we must first unify the results. The most important length scale is a, the radius perpendicular to the motion, and this will be used from now on. We will use the most appropriate force scale which is the Stokes drag on a sphere, $6\pi\mu Ua$. The frequency parameter to be used is $\lambda = (1-i)a\sqrt{(\omega/2\nu)}$ or $|\lambda| = a\sqrt{(\omega/\nu)}$.

The results of the full calculation are plotted as solid lines in figure 3.2. As can be seen, the results are qualitatively similar to those for a sphere, b/a = 1. At low frequencies, the real part of the force dominates and is almost independent of $|\lambda|$; this is the quasi-steady Stokes drag. The imaginary part of the force is small and linear with $|\lambda|$, representing a slight phase shift. At high frequency, the imaginary part of the force varies with $|\lambda|$ and is dominant; thus the phase is 90°. The real part of the force is important because it results in energy dissipation which, for example, accounts for the damping of an oscillating pendulum. It can be seen that the change in

the nature of the force from quasi-steady Stokes flow to near potential flow occurs as $|\lambda|$ changes from about 0.1 to about 100. Unfortunately, as discussed in the Appendix, useful results could be obtained for oblate spheroids only for $|\lambda| < 10$ and for prolate spheroids only for $|\lambda| b/a < 10$. The asymptotic result of section 3.3(b) may be regarded as accurate only for $|\lambda| > 100$, so there remains a gap in which the results are not known accurately. The broken lines of figure 3.2 represent a correlation based on a "patching" of the two asymptotic solutions of sections 3.3(a) and (b) with numerical coefficients determined from the full solution. To help distinguish the curves, the real part of the correlated force is shown dotted and the imaginary part is shown dashed. The derivation of this correlation will be described below.

The asymptotic results are summarized by figure 3.3. Here the components of the force are plotted as functions of the aspect ratio; for the sake of comparison a value of $|\lambda| = 10$ is used. The important feature is the touching of the curves representing the low- and high-frequency first order corrections at $b/a = 1$. As predicted in section 3.3(c), these curves have the same slope and curvature at $b/a = 1$ and they remain close to each other in the range $0.1 < b/a < 10$. It seems reasonable then to represent the force in the following way:

$$F = F_s - m_a \lambda^2 - B(\lambda)\lambda \qquad (3.145)$$

In (3.145), F_s is the Stokes drag, m_a is the added mass of the body and B will be called the Basset coefficient. Clearly, at low frequency $B(\lambda)$ is given by the first order correction of section 3.2(a), B_0 say, and at high frequency by the first order correction of section 3.2(b), B_∞ say. For aspect ratios of order unity, B_0 and B_∞ are quite close, so the form of (3.145) is quite promising. In fact, we shall see later that it is more useful to split the third term of (3.145) into two parts. The asymptotic results are summarized below.

$$F_s = -\frac{4}{3}\left[x_0 - (x_0^2 - 1)\cot^{-1} x_0\right]^{-1} \tag{3.146}$$

$$m_a = \frac{2}{9}(1+x_0^2)^{\frac{1}{2}} \frac{1 - x_0 \cot^{-1} x_0}{x_0 - (1+x_0^2)\cot^{-1} x_0} \tag{3.147}$$

$$B_0 = F_s^2 \tag{3.148}$$

$$B_\infty = \left[\frac{x_0}{(1+x_0^2)^{\frac{1}{2}}} - \frac{9}{2} m_a\right]^2 \frac{1}{3}(1+x_0^2)\left[1 - (2+x_0^2)(1+x_0^2)^{\frac{1}{2}} \sinh^{-1}\frac{1}{x_0}\right] \tag{3.149}$$

Care must be taken in choosing the sign of $(1+x_0^2)^{\frac{1}{2}}$ for a prolate spheroid when x_0 is imaginary.

Using (3.145) for the definition, B can be calculated from the exact results, as far as they are known, and some examples are shown in figures 3.4, 3.5(a), (b), (c), (d), (e), (f). Figure 3.4 shows the phase of the Basset force, $B(\lambda)\lambda$ for a few values of b/a. For a sphere, the phase is exactly 45° and even for b/a = 10, the phase never deviates by more than 3°. The deviation is always contained in the

region $0.1 < |\lambda| < 10$ and is always small. We can infer that $B(\lambda)$ is "almost real", but we will not take it to be real in the correlation. The amplitude of B is shown in figures 3.5 which also give an indication of the effect of the phase shift. The real and imaginary parts of $B(\lambda)\lambda/|\lambda|$ are plotted for different values of aspect ratio. These figures suggest that B changes smoothly from B_0 to B_∞ as the frequency increases, the imaginary part changing at slightly lower frequency. There is a slight overshoot, which is more apparent for aspect ratios closer to unity since B_0 and B_∞ are then closer to each other, but this does not appear to be significant. The dotted lines in figures 3.5 are simply scaled versions of the hyperbolic tangent function which will be used as an approximation for $B(\lambda)$. We take B to have the form:

$$B(\lambda) = \tfrac{1}{2}(B_0+B_\infty) + \tfrac{1}{2}(B_\infty-B_0)\tanh[\alpha(\log\lambda-\log\lambda_0)] \qquad (3.150)$$

The form of (3.150) is reasonable in view of the shape of the curves in figures 3.5(a)-(f), the small phase shift of figure 3.4 and the fact that B_0 and B_∞ are quite close. Equation (3.150) can be simplified since

$$\tanh[\alpha(\log\lambda-\log\lambda_0)] = \frac{\left(\frac{\lambda}{\lambda_0}\right)^{\alpha}-\left(\frac{\lambda}{\lambda_0}\right)^{-\alpha}}{\left(\frac{\lambda}{\lambda_0}\right)^{\alpha}+\left(\frac{\lambda}{\lambda_0}\right)^{-\alpha}} \qquad (3.151)$$

So we have

$$B(\lambda) = \frac{B_0+B_\infty\left(\frac{\lambda}{\lambda_0}\right)^{2\alpha}}{1+\left(\frac{\lambda}{\lambda_0}\right)^{2\alpha}} = B_\infty + \frac{B_0-B_\infty}{\left(1+\frac{\lambda}{\lambda_0}\right)^{2\alpha}} \qquad (3.152)$$

By a happy coincidence, this form of $B(\lambda)$ has the same type of phase shift as the exact solution as can be observed in figure 3.4, where the phase shift of (3.152) is shown dotted. Suitable values of α and λ_0 are to be obtained from the full theory, i.e. the solid lines of figures 3.5, in the following way.

When $|\lambda| = \lambda_0$ and $\lambda = \lambda_0 e^{-i\pi/4}$, (3.150) simplifies since

$$\tanh[\alpha(\log\lambda - \log\lambda_0)] = \tanh[\alpha \log(e^{-i\pi/4})] = \tanh(-i\tfrac{\alpha\pi}{4}) = -i\tan\tfrac{\alpha\pi}{4} \qquad (3.153)$$

So we have:

$$B(\lambda_0 e^{-i\pi/4}) = \tfrac{1}{2}(B_0+B_\infty) - \tfrac{1}{2}(B_0-B_\infty) i \tan\tfrac{\alpha\pi}{4} \qquad (3.154)$$

Thus in figure 3.5 when $|\lambda| = \lambda_0$,

$$Re\{B e^{-i\pi/4}\} = \tfrac{1}{2\sqrt{2}}\left[(B_0+B_\infty) - (B_0-B_\infty)\tan\tfrac{\alpha\pi}{4}\right] \qquad (3.155)$$

and

$$-Im\{B e^{-i\pi/4}\} = \tfrac{1}{2\sqrt{2}}\left[(B_0+B_\infty) + (B_0-B_\infty)\tan\tfrac{\alpha\pi}{4}\right] \qquad (3.156)$$

Thus, λ_0 is the value of $|\lambda|$ where the two curves are equidistant from the center-line $B = \frac{1}{2}(B_0+B_\infty)/\sqrt{2}$, and α is found from:

$$\alpha = \tfrac{4}{\pi}\tan^{-1}\left[\frac{-Im\{B e^{-i\pi/4}\} - Re\{B e^{-i\pi/4}\}}{(B_0-B_\infty)/\sqrt{2}}\right] \qquad (3.157)$$

The values obtained are displayed in table 3.1. At this point, it is convenient to re-write (3.145) as a four term correlation,

$$F = F_s - m_a\lambda^2 - B_\infty\lambda - \left[\frac{B_0-B_\infty}{1+(\frac{\lambda}{\lambda_0})^{2\alpha}}\right]\lambda \qquad (3.158)$$

b/a	0.1	0.2	0.5	1	2	5	10
λ_0	6.07	2.86	0.84	-	3.60	1.12	0.59
α	0.394	0.464	0.636	-	0.687	0.543	0.494

Table 3.1. Values of λ_0 and α for the correlation equation.

The approximations to $B(\lambda)$ derived from table 3.1 and equation (3.152) are shown as dotted lines in figures 3.4 and 3.5, and the corresponding force (3.158) is shown as broken lines in figure 3.2.

The least accurate behaviour of the correlation is at intermediate frequencies and large aspect ratios. From figure 3.5(f) we see that with b/a = 10 and $|\lambda| = 0.1$, the discrepancy in $\Im m\{B\}$ is about 0.5%; the largest error in $\Re e\{B\}$ is 0.1% at $|\lambda| = 5$. This is very satisfactory considering the complicated nature of the exact calculation and the simple form of the correlation (3.158). Figure 3.5 suggests that the values of α in table 3.1 may be a little too small. The accuracy of the correlation might be improved if another method were used to choose the values of λ_0 and α. However, there is no obvious alternative method since any other would be much more cumbersome, so no improvement will be attempted.

A very useful property of the correlation is that (3.158) may be integrated over all frequencies to provide an inverse Laplace transform of the problem (at least for some values of α); i.e. we can find the Basset force for an an arbitrary time-dependent velocity and this will be done in the next section.

Another interesting feature of the results may be observed in figure 3.3. We can now regard the two touching curves for the linear corrections as representative of the sum of the Basset force and the new force. When the aspect ratio is large, we see that the added mass is small, since the body is "streamlined", whereas the Stokes drag and Basset force increase with the length of the body. We can conclude, therefore, that for long bodies at moderately high frequencies the Basset force is the dominant one. Although the phase of $B(\lambda)$ may vary considerably from 45° for a long body, examination of the trends in table 3.1 suggests that the phase shift is confined to low frequencies when the body is long. These considerations are illustrated in figure 3.6 where the asymptotes for the forces are shown as a function of frequency for a few aspect ratios. Clearly for a body with aspect ratio 100, the Basset force is the dominant one over the range $1 < |\lambda| < 1000$.

The above discussion leads us to expect that long bodies exhibit three distinct types of behaviour depending

on the frequency of oscillation. At very low frequency, the flow is essentially quasi-steady in the neighborhood of the body and the force is dominated by the steady Stokes drag. At very high frequencies, the potential flow limit is virtually reached and the force is dominated by the virtual mass term. There is a third region of simple behaviour in which the flow is locally two-dimensional near the body, the ends of the body and the far field being relatively unimportant, and the force is dominated by the Basset force. Such flows have been discussed by Batchelor (1955). The boundaries of the regions of different behaviour are shown in figure 3.7.

3.6 INVERSION OF THE LAPLACE TRANSFORM

If we consider the force on the spheroid in arbitrary motion with velocity W(t), then the differential equation for $\Psi(r,t)$ is

$$E^4\Psi - E^2\Psi_t = 0 \qquad (3.159)$$

We now define a Laplace transform over time

$$\mathcal{L}[f(t)] = \bar{f}(s) = \int_0^\infty e^{-st} f(t)\,dt \qquad (3.160)$$

so that $\bar{\Psi}(r,s)$ satisfies the equation

$$E^4\bar{\Psi} - sE^2\bar{\Psi} = \Psi(r,0) \qquad (3.161)$$

If the fluid is initially at rest, $\Psi(r,0) = 0$, so that (3.161) becomes the same as (3.20) with $\overline{\Psi}(r,s)$ replacing $\psi(r,c^2)$. If length scale a had been used from the beginning in (3.20), c^2 would be replaced by λ^2. The force on the body $\mathcal{F}_H(t)$ transforms in the same way, so the correlation (3.153) would give:

$$\overline{\mathcal{F}_H} = \left[F_s - m_a s - B_\infty s^{1/2} - \frac{B_0 - B_\infty}{z_0 + s^\alpha} z_0 s^{1/2}\right] \overline{W}(s) \qquad (3.162)$$

with $z_0 = \lambda_0^{2\alpha}$. The Laplace transform may be inverted to give:

$$\mathcal{F}_H(t) = F_s W(t) - \frac{1}{\sqrt{\pi}} B_\infty \int_0^t \frac{dW}{d\tau}(t-\tau)^{-1/2} d\tau - m_a \frac{dW}{dt}$$

$$- (B_0 - B_\infty) \int_0^t \frac{dW}{d\tau} G(t-\tau) d\tau \qquad (3.163)$$

In equation (3.163) and what follows, the time is made dimensionless using the viscous diffusion time a^2/ν. The first three terms of (3.163) are the analogue of Basset's (1888) result for a sphere, with the Basset force given by the high frequency limit of $B(\lambda)$, viz B_∞. The fourth term has no analogy for the case of a sphere, since then $B_0 - B_\infty = 0$, and this new term will be considered in detail. The memory function G(t) is much more complicated than the $t^{-1/2}$ term in the Basset force; its Laplace transform is

$$\overline{G}(s) = \frac{z_0}{s^{1/2}} \frac{1}{s^\alpha + z_0} \qquad (3.164)$$

At high frequency, $\bar{G}(s) \sim z_0 s^{-(\frac{1}{2}+\alpha)}$, so the inverse transform for small times will be $G(t) \sim z_0 [\Gamma(\frac{1}{2}+\alpha)]^{-1} t^{\alpha-\frac{1}{2}}$. In table 3.1, we see that α is positive and typically lies in the range $0.5 < \alpha < 1.0$. Thus G(t) will always have less singular behaviour for small t than does the Basset memory function $t^{-\frac{1}{2}}$, and for $\alpha \geq 0.5$ G(t) will not be singular at all. However, at large t (small frequency) $\bar{G}(s) \sim s^{-\frac{1}{2}}$, so G(t) will have the same behaviour as $t^{-\frac{1}{2}}$.

Although (3.164) is a simple function of s, its inverse transform is difficult to find in the general case. So before we proceed with the general case, we will consider the two special cases $\alpha = \frac{1}{2}$, $\alpha = 1$, where the transform is tabulated. In these cases the inverse transforms are (Oberhettinger & Badii 1973):

$$\alpha = \tfrac{1}{2}: \quad G_{\frac{1}{2}}(t) = e^{z_0^2 t} \operatorname{erfc}(z_0 t^{\frac{1}{2}})\, z_0 \tag{3.165}$$

$$\alpha = 1: \quad G_1(t) = (-z_0)^{\frac{1}{2}} e^{-z_0 t} \operatorname{erf}[(-z_0 t)^{\frac{1}{2}}] \tag{3.166}$$

The first of these is related to the function called w(z) by Abramowitz & Stegun (1965). w(z) is given in terms of a power series in z and asymptotic inverse power series, and we get:

$$G_{\frac{1}{2}}(t) = z_0\, w(i z_0 t^{\frac{1}{2}}) = \sum_{n=0}^{\infty} z_0 \frac{(-z_0 t^{\frac{1}{2}})^n}{\Gamma(\frac{n}{2}+1)} \tag{3.167}$$

and as $t \to \infty$, $$G_{\frac{1}{2}}(t) \sim \frac{1}{\sqrt{\pi t}} \left[1 + \sum_{m=1}^{\infty} (-1)^m \frac{1.3\ldots(2m-1)}{(2z_0^2 t)^m}\right] \tag{3.168}$$

The second function (3.166) is not dignified with a symbol. In this case $\alpha = 1$, so $z_0 = \lambda_0^2$ and Abramowitz & Stegun give:

$$G_1(t) = \frac{z_0 2 t^{1/2}}{\sqrt{\pi}} \sum_{n=0}^{\infty} \frac{2^n}{1.3\ldots(2n-1)} (-z_0 t)^n \qquad (3.169)$$

which may be rearranged to give:

$$G_1(t) = z_0 t^{1/2} \sum_{n=0}^{\infty} \frac{(-z_0 t)^n}{\Gamma(n+\frac{3}{2})} \qquad (3.170)$$

The inverse transform of $\bar{G}_\alpha(s)$ is not tabulated for arbitrary values of α, but it can be found quite easily by the following nonrigorous method. We write $\bar{G}(s)$ from (3.164) in the form

$$\bar{G}(s) = z_0 s^{-\frac{1}{2}-\alpha} (1 + z_0 s^{-\alpha})^{-1} \qquad (3.171)$$

Now whenever $|s| > |z_0|^{1/2}$, we can expand the binomial as a convergent power series:

$$\bar{G}(s) = -\sum_{n=0}^{\infty} (-z_0)^{n+1} s^{-[(n+1)\alpha+\frac{1}{2}]} \qquad (3.172)$$

This form of the Laplace transform $\bar{G}(s)$ can easily be inverted to give a power series which should be valid at least for small values of t.

$$G_\alpha(t) = -\sum_{n=0}^{\infty} (-z_0)^{n+1} t^{(n+1)\alpha-\frac{1}{2}} / \Gamma[(n+1)\alpha+\tfrac{1}{2}] \qquad (3.173)$$

$$\text{i.e.} \quad G_\alpha(t) = z_0 t^{\alpha-\frac{1}{2}} \sum_{n=0}^{\infty} \frac{(-z_0 t^\alpha)^n}{\Gamma[(n+1)\alpha+\frac{1}{2}]} \qquad (3.174)$$

The power series (3.174) is uniformly convergent when $\alpha > 0$, which enhances its chances of being reliable. More

importantly, it reduces to the forms of (3.167), (3.170) when $\alpha = \frac{1}{2}$ or 1, which suggests that it is satisfactory. An additional benefit is that G(t) is real which is not genarally true when $\bar{G}(s)$ is only an approximation, and is a consequence of the form of the correlation (3.158). If we substitute $z_0 = \lambda^{2\alpha}$ in (3.174), we get the final form:

$$G_\alpha(t) = t^{-1/2} \sum_{n=1}^{\infty} \frac{(-1)^{n+1} (\lambda_0^2 t)^{\alpha n}}{\Gamma[n\alpha + \frac{1}{2}]} \tag{3.175}$$

The form of this function is shown in figure 3.8 for the values of λ_0 and α in table 3.1.

We can also invert the Laplace transform for the force derived for a nearly spherical body (3.95), when b/a is close to unity. The result is of the same form as (3.163).

$$\mathcal{F}_H(t) = F_s W(t) - \frac{1}{\sqrt{\pi}} B_\infty \int_0^t \frac{dW}{d\tau}(t-\tau)^{-1/2} d\tau - m_a \frac{dW}{d\tau} - C \int_0^t \frac{dW}{d\tau} G(t-\tau) d\tau \tag{3.176}$$

where $$B_\infty = 1 + \frac{8}{5}\epsilon + \frac{116}{175}\epsilon^2 + O(\epsilon^3) = B_0 + O(\epsilon^3) \tag{3.177}$$

$$F_s = -\left(1 + \frac{4}{5}\epsilon + \frac{2}{175}\epsilon^2 + O(\epsilon^3)\right) \tag{3.178}$$

$$m_a = \frac{1}{9}\left(1 + \frac{16}{5}\epsilon + \frac{604}{175}\epsilon^2\right) + O(\epsilon^3) \tag{3.179}$$

Equation (3.176) is made dimensionless with length-scale b and $a = b(1+\epsilon)$. In this case, the constant C is

$$C = \frac{8}{175}\epsilon^2 \tag{3.180}$$

and the memory function G is given by

$$\bar{G}(s) = \frac{1}{3+3s^{1/2}+s} = \frac{1}{\sqrt{3}\,i}\left[\frac{1}{s^{1/2}+z_1^*} - \frac{1}{s^{1/2}+z_1}\right] \qquad (3.181)$$

with $z_1 = \frac{1}{2}\sqrt{3}(\sqrt{3}+i) = \sqrt{3}e^{i\pi/6}$. From Oberhettinger & Badii (1973) we find that

$$G(t) = \frac{1}{i\sqrt{3}}\left\{\sqrt{\pi t} - z_1^* e^{z_1^{*2}t}\operatorname{erfc}(z_1^* t^{1/2}) - \sqrt{\pi t} + z_1 e^{z_1^2 t}\operatorname{erfc}(z_1 t^{1/2})\right\} \qquad (3.182)$$

$$= \frac{2}{\sqrt{3}}\,\mathrm{Im}\left\{z_1 e^{z_1^2 t}\operatorname{erfc}(z_1 t^{1/2})\right\} \qquad (3.183)$$

This can be written in the form of a power series,

$$G(t) = 2\sum_0^\infty \frac{(-3)^n t^{n/2}}{\Gamma(\frac{n}{2}+1)}\sin(n+1)\frac{\pi}{6} \qquad (3.184)$$

Equation (3.184) is real since the transform G(s) is exact in this case. The function (3.184) is shown dotted in figure 3.8.

In conclusion, we see that the concept of the Basset force is easily generalized to nonspherical bodies, and that it is the high frequency term B_∞ which in fact gives rise to the usual term with the $t^{-\frac{1}{2}}$ memory function. Then it is convenient to separate off a fourth term which, in most cases, has no singularity in the memory function, but which is comparable to the Basset force at long times. Although the general problem is very complicated, it is helpful to treat it in this way, so that all the complex behaviour is contained in one term of the force.

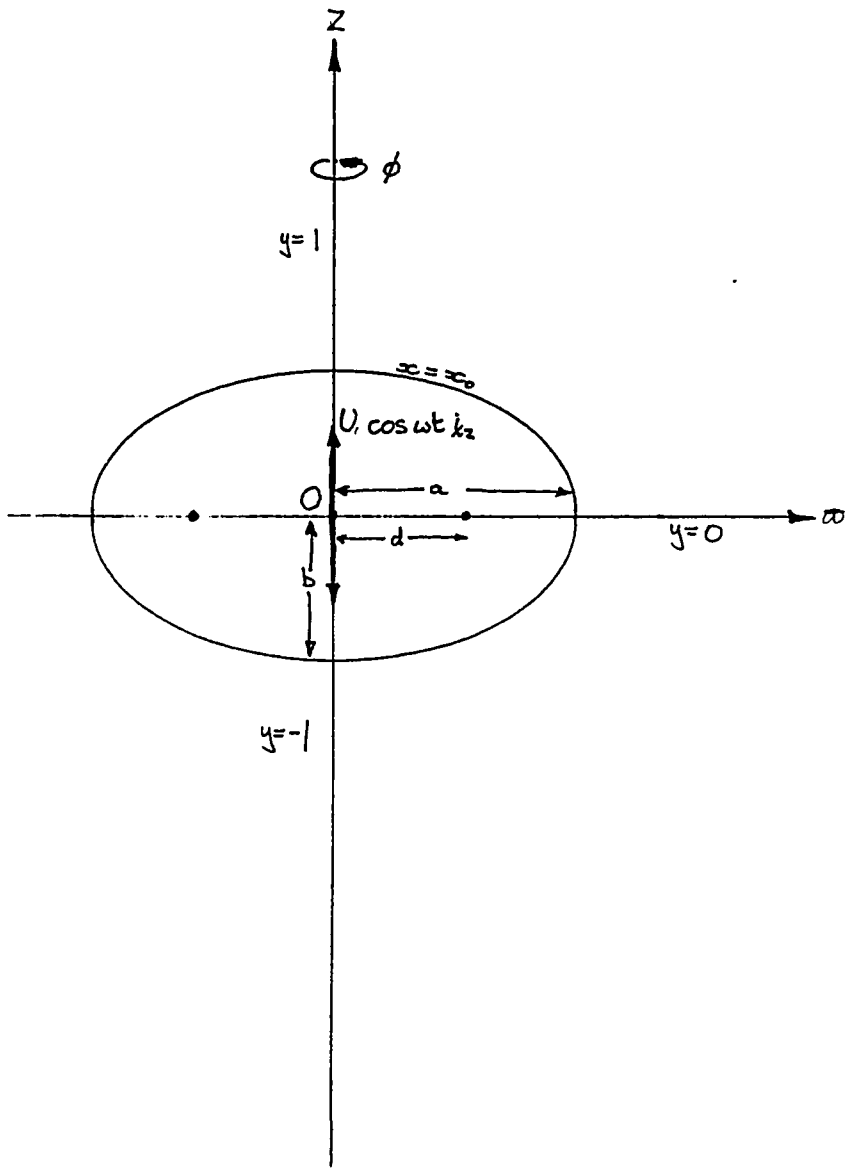

Figure 3.1(a). The geometry and coordinate system for an oblate spheroid.

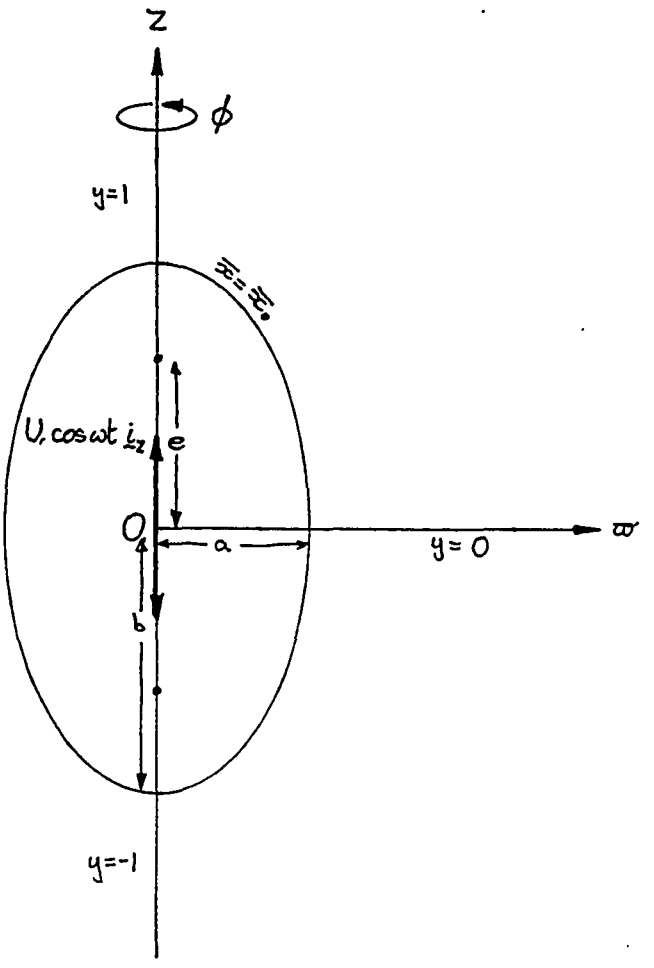

Figure 3.1(b). The geometry and coordinate system for a prolate spheroid.

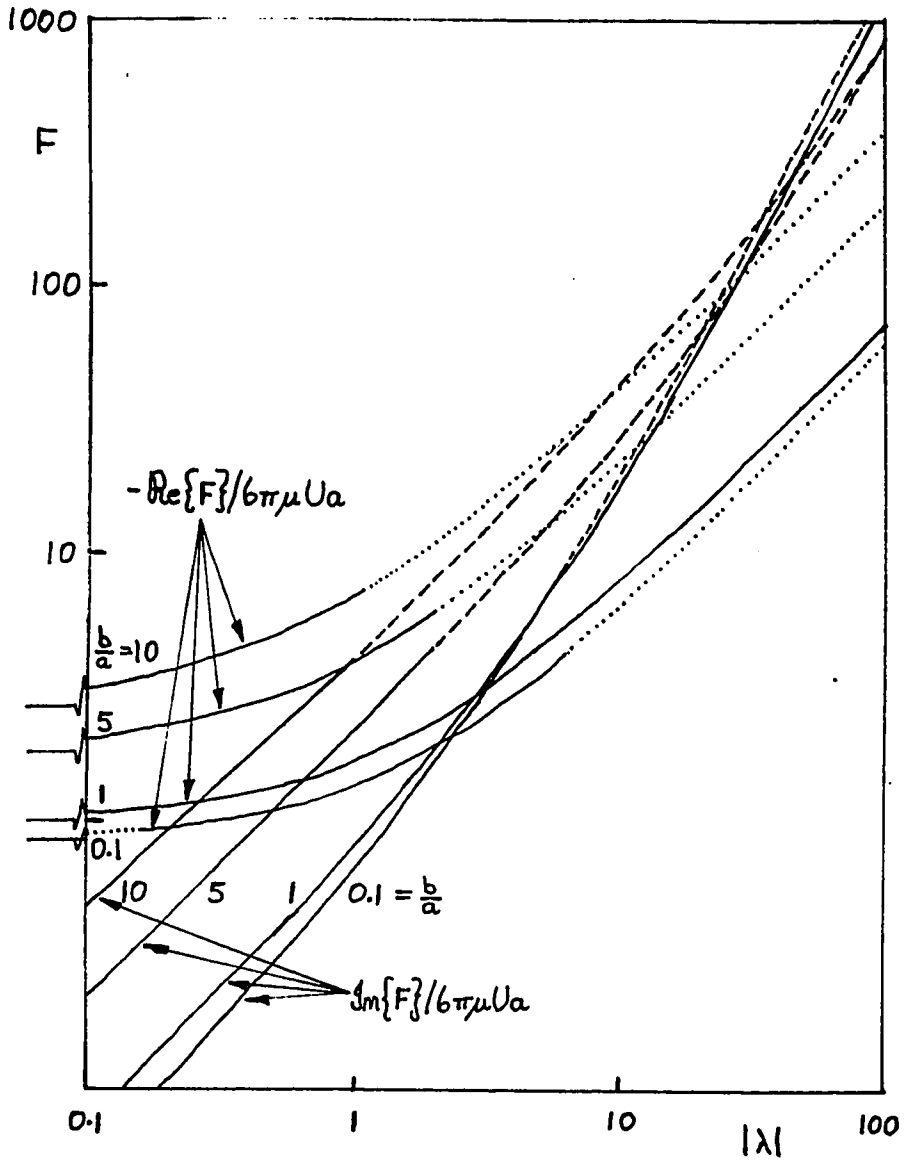

Figure 3.2. The force on an oscillating spheroid as a function of b/a and $|\lambda|$: _____ , full calculation; ..... , correlation for the real part; ----- , correlation for the imaginary part.

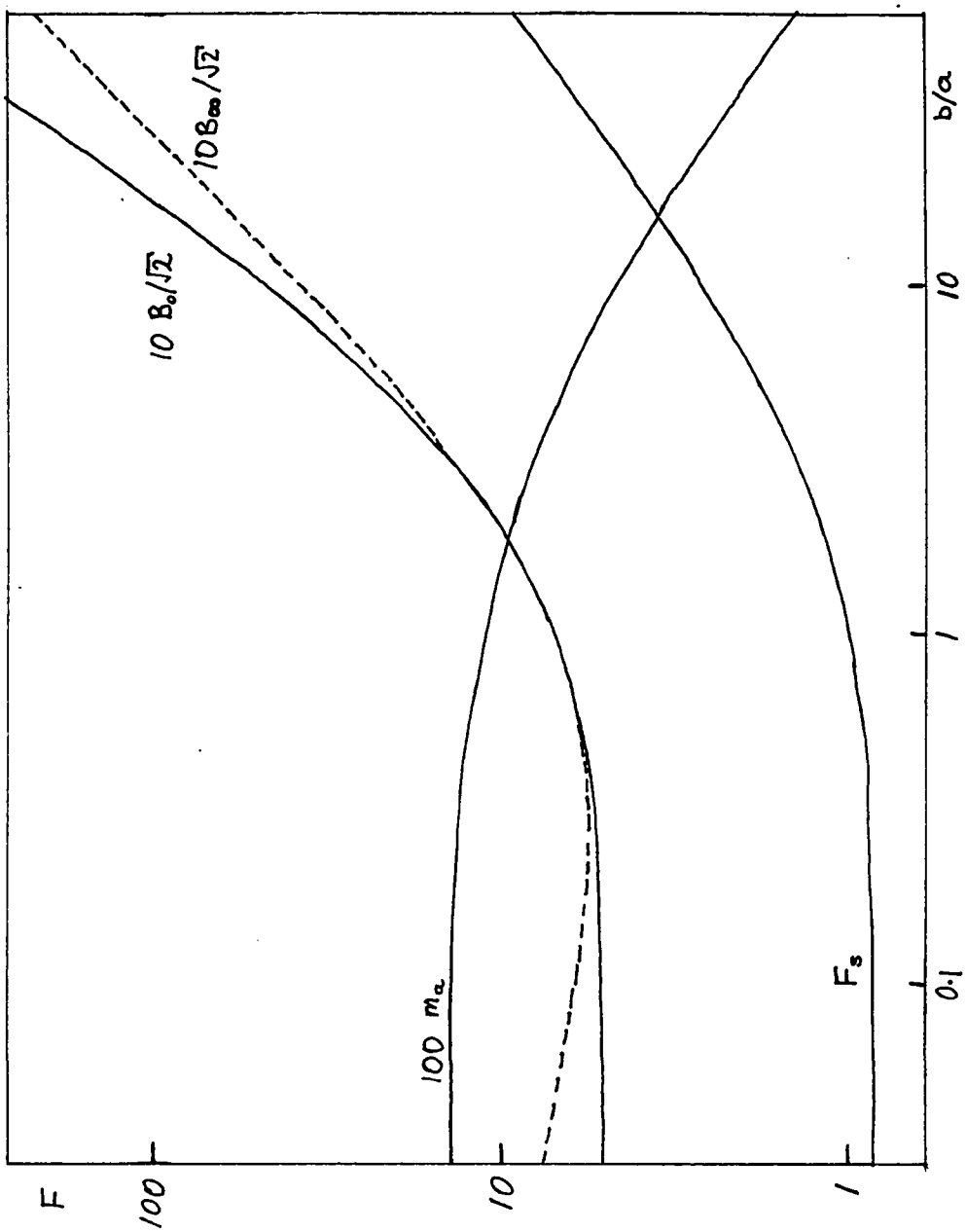

Figure 3.3. Asymptotic values of the components of the force as a function of aspect ratio. (nominal value of $|\lambda| = 10$ used for comparison.)

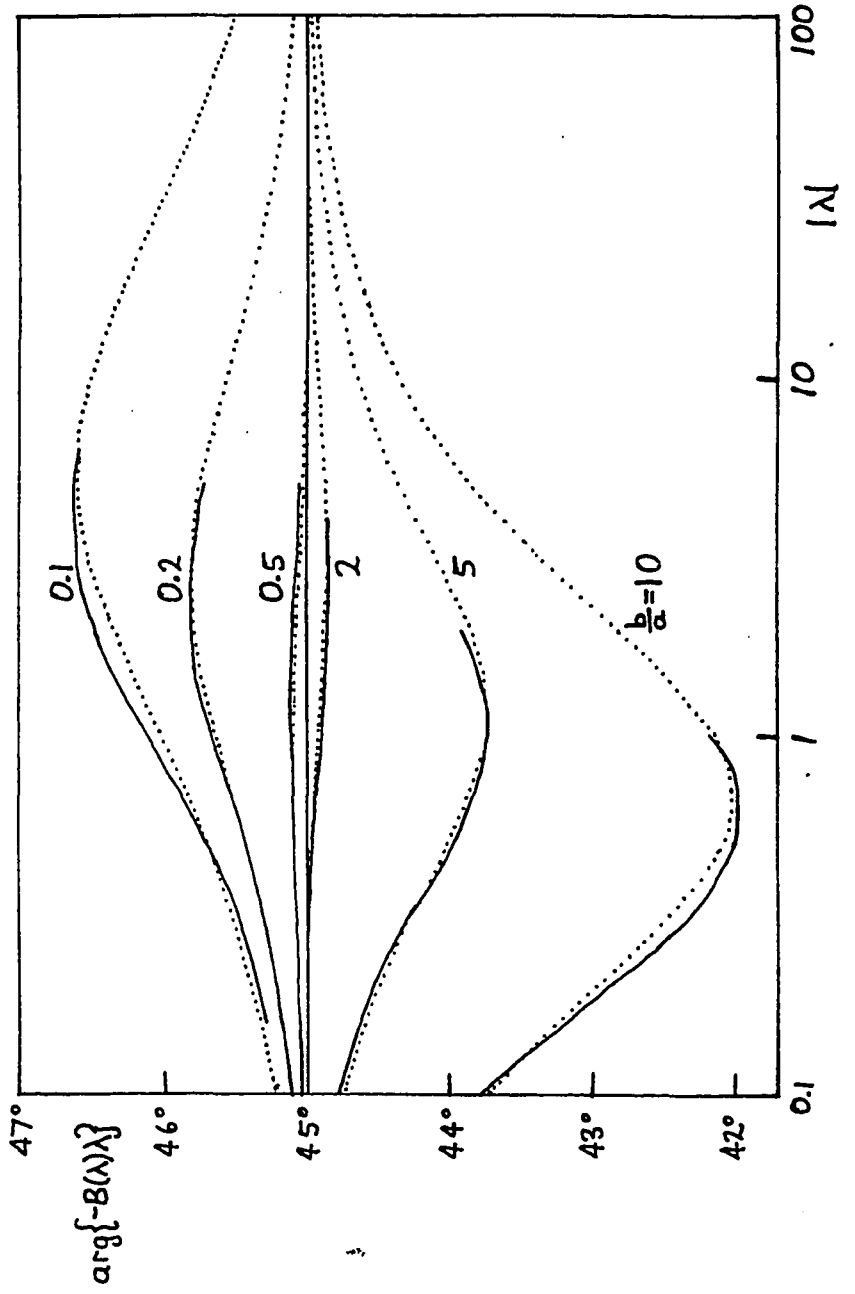

Figure 3.4. The phase of the "Basset coefficient", $B(\lambda)\lambda$ as a function of b/a and $|\lambda|$: _____ , full calculation; ..... , correlation.

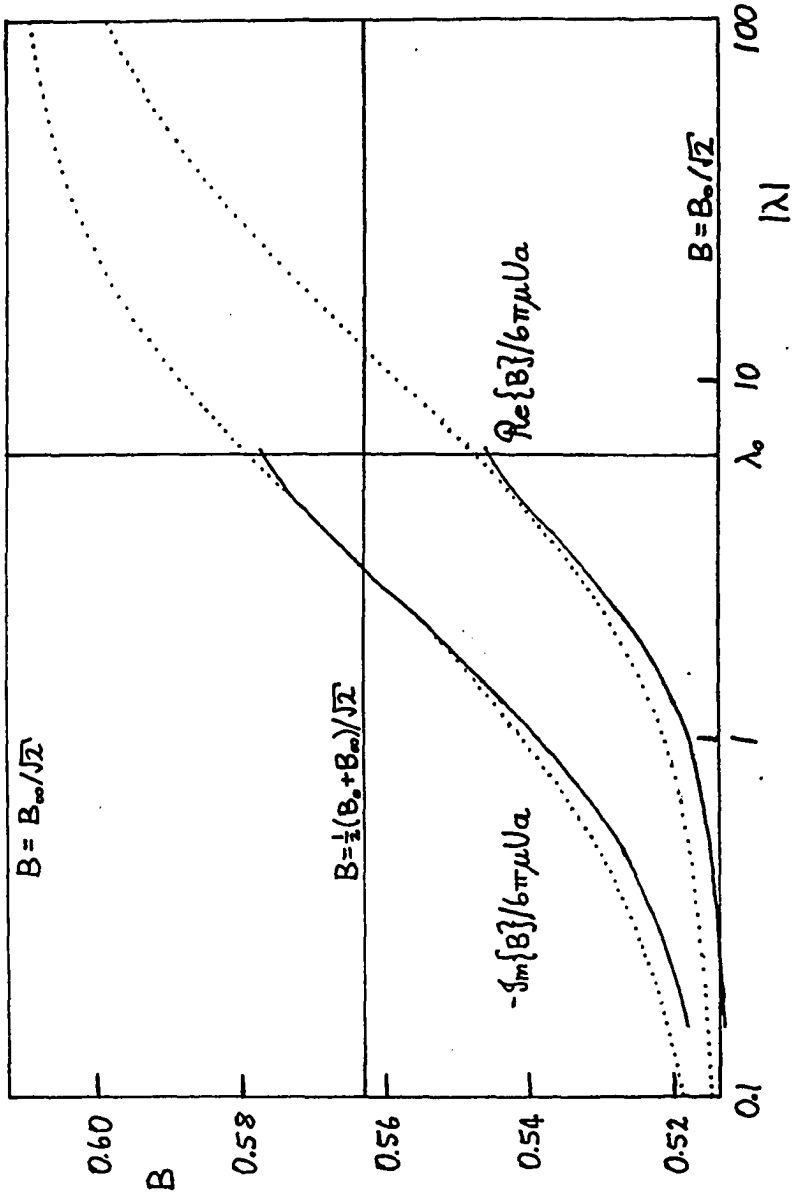

Figure 3.5. The real and imaginary components of the "Basset coefficient", $B(\lambda)\lambda/|\lambda|$ as a function of $|\lambda|$. (a) b/a = 0.1.

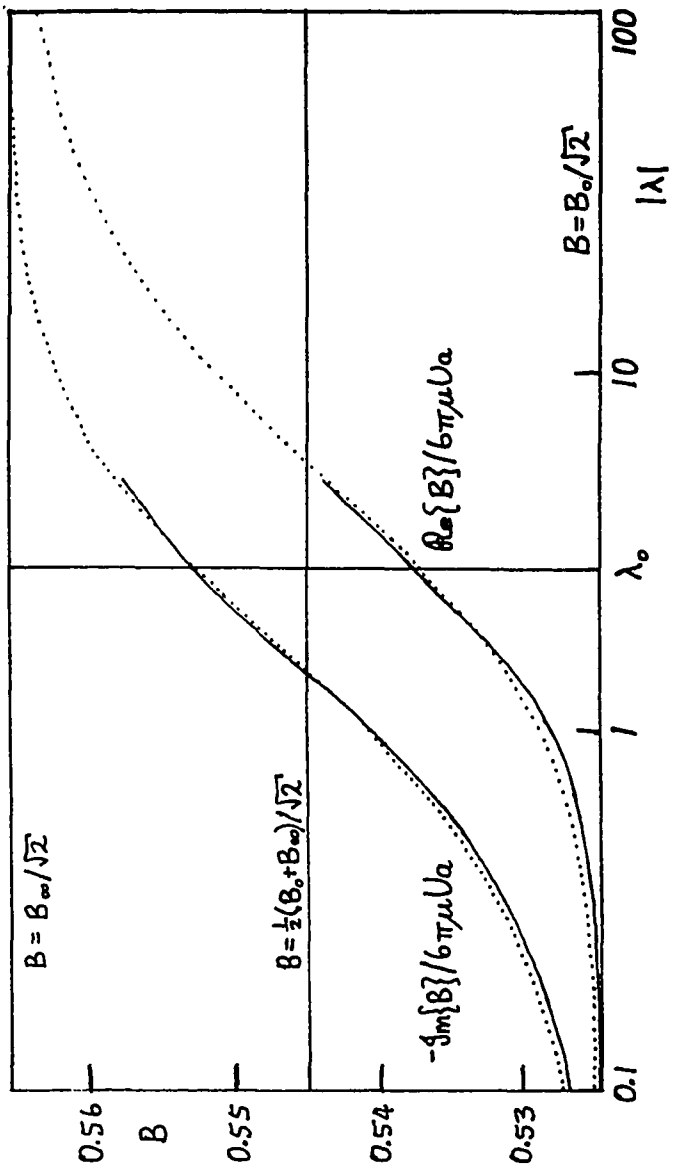

Figure 3.5. The real and imaginary components of the "Basset coefficient", $B(\lambda)\lambda/|\lambda|$ as a function of $|\lambda|$. (b) $b/a = 0.2$.

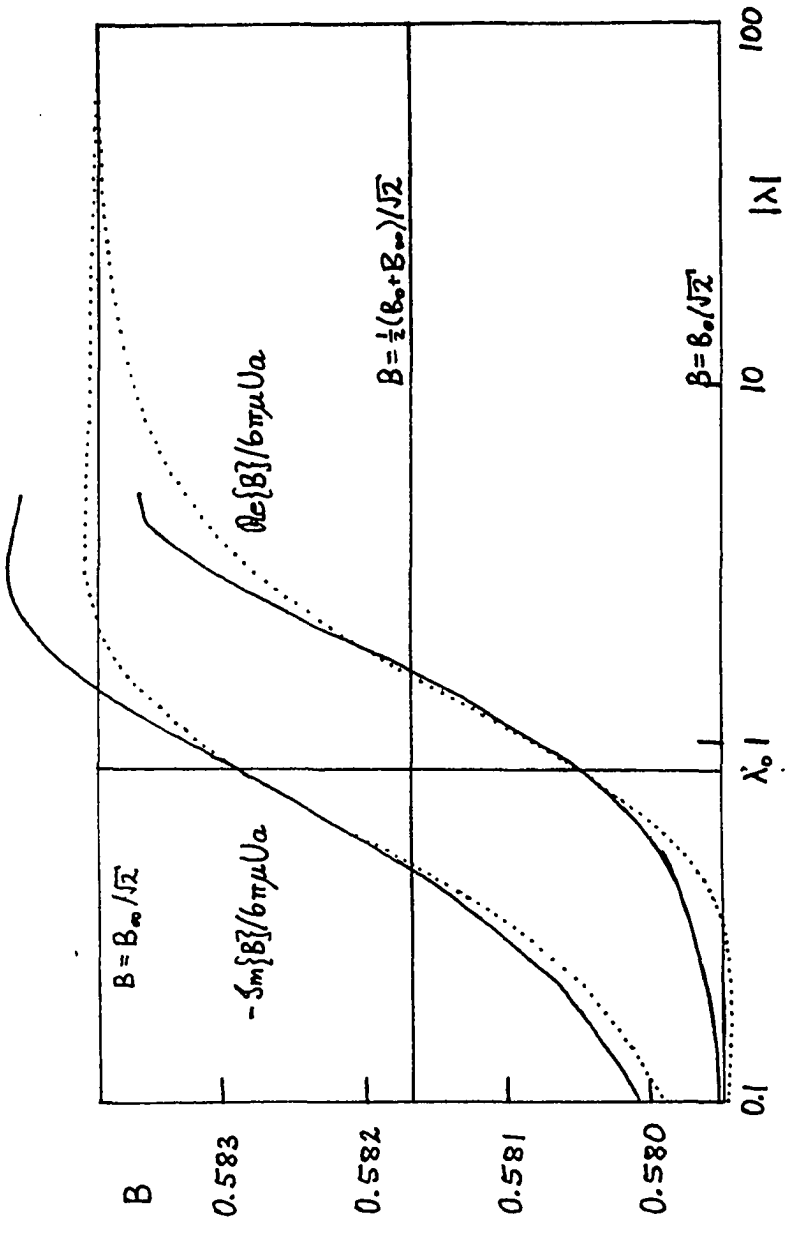

Figure 3.5. The real and imaginary components of the "Basset coefficient", $B(\lambda)\lambda/|\lambda|$ as a function of $|\lambda|$. (c) b/a = 0.5.

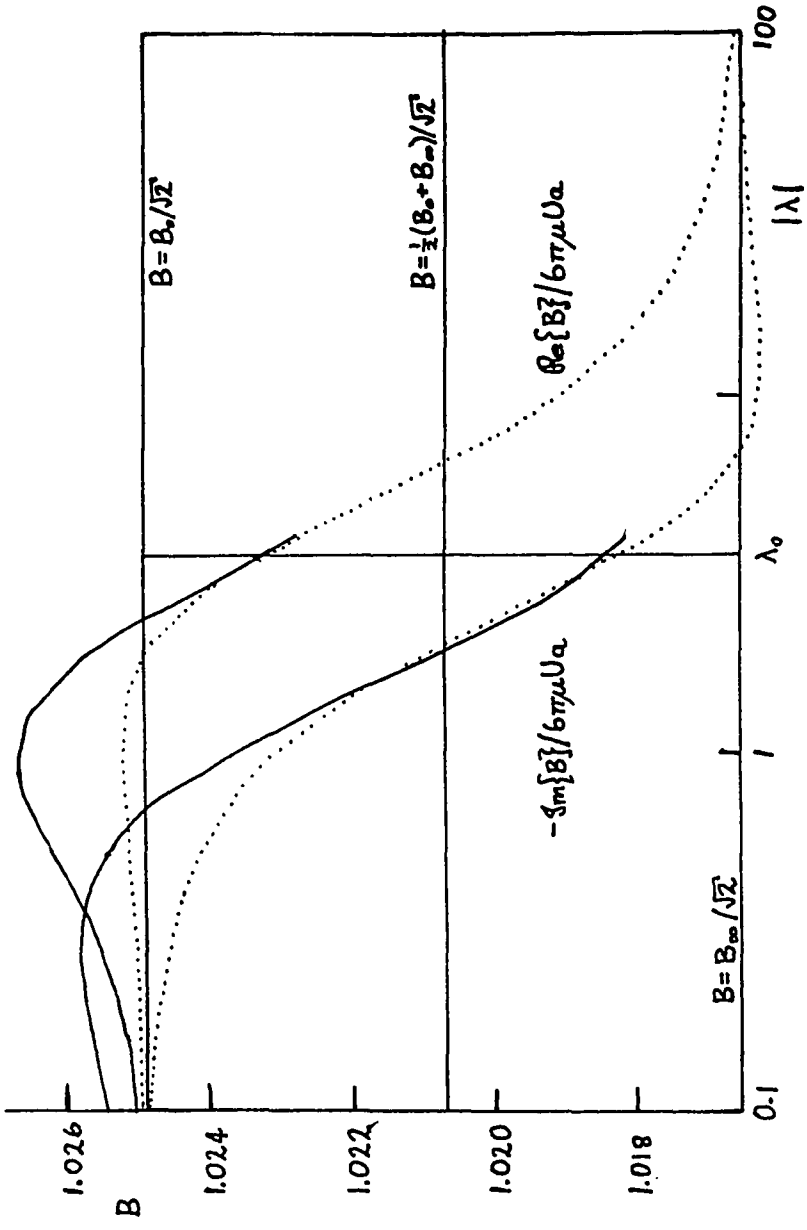

Figure 3.5. The real and imaginary components of the "Basset coefficient", $B(\lambda)\lambda/|\lambda|$ as a function of $|\lambda|$. (d) b/a = 2.

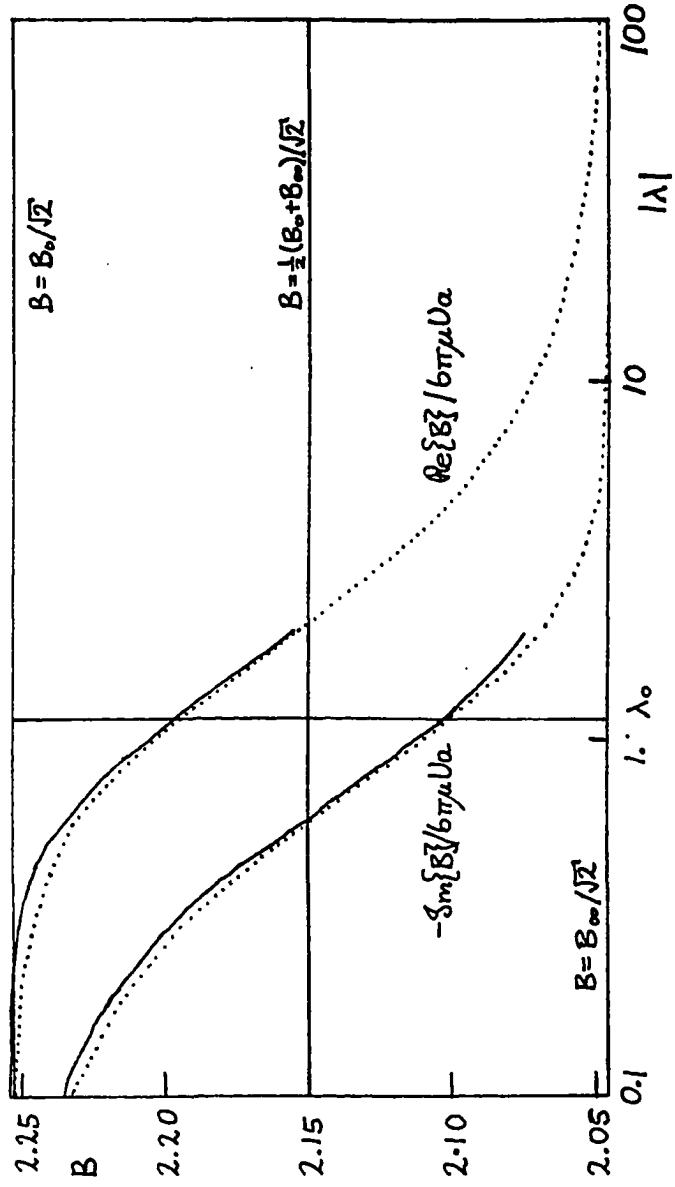

Figure 3.5. The real and imaginary components of the "Basset coefficient", $B(\lambda)\lambda/|\lambda|$ as a function of $|\lambda|$. (e) b/a = 5.

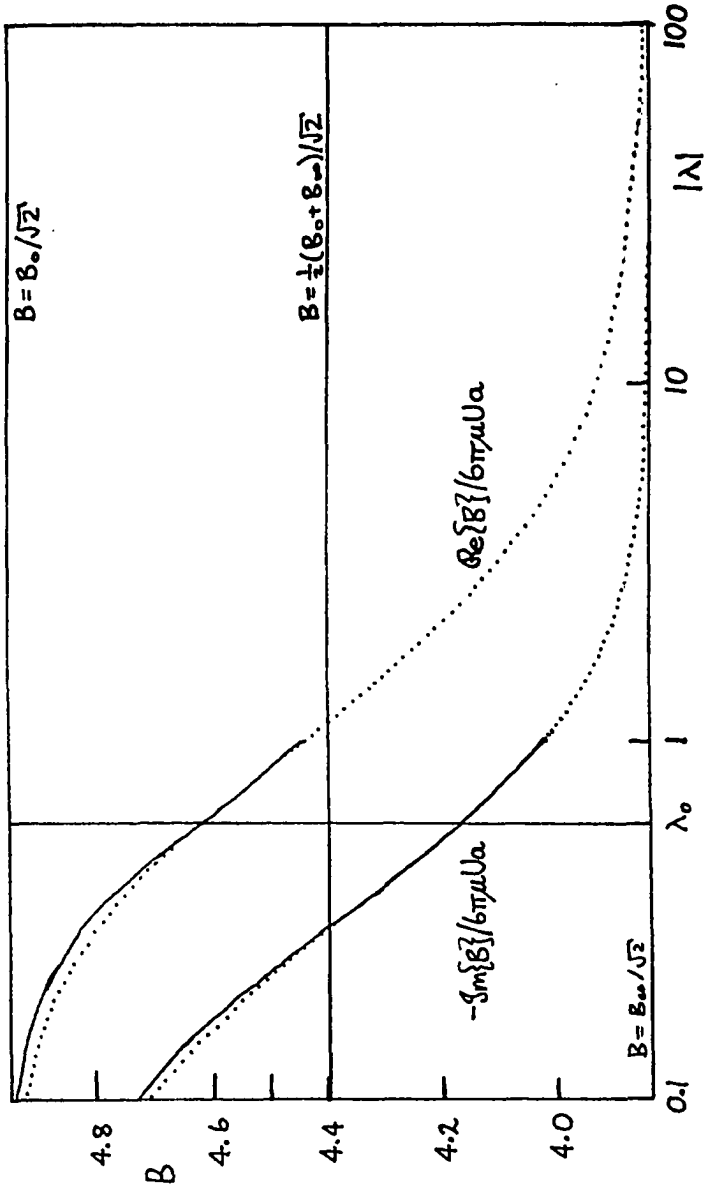

Figure 3.5. The real and imaginary components of the "Basset coefficient", $B(\lambda)\lambda/|\lambda|$ as a function of $|\lambda|$. (f) b/a = 10.

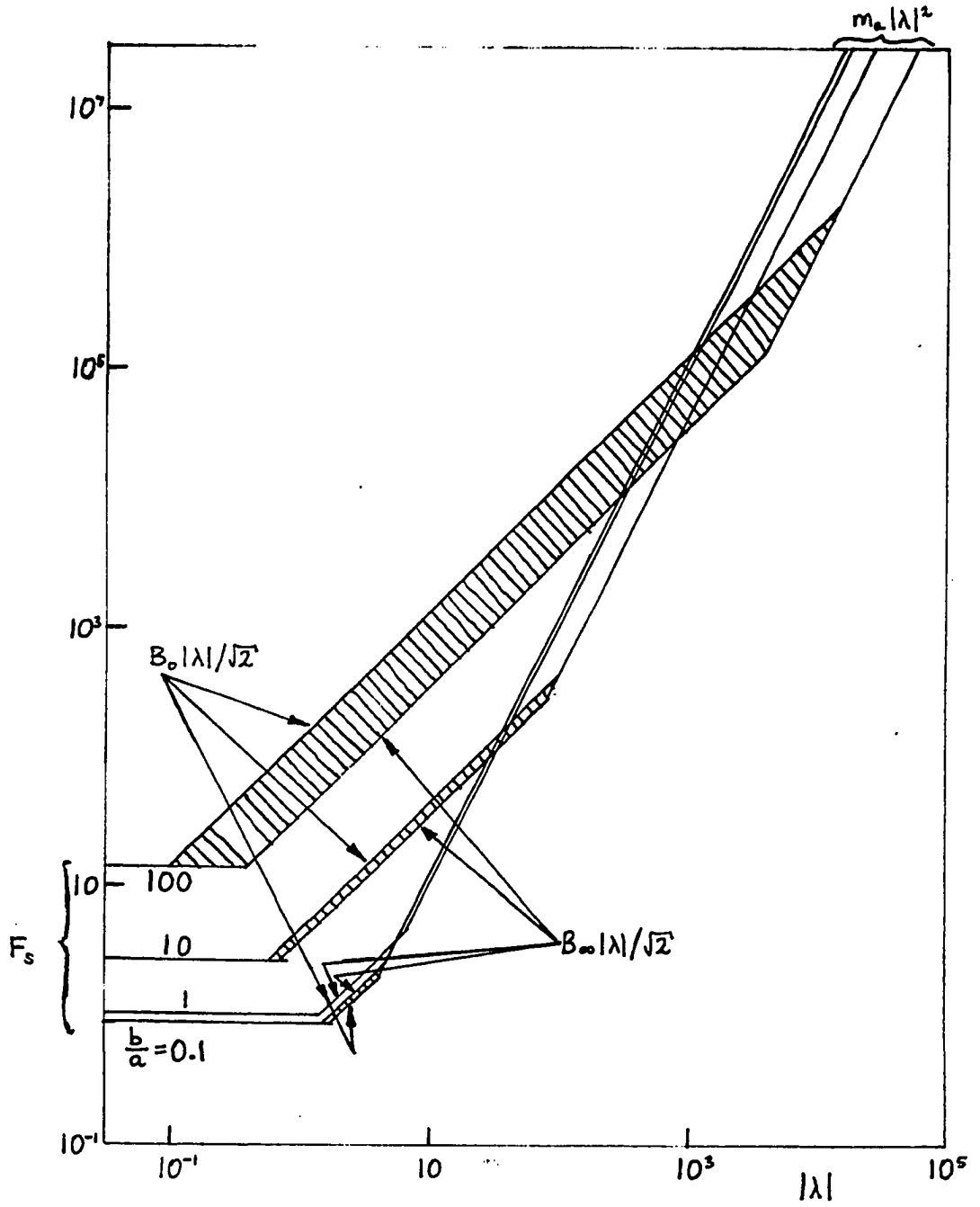

Figure 3.6. Asymptotes of the force for different aspect ratios as a function of $|\lambda|$.

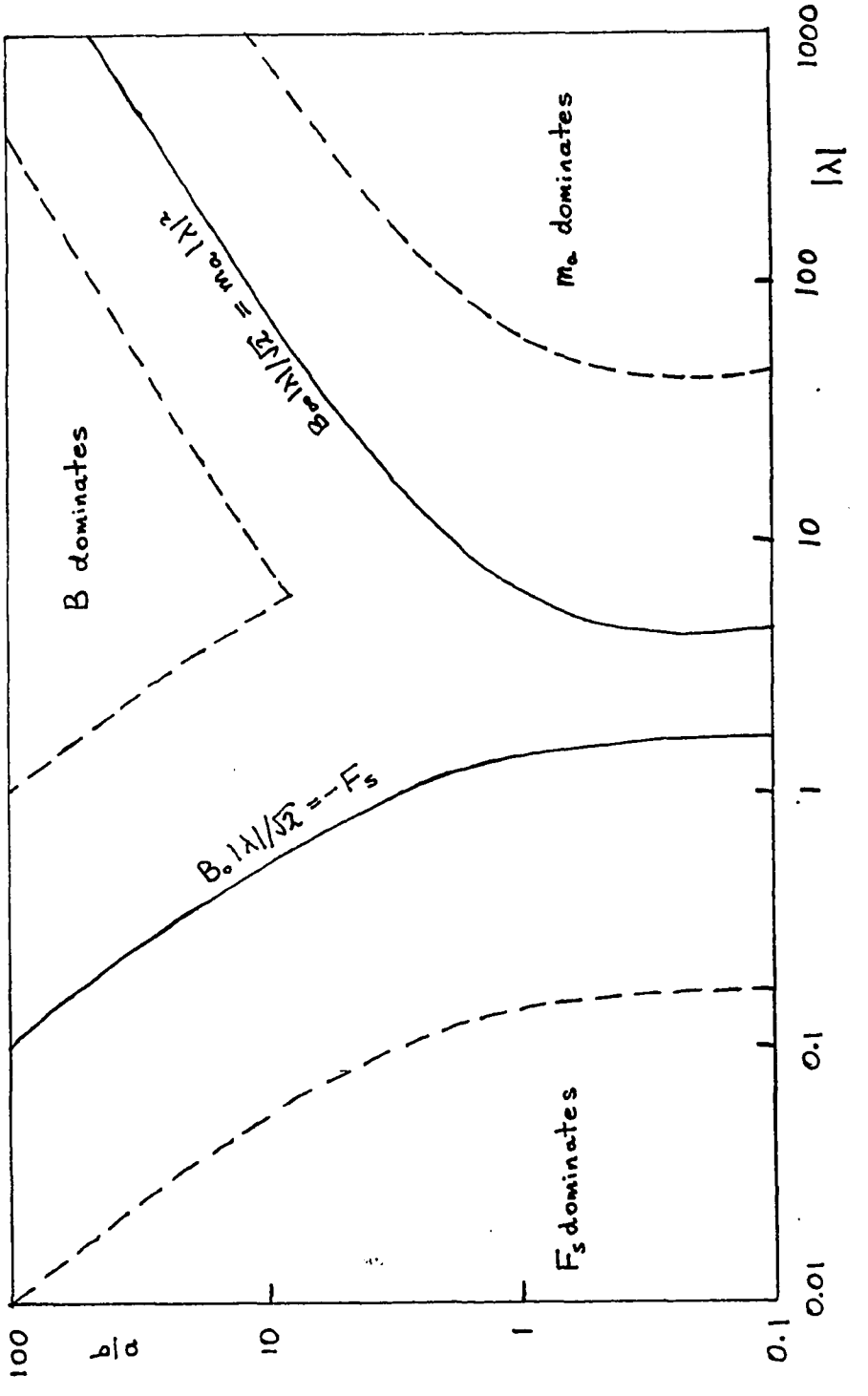

Figure 3.7. The regions of different behaviour in the parameter space of $|\lambda|$ and b/a. The dashed lines are separated from the solid lines by a factor of 10.

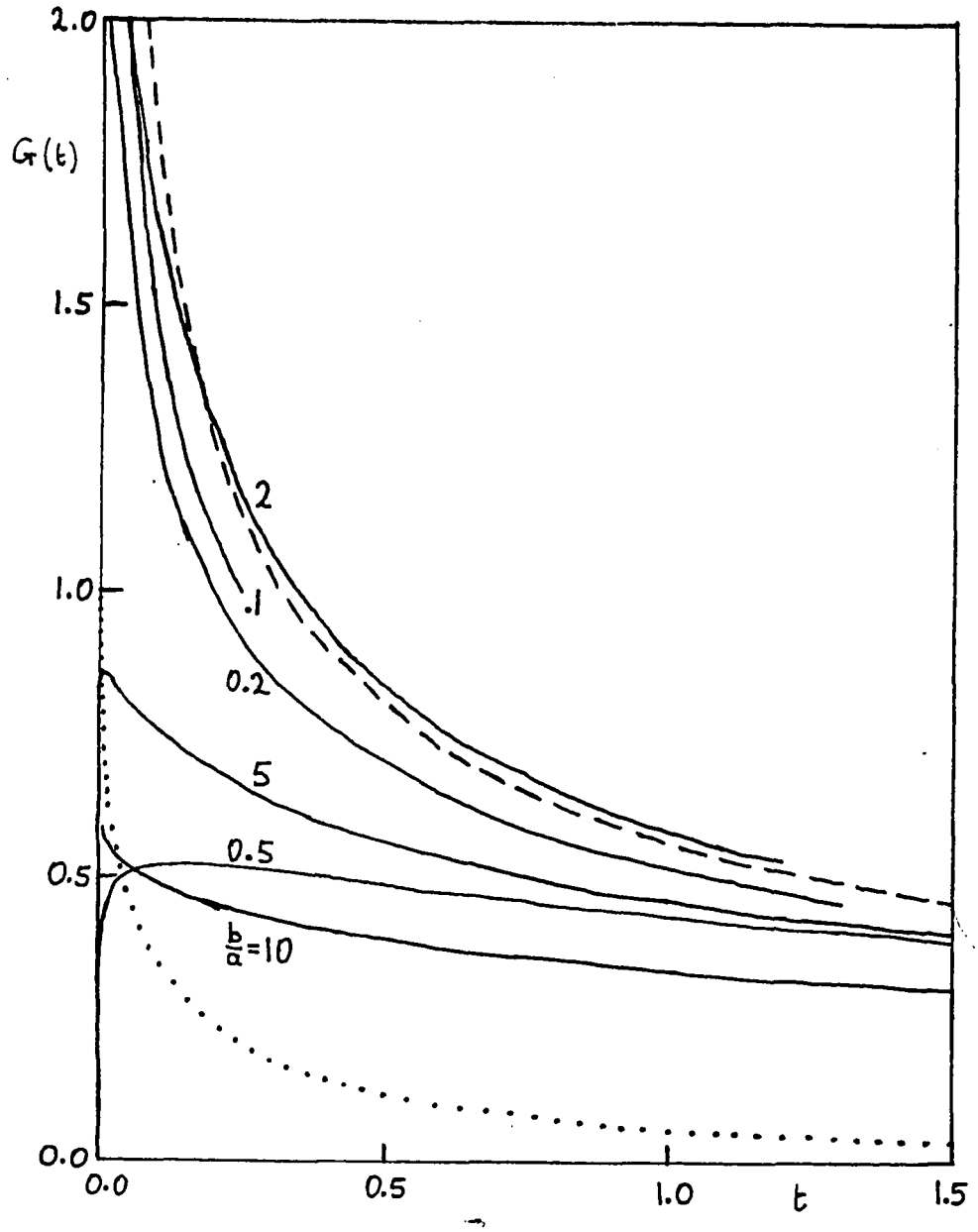

Figure 3.8. The memory function G(t) which appears in the new force term: _____ , correlation (3.175); ..... , asymptotic result for small b/a (3.184); ----- , the Basset $1/\sqrt{(\pi t)}$ memory function.

CHAPTER 4. SIMILARITY SOLUTIONS FOR THE MOTION OF A LARGE DISC NEAR A PLANE

4.1 INTRODUCTION

The draining of a fluid layer in the hydrodynamic collision of two particles or the interaction of an object with a boundary underlies a diverse spectrum of physical phenomena associated with filtration, coagulation and biological applications. In virtually all of these studies to date, these interactions have been treated either in the viscosity dominated limit, where particle and fluid inertial effects can be ignored, or in the inviscid limit where all real fluid effects are omitted. The vast majority of analyses in the viscous limit have been based on either the quasi-steady Stokes equation in the limit of zero Reynolds number or lubricating layer theories where the Reynolds number based on gap height is small and all inertial effects in the fluid layer can be neglected. The latter approximation has been used in the recent theory of Davis, Serayssol & Hinch (1985), the first analysis which attempts to address the elastohydrodynamic collision and rebound of solid particles from a wall in a viscous fluid.

The problem of the unsteady collision interaction of a finite particle with a boundary is one of the most basic in the study of viscous fluids. Depending on the initial

velocity of the particle, the Reynolds number based on the instantaneous height of the fluid gap can vary continuously from very large values where inertial effects are dominant to very small values during collision when the fluid gap is very narrow. The treatment of the nonlinear regime, in particular, has seemed to be insurmountably difficult. The problem of the near collision approach, however, has an important simplification in that the boundary geometry in the region of near contact will be nearly parallel, at least for a blunt object, and the boundaries may be flattened by elastic deformation. Therefore, important insights can first be obtained by examining the fully nonlinear problem for the simple inelastic parallel wall geometry. For mathematical simplicity, we consider an object with a flat circular bottom moving towards a parallel plane surface, as shown in figure 4.1, and we will assume that the initial gap height h_o is much smaller than the disc radius a. The fluid motion in the gap can be visualized as a time-dependent axisymmetric double stagnation point flow.

The problem described has already been studied in the case where the body is dropped from rest and falls under the action of a constant normal force. (Weinbaum, Lawrence & Kuang and Lawrence, Kuang & Weinbaum 1985. These papers will henceforth be referred to as WLK 1 and LKW 2.) In the present chapter we are interested primarily in the motion of a body under the influence of its own inertia and fluid

inertia in the absence of an applied force. For a viscous fluid, there will be dissipation of energy and, in the absence of elasticity, the body will come to rest without recoil at some distance from the plane. It is this distance, as well as the actual process of arrest, which is of fundamental interest. In WLK 1 and LKW 2, the draining of the fluid layer after the body is dropped from rest was considered. This choice of initial condition limits the range of solutions available and in the current chapter the initial velocity will be arbitrary. This enables us to examine the relative importance of the applied force and the initial momentum of the body and fluid.

It was shown in WLK 1 that the parallel wall geometry leads to a separation of the radial coordinate in the equations of motion. This separation is the time-dependent equivalent of the separation found by Homann (1936) for a steady axisymmetric stagnation point boundary layer. It is interesting that analogous forms exist for the two-dimensional version of this problem (Secomb, 1978) and for the fluid motion in a tube which contracts uniformly along its length (Uchida & Aoki ,1977). In each case, there is stagnation flow at the origin of coordinates, the streamwise velocity is proportional to the streamwise coordinate, and the perpendicular velocity is independent of the streamwise coordinate. In all these problems the number of independent variables is reduced by one and the reduced equations lead

to exact numerical solutions of the Navier-Stokes equations. Another family of such solutions was described by Batchelor (1951) who generalized the rotating disc problem of von Karman (1921). The basic equations are all of modified boundary layer type; the terms retained in the governing equations are exactly those retained in the boundary layer equations except that the pressure is no longer constant across the viscous layer and a different normal momentum equation is employed. Some of the above examples are discussed by Schlichting (1979).

Yang (1958) showed that for a time-dependent two-dimensional stagnation point flow, a further simplification can be obtained if the outer flow has the special dimensionless form,

$$u_\infty = \frac{x}{1-\alpha t} \qquad (4.1)$$

In this case a similarity solution is found and the number of independent variables is further reduced, so the flow is determined in terms of a function of a single variable. Uchida & Aoki (1977) found that a particular time-dependence of the tube radius also leads to a similarity solution; in fact this also leads to a streamwise velocity like (4.1). These two solutions have no special physical interpretation, rather the time-dependence is introduced artificially as a mathematical convenience in the solution. We will show that a similar solution arises naturally in the present problem and that it has a simple physical interpretation.

When the governing equations are cast in dimensionless form, we find that in the general case there are three dimensionless parameters governing the motion. These are $Re_0 = h_0|w_0|/\nu$, $\beta = 4mh_0/\pi\rho a^4$ and $\gamma = V_0^2/w_0^2$, in which ν and ρ are the kinematic viscosity and density of the fluid, m and w_0 are the mass and initial velocity of the disc, and $V_0 = (4\tilde{\mathcal{F}}_A/\pi\rho a^2)^{1/2}(h_0/a)$ is a velocity scale based on the initial gap height and the characteristic inertial time required to drain the fluid under an applied force $\tilde{\mathcal{F}}_A$ which includes gravity. The first parameter is the Reynolds number based on the initial gap height, the second parameter is the ratio of the contribution to the dynamic equation of the inertia of the body to that of the inertia of the fluid, and γ is the ratio of the applied force to the pressure force induced by the inertia of the fluid. The parameter values can vary greatly depending on the type of collision considered. Re_0 may be very small for microscopic particles or quite large for large particles (e.g. for a large snowflake hitting a window $Re_0 \sim 10^3$). β is typically $\ll O(1)$ for liquids and for small gap height, but may be large for solid particles in a gas (e.g. for a penny dropped in a puddle of water $\beta \sim 10^2$, but for the snowflake hitting a window $\beta \sim 10^2$). Finally, γ depends on the nature of the problem ; if there is no applied force γ is zero, if there is no initial velocity γ is infinite. Hence for a given body and fluid γ may take any value.

In the present chapter we are principally interested in two problems: (i) the near collision arrest of an object driven solely by inertia in the absence of an applied force and (ii) the modification of this flow when an applied force is present with inertia playing a subsidiary role. For the first of these problems the reduced equation simplifies since $\gamma = 0$; for the second, only two parameters are required since we can define a modified Reynolds number $\overline{Re}_o = h_o V_o / \nu$ based on V_o and the parameter γ is replaced by unity.

The equations of motion will be treated in the inviscid limit for all values of β and γ and for real fluids with finite Re_o we shall consider the two problems mentioned above. In the case of finite Re_o, it is possible to define a time-dependent Reynolds number; this will enable us to obtain a single solution curve which is valid for the entire range of Reynolds numbers from the initial value to zero at final arrest. This solution is divided into three parts. The first part is a boundary layer solution valid for $Re_o > O(100)$ which is an exact similarity solution when $\beta = 0$, the second part is a numerical solution for $O(0.1) < Re_o < O(100)$ and the third part is a low Reynolds number analysis. Amongst other things, this solution predicts the ultimate position of rest of the body in the absence of an applied force.

4.2 GOVERNING EQUATIONS

The equations of motion for the body and fluid were derived in WLK 1, but a slightly different approach is used here. Since the flow is axisymmetric, it is beneficial to introduce a stream function ψ so that the radial velocity is $u = \psi_z/r$ and the axial velocity is $w = -\psi_r/r$. The continuity equation is thereby satisfied and the vorticity equation takes the well-known form:

$$\nu E^4\psi - r\left(\psi_z\frac{\partial}{\partial r} - \psi_r\frac{\partial}{\partial z}\right)\frac{1}{r^2}E^2\psi - E^2\psi_t = 0 \qquad (4.2)$$

A subscript denotes differentiation and E^2 is the generalized axisymmetric potential operator given by

$$E^2 = r\frac{\partial}{\partial r}\frac{1}{r}\frac{\partial}{\partial r} + \frac{\partial^2}{\partial z^2} \qquad (4.3)$$

We expect that for small values of (a/h), the dynamically important effects will be contained within the narrow gap region $0 \leqslant r \leqslant a$, $0 \leqslant z \leqslant h$. The boundary conditions for this region are:

$$\text{on } r=0: \quad \psi = 0, \qquad \psi_r = 0 \qquad (4.4)$$

$$\text{on } z=0: \quad \psi = 0, \qquad \psi_z = 0 \qquad (4.5)$$

$$\text{on } z=h(t): \quad \psi = -\tfrac{1}{2}r^2h_t, \quad \psi_z = 0 \qquad (4.6)$$

These conditions suggest a trial solution of the form

$$\psi = r^2F(z,t), \qquad u = rF_z, \qquad w = -2F \qquad (4.7)$$

This form of Ψ satisfies (4.2) provided that F is a solution of the simpler equation:

$$\nu F_{zzzz} + 2FF_{zzz} - F_z F_{zzz} = 0 \qquad (4.8)$$

The separation of the streamwise coordinate is similar to that found by Uchida & Aoki (1977) and Secomb (1978) for two-dimensional flow and axial flow in a pipe, and is characteristic of stagnation point flows.

Equation (4.8) may be integrated with respect to z to give

$$\nu F_{zzz} + 2FF_{zz} - F_z^2 - F_{zt} = A(t) \qquad (4.9)$$

A(t) is an arbitrary function which may be found by reference to the momentum equation. The latter gives two equations for the derivatives of the pressure,

$$p_z = -2\rho\,(\nu F_{zz} - F_t + 2FF_z) \qquad (4.10)$$

and

$$p_r = r\rho\,(\nu F_{zzz} + 2FF_{zz} - F_z^2 - F_{zt}) = r\rho A(t) \qquad (4.11)$$

From (4.11) we conclude that

$$p(r,z,t) = \tfrac{1}{2}\rho r^2 A(t) + B(z,t) \qquad (4.12)$$

where from (4.10)

$$B_z = -2\rho\,(\nu F_{zz} - F_t + 2FF_z) \qquad (4.13)$$

We integrate (4.13) making use of (4.6) to give

$$B = -2\rho\left(\nu F_z + F^2 - \tfrac{1}{4}h_t^2 + \int_z^h F_t\,dz'\right) + p_0(t) \qquad (4.14)$$

where p_o is the pressure at the centre of the underside of the disc.

A(t) is related to the hydrodynamic force on the disc which we now calculate. The normal component of the viscous stress is $\mu\frac{\partial w}{\partial z}$, which is necessarily zero on the disc, and the pressure is given by:

$$p(r,h,t) = \tfrac{1}{2}\rho r^2 A(t) + p_o(t) \qquad (4.15)$$

The above analysis is not valid near the edge of the disc. However, in purely viscous flow, exit effects would be confined to within one gap height of the edge (c.f. Dagan, Weinbaum & Pfeffer 1982), and in inviscid flow exit effects would not be important within the gap. We define a_o to be the radius of the inner region so that for $r < a_o$, the flow satisfies the above assumptions and so that

$$\frac{a-a_o}{a} = O\left(\frac{h_o}{a}\right) \quad \text{as} \quad \left(\frac{h_o}{a}\right) \longrightarrow 0 \qquad (4.16)$$

In incompressible flow the pressure includes an arbitrary additive constant, so we may take the ambient pressure in the external domain to be zero. The pressure at the point (a_o,h) will differ from zero by Δp, the exit pressure drop. Equation (4.15) gives:

$$\Delta p = \tfrac{1}{2}\rho a_o^2 A(t) + p_o(t) \qquad (4.17)$$

For a high Reynolds number exit flow, the pressure is constant across the edge to $O(h_o/a)$, whereas for very

viscous flow we expect that $\Delta p/p_o = O(h_o/a)$. Thus for all regimes of flow,

$$p_o(t) = -\tfrac{1}{2}\rho a^2 A(t)[1 + O(h_o/a)] \tag{4.18}$$

so
$$p(r,h,t) = \tfrac{1}{2}\rho(r^2-a^2)A(t)[1 + O(h_o/a)] \tag{4.19}$$

We integrate the pressure over the underside of the disc to get the hydrodynamic force on the disc.

$$\mathcal{F}_H = -\tfrac{\pi}{4}\rho a^4 A(t)[1 + O(h_o/a)] \tag{4.20}$$

The error term in (4.20) contains parts due to the external flow, the inaccuracy of (4.15) near the edge of the disc, and the unknown, small, constant pressure increase within the gap due to the exit pressure drop. The third contribution will often be dominant and it is estimated by $\Delta p \pi a^2$.

The hydrodynamic force is balanced by the acceleration of the disc and an applied downward force $\mathcal{F}_A$ to give:

$$\mathcal{F}_H = m h_{tt} + \mathcal{F}_A \tag{4.21}$$

in which m is the mass of the disc. Finally, we have the dynamic equation for the motion,

$$\nu F_{zzz} + 2F F_{zz} - F_z^2 - F_{zt} = \frac{-4}{\pi\rho a^4}(m h_{tt} + \mathcal{F}_A) \tag{4.22}$$

This equation is valid in the limit as $(h_o/a) \to 0$. The coupled system of equations for F and h is completed by the boundary conditions on F,

$$\text{on } z=0: \quad F=0, \quad F_z=0 \tag{4.23}$$

$$\text{on } z=h(t): \quad F_z=0, \quad h_t=-2F \tag{4.24}$$

We may also specify initial conditions for F and h;

$$\text{when } t=0: \quad F=F_0(z), \quad h=h_0 \tag{4.25}$$

The initial velocity of the disc, w_0, is then given by;

$$w_0 = -2F_0(h_0) \tag{4.26}$$

we may now cast the system of equations in dimensionless form by defining $F^* = F/|w_0|$, $F_0^* = F_0/|w_0|$, $h^* = h/h_0$, $z^* = z/h_0$, $t^* = t|w_0|/h_0$. We drop the asterisks to get:

$$F_{zt} + F_z^2 - 2FF_{zz} - \frac{1}{Re_0}F_{zzz} = \beta h_{tt} + \gamma \tag{4.27}$$

The boundary conditions are unchanged and the initial conditions become:

$$\text{when } t=0: \quad F=F_0(z), \quad h=1 \tag{4.28}$$

$$\text{with} \qquad h_t = -1 = -2F_0(1) \tag{4.29}$$

The three dimensionless parameters are:

initial Reynolds number $$Re_0 = \frac{h_0|w_0|}{\nu} \tag{4.30}$$

inertia parameter $$\beta = \frac{4m}{\pi\rho a^2 h_0}\left(\frac{h_0}{a}\right)^2 \tag{4.31}$$

forcing parameter $$\gamma = \frac{4\gamma_A}{\pi\rho a^2 w_0^2}\left(\frac{h_0}{a}\right)^2 \tag{4.32}$$

The regimes of motion are determined by the values of these parameters which represent the ratios of forces, fluid inertia : viscous, body inertia : fluid inertia, applied force : fluid inertia respectively.

4.3 INVISCID SOLUTION

If the initial Reynolds number is very large, the effects of viscosity will be confined in space to thin boundary layers and in time towards the end of the motion. For a large part of the motion the inviscid equations will give a good representation of the solution. These equations are:

$$F_{zt} + F_z^2 - 2FF_{zz} = \beta h_{tt} + \gamma \qquad (4.33)$$

where on $z=0$: $F=0$ (4.34)

on $z=h(t)$: $F=-\frac{1}{2}h_t$ (4.35)

and when $t=0$: $h=1$, $F=F_0(z)$, $h_t=-1=-2F_0(z)$ (4.36)

The differential equation can be satisfied by taking $F = \Phi(t)z$ to give:

$$\Phi_t + \Phi^2 = \beta h_{tt} + \gamma \qquad (4.37)$$

with $$h_t = -2h\Phi \qquad (4.38)$$

when $t=0$: $h=1$, $\Phi=\frac{1}{2}$ (4.39)

Equation (4.39) requires that

$$F_0(z) = \tfrac{1}{2}z \qquad (4.40)$$

Now in inviscid flow, the instantaneous stream function is determined uniquely by the boundary conditions, so if the boundary conditions are to hold at the initial instant, then F_0 must have the form of (4.40). Alternatively we may regard $F_0(z)$ as an unknown function which is determined as part of the solution.

We must solve the coupled equations (4.37), (4.38) for h and Φ subject to initial condition (4.39). First, we eliminate Φ from (4.37) using (4.38) to give:

$$(\beta+\tfrac{1}{2h})h_{tt} - \tfrac{3}{4}(\tfrac{h_t}{h})^2 + \gamma = 0 \qquad (4.41)$$

Equation (4.41) was derived in WLK 1 with a different scaling so that γ was replaced by unity. For this case, with the initial condition $h=1$, $h_t = 0$, it was solved numerically for all β and an analytic solution was given for $\beta = 0$ (c.f. case (ii) below). Since (4.41) does not contain t explicitly, we can obtain a first integral by introducing $J(h) = \tfrac{1}{2}h_t^2$, so that $J' = h_{tt}$. Then we have:

$$J' - \frac{3J}{h(1+2\beta h)} = \frac{-2h\gamma}{1+2\beta h} \qquad (4.42)$$

This equation is of standard form and has the solution:

$$J(h) = h^3\left(\frac{1+2\beta}{1+2\beta h}\right)^3\left\{\tfrac{1}{2} + \left(\frac{2\gamma}{(1+2\beta)^3}\right)\left[4\beta^2(1-h) + 4\beta\log(\tfrac{1}{h}) + \tfrac{1}{h} - 1\right]\right\} \qquad (4.43)$$

Now $h_t = -\sqrt{2J(h)}$, so we have formally,

$$t = \int_h^1 \left[2J(\alpha)\right]^{-\frac{1}{2}}\, d\alpha \qquad (4.44)$$

This integral is not amenable to analytical calculation in the general case, but may be evaluated in the following special cases.

<u>case (i) $\gamma = 0,\ \beta \neq 0$</u>

In this case J(h) reduces to:

$$J(h) = \tfrac{1}{2}h^3\left(\frac{1+2\beta}{1+2\beta h}\right)^3 \qquad (4.45)$$

So we have:

$$t = \int_h^1 \frac{(1+2\beta x)^{3/2}}{(1+2\beta)^{3/2}x^{3/2}}\,dx \qquad (4.46a)$$

$$= (1+\tfrac{1}{2\beta})^{-3/2}\int_h^1 (1+\tfrac{1}{2\beta x})^{3/2}dx \qquad (4.46b)$$

Equation (4.46b) is integrated using the substitution $1+\frac{1}{2\beta x} = q^2$ to give:

$$t = \frac{1}{\beta}(1+\tfrac{1}{2\beta})^{-\frac{3}{2}}\left[(1+\tfrac{1}{2\beta h})^{\frac{1}{2}}(1-\beta h) - (1+\tfrac{1}{2\beta})^{\frac{1}{2}}(1-\beta) - \tfrac{3}{2}\coth^{-1}(1+\tfrac{1}{2\beta h})^{\frac{1}{2}} + \tfrac{3}{2}\coth^{-1}(1+\tfrac{1}{2\beta})^{\frac{1}{2}}\right] \qquad (4.47)$$

This transcendental equation cannot be inverted to give h(t). From (4.38) and (4.45) Φ is given by

$$\Phi = \frac{-h_t}{2h} = \tfrac{1}{2}h^{1/2}\left(\frac{1+2\beta}{1+2\beta h}\right)^{\frac{3}{2}} \qquad (4.48)$$

Solutions (4.47) and (4.48) are shown in figures 4.2(a) and 4.2(b) respectively.

The dimensionsless hydrodynamic force on the disc is βh_{tt}, which from (4.19), (4.20), and (4.21) is proportional to $p_o(t)$, A(t) and $\mathcal{Y}_H(t)$. From equation (4.45) we have:

$$h_{tt} = J'(h) = \tfrac{3}{2}h^2\frac{(1+2\beta)^3}{(1+2\beta h)^2} \qquad (4.49)$$

The solutions for Φ, which is proportional to radial velocity, and h_{tt} shown in figures 4.2(b) and 4.2(c) are of particular interest. We see that both Φ and h_{tt} are strongly dependent on β. For small β, h_{tt} or the fluid pressure decays monotonically as does the radial velocity. For large β, the force is relatively small except for a short time near $t = 1$, when the body is rapidly brought to a stop by a very large force, which approaches a unit impulse as $\beta \to \infty$. The force comes from the large pressure generated under the body by the large radial velocities which arise as the gap becomes very narrow. This is evident from the comparison of the $\beta = 50$ curves in figure 4.2(b) and 4.2(c) where the maxima of the h_{tt} and Φ curves are coincident. If equation (4.37) is multiplied by h_t, the right hand side is immediately recognized as the time derivative of the kinetic energy of the body; the time integral of this term is the work done by the body in transferring its own energy to the surrounding fluid. When β is small, most of the kinetic energy is contained in the fluid which has a chance to escape at the edge of the body and there is only a minor transfer of kinetic energy to the fluid in the gap before final arrest. For large β, however, the escaping fluid contains only a small portion of the total kinetic energy with the result that very large accelerations and dynamic pressures can be built up in the near collision or impact region. This behaviour has important implications for the

collision and recoil of an elastic body which are discussed in the concluding section.

<u>case (ii) $\beta = 0$, $\gamma \neq 0$</u>

In this case the equation for Φ, (4.37), becomes decoupled from h, so it is easier to proceed directly. We have to solve:

$$\Phi_t + \Phi^2 = \gamma \tag{4.50}$$

with when $t=0$: $\Phi = \frac{1}{2}$ (4.51)

This problem has different solutions depending on the value of γ.

If $\gamma = \frac{1}{4}$, then $\Phi = \frac{1}{2}$ (4.52)

If $\gamma < \frac{1}{4}$, then $\Phi = \gamma^{1/2} \coth[\gamma^{1/2}(t+c)]$ (4.53)

with $c = \gamma^{-1/2} \coth^{-1}(4\gamma)^{-1/2}$ (4.54)

If $\gamma > \frac{1}{4}$, then $\Phi = \gamma^{1/2} \tanh[\gamma^{1/2}(t+c)]$ (4.55)

with $c = \gamma^{-1/2} \tanh^{-1}(4\gamma)^{-1/2}$ (4.56)

Then we use (4.38) to find the respective solutions for h:

$\gamma = \frac{1}{4}$, $h = e^{-t}$ (4.57)

$\gamma < \frac{1}{4}$, $h = \operatorname{cosech}^2[\gamma^{1/2}(t+c)] / \operatorname{cosech}^2(c\gamma^{1/2})$ (4.58)

$\gamma > \frac{1}{4}$, $h = \operatorname{sech}^2[\gamma^{1/2}(t+c)] / \operatorname{sech}^2(c\gamma^{1/2})$ (4.59)

These solutions for h and Φ are shown in figures 4.3(a), 4.3(b). Comparison of figures 4.2(a), 4.2(b), 4.3(a) and 4.3(b) clearly shows the difference between draining behaviour under a force due to body inertia and a constant applied force such as gravity. For a constant applied force with $\gamma > \frac{1}{4}$ the radial velocity asymptotically approaches a constant value for which the dynamic pressure force in the fluid gap just balances the applied force. The radial velocity cannot, therefore, exhibit a local maximum as a function of time, nor can there be a pressure overshoot when $\beta = 0$.

<u>case (iii) $\beta = 0$, $\gamma = 0$</u>

This is the simplest case of all; we must solve:

$$\Phi_t + \Phi^2 = 0 \quad \text{with } \Phi = \tfrac{1}{2} \text{ when } t = 0 \qquad (4.60)$$

This gives $$\Phi = \frac{1}{t+2} \qquad (4.61)$$

Then (4.38) gives: $$h = \frac{4}{(t+2)^2} = 4\Phi^2 \qquad (4.62)$$

The foregoing inviscid solutions for Φ and h describe a large part of the motion in the case of very large Re_o and may be used as a basis for including small viscous effects in a boundary layer theory for large Re_o.

4.4 SOLUTION PROCEDURE FOR VISCOUS CASE

There are two main problems of interest in solving (4.27). The first is the hydrodynamic arrest by viscous dissipation of a moving body approaching a solid boundary, where the driving force for the motion is the initial momentum of the body and fluid. The second problem is that of complete draining of the fluid in the gap under the action of a constant applied force. The solution procedure for these two problems is outlined below.

(a) hydrodynamic arrest

The body will come to rest before reaching the plane only if there is no applied force, i.e. we must take $Y = 0$. From equation (4.27) we are left with a two-parameter family of solutions for different values of β and Re_o. The initial stream function $F_o(z)$ is unknown, but it must reflect the previous history of the motion and the instantaneous Reynolds number based on gap height when the solution is started. If Re_o and the initial gap height are large, we would expect $F_o(z)$ to be very close to the inviscid solution found in section 3, except for the presence of thin boundary layers on the top and bottom walls. On the other hand, for smaller values of Re_o we would expect the velocity profile F_{oz} to be more or less parabolic. In fact a suitable form

for $F_o(z)$ will emerge as part of the solution which is described below.

We consider for the moment the solution for a given value of β and a large Re_o. On physical grounds, we expect both the dimensionless gap height h and the descent rate $|h_t|$ to decrease monotonically as the motion progresses. We can define a time-dependent Reynolds number, $Re(t) = Re_o h|h_t|$, which will decrease monotonically from Re_o to zero during the motion. When Re_o is very large we could, for example, choose the inviscid flow as a realistic initial condition, but when Re_o is not large, the form of the initial condition is not obvious. However, a suitable candidate is available in the form of the instantaneous solution for large Re_o at the appropriate time when Re(t) has the desired value. This solution will be a good choice for the initial stream function provided that it is independent of the large value used for Re_o. In this way, the solution should become independent of the actual initial conditions and exhibit a similarity behaviour in which the memory of the detailed initial profile is lost.

The above argument provides us with two benefits. Firstly, the initial condition chosen for the stream function is, in a sense, the most natural one. Secondly, we need only one solution of the problem to cover the whole range of Re_o at a given β. To obtain the solution for

smaller Re_o, we simply discard the portion of the solution with $Re(t) > Re_o$ and re-scale the remaining portion of the motion to give unit initial conditions.

(b) draining under a constant force

When a force is applied, the body will not come to rest until it is in contact with the plane, a process which takes an infinite time. There are two cases which are of particular interest - (i) the body is dropped from rest, and (ii) the body arrives from "far away" with non-zero initial velocity. In both cases, the velocity scale is determined by the applied force, so we use a different velocity scale, namely $V_o = (h_o/a)(4\mathcal{F}_A/\pi\rho a^2)^{1/2}$. Then we find that $\gamma = V_o^2/w_o^2$ and equation (4.27) becomes:

$$F_{zt} + F_z^2 - 2FF_{zz} - F_{zzz}/Re_o\gamma^{1/2} = \beta h_{tt} + 1 \qquad (4.63)$$

where when $t=0$: $h=1$, $h_t = -\gamma^{-1/2}$, $F = F_o(z)$ (4.64)

If we redefine the Reynolds number so that $\overline{Re}_o = Re_o\gamma^{1/2} = h_o V_o/\nu$ and define $\overline{w}_o = -\gamma^{-1/2}$, then we have:

$$F_{zt} + F_z^2 - 2FF_{zz} - F_{zzz}/\overline{Re}_o = \beta h_{tt} + 1 \qquad (4.65)$$

where when $t=0$: $h=1$, $h_t = \overline{w}_o$, $F = F_o(z)$ (4.66)

Equation (4.65) is the same as (4.27) with $\gamma = 1$. The only difference is in the initial value of h_t. It is clear then,

that by replacing γ by zero or unity in (4.27), we can solve the two problems of major interest, provided we allow a little more flexibility in the initial value of h_t. Thus we do not need to consider arbitrary values of γ in (4.27).

In case (i) when the body is dropped from rest, both $\overline{W}_0$ and $F_0(z)$ are zero. The solution of (4.65) is essentially different for each combination of $\overline{Re}_0$ and β, so the full two-parameter family of solutions is needed. This case will be discussed further in Chapter 5.

In case (i) the initial condition is unspecified and, as in section (a) above, we must find the initial stream function as part of the solution; we must also find the appropriate value of $\overline{W}_0$. The time-dependent Reynolds number for this problem is $\overline{Re}(t) = \overline{Re}_0 h^2(t)$, since V_0 is proportional to h_0. The behaviour is qualitatively the same as that for problem (a) and the same method of solution may be applied. For a given value of β, we take $\overline{Re}_0$ to be very large and use the inviscid solution as the initial condition. The sequence of states with smaller $\overline{Re}(t)$ then gives the initial conditions for each smaller value of $\overline{Re}_0$. Again only one solution of the problem is needed to cover the whole range of $\overline{Re}_0$ for a given β.

The solution method outlined above enables us to simplify the range of parameters and starting conditions for the solution. Instead of a three parameter family of

solutions with unknown initial conditions, we only need to find two one-parameter families of solutions for the two problems (a) and (b). The extra degrees of freedom have been removed by choosing the most convenient (and realistic) initial conditions. In addition, the equations for F and h decouple when $\beta = 0$. This will enable us to find new boundary layer type similarity solutions to the Navier-Stokes equations in which the inviscid outer flow has a meaningful physical interpretation (sections 4.5, 4.6). This simplification is not possible for non-zero β; since these solutions require much more numerical computation, we shall only present results for $\beta = 0$.

4.5 VISCOUS DRAINING FOR SMALL β AND CONSTANT APPLIED FORCE

We see from (4.31) that for many problems $\beta << 1$ since it is the ratio of the mass of the body to the mass of the fluid in the gap multiplied by the factor $(h_o/a)^2$, which is assumed to be small. This case also includes the latter part of any draining motion for a constant applied force, since for draining $h \longrightarrow 0$ at large times. We will tackle this problem first since its solution is the simpler of the two cases and serves as a guide for the arrest problem to be discussed in section 4.6.

(a) boundary layer solution

The method described in section 4.4 requires that we should choose $\overline{Re}_o$ to be large and suggests that we use the inviscid solution with fully established top and bottom boundary layers as the initial condition. We shall begin by analyzing the boundary layer for large $\overline{Re}_o$. The "outer" flow is given by the displaced inviscid stagnation point,

$$F = (z - \delta(t))\,\Phi(t) \tag{4.67}$$

where $\delta(t)$ is the boundary layer displacement thickness defined by:

$$\delta(t) = \int_0^{\frac{h}{2}} (1 - F_z/\Phi)\, dz \tag{4.68}$$

We may use the symmetry of the flow about $z = h/2$ to replace boundary conditions (6.24) by:

$$\text{on } z = \tfrac{1}{2}h(t): \quad F = -\tfrac{1}{4}h_t, \quad F_{zz} = 0 \tag{4.69}$$

Then the inviscid part of the flow gives:

$$\Phi' + \Phi^2 = 1 \tag{4.70}$$

$$(h - 2\delta)\Phi = -\tfrac{1}{2}h_t \tag{4.71}$$

where $$\text{at } t = 0: \quad h = 1, \quad h_t = \overline{w}_o \tag{4.72}$$

The above set of equations cannot be solved immediately because of the presence of δ which depends on the detailed structure of the boundary layer. The boundary layer scaling

is $F = \overline{Re}_o^{-\frac{1}{2}} f(\zeta,t)$ with $\zeta = \overline{Re}_o^{1/2} z$. Equations (4.65), (4.23), (4.69) and (4.66) become:

$$f_{\zeta t} + f_\zeta^2 - 2ff_{\zeta\zeta} - f_{\zeta\zeta\zeta} = 1 \qquad (4.73)$$

subject to boundary and initial conditions:

$$\text{on } \zeta = 0: \quad f = 0, \quad f_\zeta = 0 \qquad (4.74)$$

$$\text{as } \zeta \to \infty: \quad f_\zeta \sim \Phi(t) \qquad (4.75)$$

$$\text{when } t = 0: \quad f = f_0(\zeta) \qquad (4.76)$$

Equations (4.70) and (4.73)-(4.76) are independent of h(t) and so can be solved independently of (4.71) and (4.72). This simplification is a direct result of setting $\beta = 0$ which decouples the equation for F from that for h. There remains only a secondary coupling in the boundary condition. The inviscid problem for Φ is completely decoupled from h and hence δ. Thus we are able to obtain an exact solution with all higher order boundary layer effects implicitly included. The freedom of choice of initial condition then allows us to find an exact similarity solution of the whole problem which is valid provided separate boundary layers exist at the top and bottom boundaries.

The solutions of (4.70) are (c.f. (4.52)-(4.56)):

$$\Phi = 1, \quad \Phi = \coth(t+c), \quad \Phi = \tanh(t+c) \qquad (4.77)$$

For large t all three of the solutions (4.77) have the same limiting behaviour, namely $\Phi \to 1$. In fact the third solution with c = 0 describes the inviscid solution given in WLK 1 for the start up motion from rest of a body with $\beta = 0$ subject to a constant applied force. During this initial start up motion, the body is accelerated until the radial velocity and pressure in the inviscid core achieves a steady distribution which just balances the applied force. Thus for any motion in which there is an inviscid core at large time in which the applied force is balanced by the pressure distribution in the gap, $\Phi \to 1$ and the boundary layers are steady. Therefore, we may set $f(\zeta,t) = f(\zeta) = f_0(\zeta)$, with

$$f'^2 - 2ff'' - f''' = 1 \tag{4.78}$$

$$\text{on } \zeta = 0: \quad f = 0, \; f' = 0 \tag{4.79}$$

$$\text{as } \zeta \to \infty: \quad f' \to 1 \tag{4.80}$$

Equations (4.78)-(4.80) are simply those for the steady stagnation point boundary layer, first solved by Homann (1936) and solved more completely by Frössling (1940). What seemed to be a complicated time-dependent boundary layer flow is in fact a simple steady one. The only time-dependence is in the equation for h(t):

$$h_t = -2h + 4\delta \tag{4.81}$$

$$h = 1 \quad \text{when} \quad t = 0 \tag{4.82}$$

These equations have solution:

$$h = e^{-2t} + 2\delta(1-e^{-2t}) \tag{4.83}$$

where δ is the constant value:

$$\delta = \overline{Re}_o^{-1/2} \lim_{\zeta \to 0} (\zeta - f) = 0.568902 (\overline{Re}_o^{-1/2}) \tag{4.84}$$

The initial disc velocity is

$$h_t = -\overline{w}_o = -2 + 4\delta \tag{4.85}$$

The above solution is exact whenever there are distinct boundary layers in the flow, but is not valid after the boundary layers begin to merge. The function f is within 10^{-7} of unity at $\zeta = 4$ and we take this to be the edge of the boundary layer. This "edge" reaches the channel mid-plane when $\zeta = 4$ corresponds to $z = h/2$, i.e when $\overline{Re}_o h^2 = 64$. But $\overline{Re}_o h^2 = \overline{Re}(t)$, so we may take the above solution to be valid whenever $\overline{Re}(t) > 64$. When this limit is passed, the solution must be continued numerically, since the nonlinear interaction of the two boundary layers is too complicated to describe analytically.

(b) numerical solution

We take $\overline{Re}_\delta = 64$ and use the boundary layer solution to equations (4.78) -(4.80) as the initial condition. First, equation (4.78) for $f(\zeta)$ is integrated up to $\zeta = 8$ using a shooting method with interval halving to find $f''(0)$ and a fifth order Runge-Kutta-Verner method of integration. To avoid large errors at the symmetry boundary, $z = h/2$, the derivative of the stream function is taken to be $F_z(z) \cdot F_z(1-z)$, with $z = \zeta/8$.

The moving boundary is inconvenient for numerical integration and we introduce a new scaled coordinate $x = z/h(t)$ which is constant at $z = h$. We also define a scaled velocity $U = F_z = F_x/h$ whose time derivative is:

$$U_t = 1 + U_{xx}/\overline{Re}_\delta h^2 + U_x h_t x/h + 2FU_x/h - U^2 \qquad (4.86)$$

The boundary conditions in terms of these new scaled variables are:

$$\text{on } x=0: \quad F=0, \quad U=0 \qquad (4.87)$$

$$\text{on } x=\tfrac{1}{2}: \quad U_x=0, \quad h_t=-4F \qquad (4.88)$$

The space dimension is now discretized so that x is restricted to the values x_I, $I = 1,\ldots,n$ with $x_1 = 0$, $x_{n-1} = 0.5$ and $x_I - x_{I-1} = \Delta x = 0.5/(n-2)$. It is advantageous to choose $n-2 = 2^m$, so that Δx may be doubled without needing to interpolate. For our problem $n = 130$ was

adequate to keep the error below 10^{-5}. The discretization leaves a set of n+1 ordinary differential equations for U_I and h. We represent the derivatives of U and F by finite differences accurate up to $O(\Delta x^4)$ and then explicitly evaluate the Δx^4 terms to give a conservative estimate of the error. When the estimated error is very small, the space step Δx can be doubled to speed up the integration. Equations (4.86)-(4.88) rewritten in the discretized variables are integrated forward in time as far as is necessary using the aforementioned Runge-Kutta-Verner method.

The truncation and integration errors for each time derivative are controlled to a relative magnitude of $10^{-5}t$. This estimate is very conservative, so the results can be regarded as very accurate. In fact, the integration need only be carried up to moderate values of t, since then Re(t) is very small, and the low Reynolds number analytic theory described next can be applied.

(c) low Reynolds number solution

The final stage of draining will occur with $\overline{Re}(t)$ very small, so the motion is governed by the equations with small $\overline{Re}_o$. The motion is very slow, so we set $F = \overline{Re}_o f$ and $t = T/\overline{Re}_o$ with f and T of order unity. Equation (4.65) becomes:

$$f_{zzz} + 1 = \overline{Re}_o^2 (f_{zT} + f_z^2 - 2ff_{zz}) \tag{4.89}$$

The associated boundary and initial conditions are:

$$\text{on } z=0: \quad f=0, \; f_z=0 \tag{4.90}$$

$$\text{on } z=h(T): \quad f=-\tfrac{1}{2}h_T, \; f_z=0 \tag{4.91}$$

$$\text{when } T=0: \quad h=1, \; h_T=\overline{w}_o/\overline{Re}_o=\tilde{w}_o, \; f=f_o(z) \tag{4.92}$$

The initial conditions $\tilde{w}_o$ and $f_o(z)$ must correspond to the final stages of the numerical solution. However, there is a "natural" condition which is in fact the same as the numerical solution at the appropriate time.

We pose an expansion:

$$f(z,T;\overline{Re}_o) \sim \sum_0^\infty \tilde{f}_{2n}(z,h(T))\overline{Re}_o^{2n} \tag{4.93}$$

which must be asymptotic for fixed z, T as $\overline{Re}_o \to 0$. The problems for the first two terms are:

$$\tilde{f}_{ozzz} + 1 = 0 \tag{4.94}$$

$$\tilde{f}_{2zzz} = \tilde{f}_{ozT} + \tilde{f}_{oz}^2 - 2\tilde{f}_o\tilde{f}_{ozz} \tag{4.95}$$

with $$\text{on } z=0: \quad \tilde{f}_o=0, \; \tilde{f}_{oz}=0, \; \tilde{f}_2=0, \; \tilde{f}_{2z}=0 \tag{4.96}$$

$$\text{on } z=h(T): \quad \tilde{f}_{oz}=0, \quad \tilde{f}_{2z}=0 \tag{4.97}$$

The solutions to these problems were given in WLK 1 and are:

$$\tilde{f}_o = \tfrac{1}{12}z^2(3h-2z) \tag{4.98}$$

$$\tilde{f}_2 = \tfrac{1}{48}z^2h_T(z^2-2h^2) - \tfrac{1}{5040}z^2(2z^5-7z^4h+14h^5) \tag{4.99}$$

We must solve for h; we again assume an asymptotic expansion:

$$h(T;\overline{Re_o}) \sim \sum_0^\infty \tilde{h}_{2n}(T)\,\overline{Re_o}^{2n} \tag{4.100}$$

The first two problems are:

$$\tilde{h}_{oT} + \tfrac{1}{6}\tilde{h}_o^3 = 0 \tag{4.101}$$

$$\tilde{h}_{2T} + \tfrac{1}{2}\tilde{h}_o^2\tilde{h}_2 = \tfrac{1}{24}\tilde{h}_o^4\tilde{h}_{oT} + \tfrac{1}{280}\tilde{h}_o^7 \tag{4.102}$$

with $\tilde{h}_o = 1, \quad \tilde{h}_2 = 0$ when $t = 0$. (4.103)

The solutions of (4.101)-(4.103) are:

$$\tilde{h}_o = (1 + \tfrac{1}{3}T)^{-1/2} \tag{4.104}$$

$$\tilde{h}_2 = -\tfrac{17}{1680}\left[(1+\tfrac{1}{3}T)^{-\frac{3}{2}} - (1+\tfrac{1}{3}T)^{-\frac{5}{2}}\right] \tag{4.105}$$

$$= -\tfrac{17}{1680}\left(\tilde{h}_o^3 - \tilde{h}_o^5\right) \tag{4.106}$$

One notices that the numerical coefficients in $\tilde{f}_2$ and $\tilde{h}_2$ are much smaller than those in $\tilde{f}_o$ and $\tilde{h}_o$; examination of the problems for $\tilde{f}_4$ and $\tilde{h}_4$ indicates that the trend continues. The relative contribution to h of $\tilde{h}_2$ is largest when T = 3, when the ratio is $\tilde{h}_2/\tilde{h}_o \approx 1/43$. Hence, we may conservatively estimate the error in the two term series for h by $\frac{1}{43}(\overline{Re_o})^4$. For this error to be less then 10^{-5}, we must have $\overline{Re_o} < 0.14$. This means that the numerical calculation in (b) must be carried at least up to Re(t) = 0.14, i.e. until h(t) < 0.05. This occurs when $t \approx 21$. The solution gives:

$$\tilde{W}_0 = -\frac{1}{6} - \frac{17}{5040}\,\overline{Re}_0^2 + O(\overline{Re}_0^4) \qquad (4.107)$$

and the initial stream function $f_0(z)$ comes from (4.98) and (4.99) with $h = 1$ and $h_\tau = \tilde{W}_0$.

The solutions given in sections (a), (b) and (c) together constitute the complete solution of the problem for arbitrary $\overline{Re}_0$ and for all time. The change in velocity profile from boundary layer type to parabolic is illustrated in figure 5.4, which gives the profiles calculated numerically as in (b) starting at $\overline{Re}_0 = 64$. The effect of $\overline{Re}_0$ on the descent of the body is shown in figure 5.5(a); here h(t) is shown for many values of $\overline{Re}_0$. The matching of the three solutions from sections (a), (b) and (c) is illustrated in figure 4.5(b) which shows the height calculated by each method for $\overline{Re}_0 = 64$. The small $\overline{Re}_0$ solution from section (c) is scaled so that it agrees with the tail end of the numerical solution. The close correspondence between the asymptotic similarity solution (a) and the intermediate $\overline{Re}_0$ numerical solution is maintained to $t \sim 2.0$.

4.6 HYDRODYNAMIC ARREST WITH SMALL β

As discussed earlier, the parameter β represents the ratio of the forces due to the inertia of the body to those due to the inertia of the fluid. It might, therefore,

appear unreasonable to consider the case $\beta = 0$ for hydrodynamic arrest because if we neglect both the inertia of the body and the applied force there is no apparent forcing in the problem. However, if the gap is sufficiently small, the fluid within it may have a large radial velocity so that the momentum posessed by the fluid at the initial instant is much larger than that of the body which is moving much more slowly in the axial direction. Thus, the forcing of the problem comes from the initial conditions and there is no contradiction in examining the limit $\beta = 0$.

The solution of this problem is more complicated than that given in section 4.5, but it has the same three components - an exact similarity boundary layer solution for large Re_o or $Re(t)$, a numerical solution for intermediate Re_o or $Re(t)$ and a low Reynolds number solution.

(a) boundary layer solution

As in section 4.5, the "outer" inviscid flow is given by:

$$F = (z - \delta(t))\, \Phi(t) \qquad (4.108)$$

with $\delta(t)$ defined by (4.68). However, $\Phi(t)$ is now governed by a different equation,

$$\Phi' + \Phi^2 = 0 \qquad (4.109)$$

whose solution is:

$$\Phi = \frac{1}{t+c_1} \tag{4.110}$$

in which c_1 is an arbitrary constant to be determined from the initial condition. The boundary layer scaling is the same as in section 4.5 and the equations are:

$$f_{\zeta t} + f_\zeta^2 - 2ff_{\zeta\zeta} - f_{\zeta\zeta\zeta} = 0 \tag{4.111}$$

where on $\zeta = 0$: $f = 0,\ f_\zeta = 0$ (4.112)

as $\zeta \to \infty$: $f_\zeta \sim \Phi(t)$ (4.113)

when $t = 0$: $f = f_0(\zeta)$ (4.114)

As before, setting $\beta = 0$ has decoupled the problem for f from that for h, so we can solve for f independently of h. Equations (4.111)-(4.114) describe a time-dependent axisymmetric stagnation point boundary layer flow which is analogous to the two-dimensional form studied by Yang (1958). The particular form of Φ (4.110) allows us to find a time-dependent similarity scaling:

$$f = \Phi^{1/2} g(\eta) \quad \text{with} \quad \eta = \Phi^{1/2}\zeta \tag{4.115}$$

Then using (4.109) we derive the similarity problem:

$$g''' + 2gg'' - g'^2 + \tfrac{1}{2}\eta g'' + g' = 0 \tag{4.116}$$

where on $\eta = 0$: $g = 0,\ g' = 0$ (4.117)

and as $\eta \to \infty$: $g' \to 1$ (4.118)

We define the number d by

$$d = \int_0^\infty (1-g')\,d\eta = \lim_{\eta\to\infty}(\eta - g) = 0.601159 \qquad (4.119)$$

Then $$\delta = Re_0^{-\frac{1}{2}}\,\Phi^{-\frac{1}{2}}\,d \qquad (4.120)$$

The equation for h(t) becomes :

$$h_t + 2h\Phi = 4\delta\Phi = 4dRe_0^{-\frac{1}{2}}\Phi^{\frac{1}{2}} \qquad (4.121)$$

This has solution:

$$h = \frac{c_2}{(t+c_1)^2} + \frac{8}{5}d\,Re_0^{-\frac{1}{2}}(t+c_1)^{\frac{1}{2}} = c_2\Phi^2 + \frac{8}{5}\delta \qquad (4.122)$$

We now apply initial conditions :

$$\text{when } t=0: \quad h=1, \quad h_t=-1 \qquad (4.123)$$

to get :

$$c_1^{\pm} = 2 + 8d^2/Re_0 \pm 4\sqrt{2}\,d\,Re_0^{-\frac{1}{2}}(1+2d^2/Re_0)^{1/2} \qquad (4.124)$$

and $$c_2 = \frac{1}{5}c_1^2(1+2c_1) \qquad (4.125)$$

For large Re_0, we have $c_1^{\pm} \approx 2$, $c_2 \approx 4$. To find the correct sign for c_1 in (4.124), we use (4.110) and (4.121) to obtain $\Phi(0) = 1/c_1 = h_t(0)/(4\delta(0)-2h(0)) = 1/(2-4\delta(0))$; this shows that $c_1 = 2-4\delta(0) < 2$, so we choose $c_1 = c_1^-$.

Once again an apparently difficult time-dependent boundary layer problem has been greatly simplified by the use of "natural" initial conditions. The above solution is again exact whenever there are distinct boundary layers. The function g' is within 10^{-8} of unity at $\eta = 4$ and it is

convenient to take this as the edge of the boundary layer, consistent with section 5.5. At the time when $\eta = 4$ corresponds to $z = h/2$, we have $4 = \Phi t Re_o^{\frac{1}{2}} h/2$, i.e. $Re_o \Phi h^2 = 64$. Now for large Re(t), $h_t \approx -2h\Phi$, so $Re(t) \approx 2Re_o \Phi h^2$. Hence the boundary layer solution is valid whenever $Re(t) > 128$. As before, this estimate is very conservative and the solution is still quite accurate at lower Reynolds numbers.

(b) numerical solution

The solution procedure is identical to that described in section 4.5, except that we use an initial Reynolds number of 128. The flow decelerates rapidly so that time derivatives become very small. Because of this, the error control is relaxed slightly - the relative error control of 10^{-5} is retained only until the absolute value falls below 10^{-2}, when an absolute error of up to 10^{-7} is allowed.

(c) low Reynolds number solution

The time scale used in section 4.5(c) is inappropriate for this problem since there is no forcing and the flow would be identically zero. In the low Reynolds number limit, the inertia forces are tiny, so this part of the motion is just a rapid deceleration to zero flow, i.e. the

actual arrest of the body. We introduce a short time scale $t = Re_o \tau$, then we have:

$$F_{zzz} - F_{z\tau} = Re_o (F_z^2 - 2FF_{zz}) \tag{4.126}$$

with on $z=0$: $F=0$, $F_z=0$ (4.127)

$$\text{on } z=h(\tau): \quad F_z=0, \quad h_\tau = -2Re_o F \tag{4.128}$$

$$\text{when } \tau=0: \quad h=1, \quad h_\tau = -Re_o, \quad F=F_o(z) \tag{4.129}$$

A suitable form for $F_0(z)$ is to be determined. We notice that h_τ is small, so h will remain close to unity and we therefore pose asymptotic expansions of the form:

$$h(\tau; Re_o) \sim 1 + Re_o \tilde{h}_1(\tau) + Re_o^2 \tilde{h}_2(\tau) \tag{4.130}$$

$$F(z,\tau; Re_o) \sim \tilde{F}_o(z,\tau) + Re_o \tilde{F}_1(z,\tau) + Re_o^2 \tilde{F}_2(z,\tau) \tag{4.131}$$

The zero order problem is:

$$\tilde{F}_{ozzz} - \tilde{F}_{oz\tau} = 0 \tag{4.132}$$

where on $z=0$: $\tilde{F}_o = 0$, $\tilde{F}_{oz} = 0$ (4.133)

and on $z=1$: $\tilde{F}_{oz} = 0$ (4.134)

The boundary layer condition has been "moved" to $z = 1$ by expanding in a Taylor series about $z = 1$. The general solution to (4.132)-(4.134) is:

$$\tilde{F}_o = \sum_1^\infty a_n (1 - \cos n\pi z) e^{-n^2\pi^2\tau} \tag{4.135}$$

The a_n are to be determined from the initial condition. The solution is very strongly damped and after a short while it will be dominated by the leading term. Hence the "natural" initial condition is:

$$\text{when } \tau = 0: \quad \tilde{F}_0 = a_1(1-\cos \pi z) \tag{4.136}$$

and the solution is then:

$$\tilde{F}_0 = a_1(1-\cos \pi z)e^{-\pi^2 \tau} \tag{4.137}$$

The first order problem for h is:

$$\tilde{h}_{1\tau} = -2\tilde{F}_0 \quad \text{on } z=1 \tag{4.138}$$

$$= -4a_1 e^{-\pi^2 \tau} \tag{4.139}$$

$$\text{Thus} \qquad \tilde{h}_1 = -\frac{4a_1}{\pi^2}(1-e^{-\pi^2 \tau}) \tag{4.140}$$

The second initial condition is:

$$\text{when } \tau = 0: \quad \tilde{h}_{1\tau} = -1 \tag{4.141}$$

$$\text{Therefore we have} \qquad a_1 = \frac{1}{4} \tag{4.142}$$

The next order problem is:

$$\tilde{F}_{1zz\tau} - \tilde{F}_{1z\tau} = \tilde{F}_{0z}^2 - 2\tilde{F}_0 \tilde{F}_{0zz} \tag{4.143}$$

$$\text{with} \qquad \text{on } z=0: \quad \tilde{F}_1 = 0, \quad \tilde{F}_{1z} = 0 \tag{4.144}$$

$$\text{on } z=1: \quad \tilde{F}_{1z} + h_1 \tilde{F}_{0zz} = 0 \tag{4.145}$$

The forcing in (4.143) has time-dependence $e^{-2\pi^2\tau}$ which is very strongly damped. Hence the only important contribution is of the same form as (4.137), forced by the $(1 - \cos \pi z)$ term in the initial condition and by (4.145). However, we can arrange that this term is zero by absorbing any contribution into the zero order solution. Hence we can neglect the first and higher order corrections to F. Thus, we have:

$$h = 1 - \frac{1}{\pi^2}(1 - e^{-\pi^2\tau}) Re_0 + O(Re_0^2) \qquad (4.146)$$

and the final position of the disc is given by:

$$h_\infty = 1 - \frac{1}{\pi^2} Re_0 + O(Re_0^2) \qquad (4.147)$$

As in section 4.5, it seems that the numerical coefficients will become smaller with increasing powers of Re_0, so we may estimate the error in (4.147) as roughly $\frac{1}{10}Re_0^2$. Then we have five-figure accuracy provided $Re_0 < 10^{-2}$. Hence the numerical calculation must be continued until $Re(t) = 10^{-2}$. This occurs at $t \approx 8.5$.

An unusual feature of the above solution is that the velocity profile ultimately takes on the shape of a half sine wave rather than the parabolic form usually associated with low Reynolds number flow. The evolution of the velocity profile is shown in figure 5.6. The effect of Re_0 on the arrest of the body is shown in figure 4.7(a) and the matching of solutions (a), (b) and (c) is illustrated in figure

4.7(b). Figure 4.8 shows the ultimate gap height h_∞ as a function of Re_0. This is determined using (4.147), the numerical solution and, if necessary, (4.122). We see that h_∞ varies appreciably only for Reynolds numbers in the range $1 < Re_0 < 10^4$.

4.7 CONCLUDING REMARKS

Equation (4.27) contains three parameters Re_0, β and γ, and while we have indicated the solution procedure for every regime, numerical results have been presented in the inviscid limit $Re_0 \to \infty$ for either $\gamma = 0$ or $\beta = 0$, and for viscous fluids only for the limiting case $\beta \to 0$. The inviscid results clearly indicate that for $\beta \neq 0$ the finite Re_0 solutions will depart substantially from the curves in figures 4.6-4.8. The effect of viscosity on the solutions of section 4.3 would be to slow the descent rate in general and to damp the singular behaviour for large β observed in the solutions for Φ and h_{tt} in figures 4.2(b), 4.2(c). In the case $\gamma = 0$, the viscous forces would cause the premature arrest of the body before contact as explained in section 4.4. For large β the inertia of the body provides an important source of energy which must be dissipated by viscous stresses before the body comes to rest. The dramatic acceleration of the core flow shown in figure 4.2(b) is in sharp contrast to the decelerating core flow of

figure 4.6. At high initial Reynolds number and large β the rapid acceleration of the core flow would still occur leading to the equivalent of the start-up boundary layers that result from impulsively started motions in pipe and channel flows. The subsequent rapid deceleration of the fluid in the core would lead to a complicated overshoot in the boundary layer velocity profile. At lower initial Reynolds number, the effects of viscosity would be felt more quickly; the acceleration of the core flow would be damped and the increase in gap pressure would be diminished.

Real impact problems are further complicated by the elastic deformation of the boundaries which can lead to a damped oscillation of the body after near contact as discussed by Davis, Serayssol & Hinch (1986). In the latter theory, which is based on a viscosity dominated lubricating layer analysis, the inertia of the fluid is neglected and thus there can be no transfer of kinetic energy from the body to the fluid in the gap as observed in figures 4.2(b), 4.2(c). A large inviscid pressure loading in the near contact region cannot develop and the energy of elastic deformation is completely dissipated by the viscous stresses in the fluid layer. The body is incapable of rebound in this viscosity dominated limit. In contrast, if the pressure loading leading to elastic deformation is largely of an inviscid nature (the high Re_o, large β case just discussed), the viscous dissipation will not absorb all the

elastic recoil energy and the body should be capable of rebound. This more complicated problem is discussed in Chapter 6.

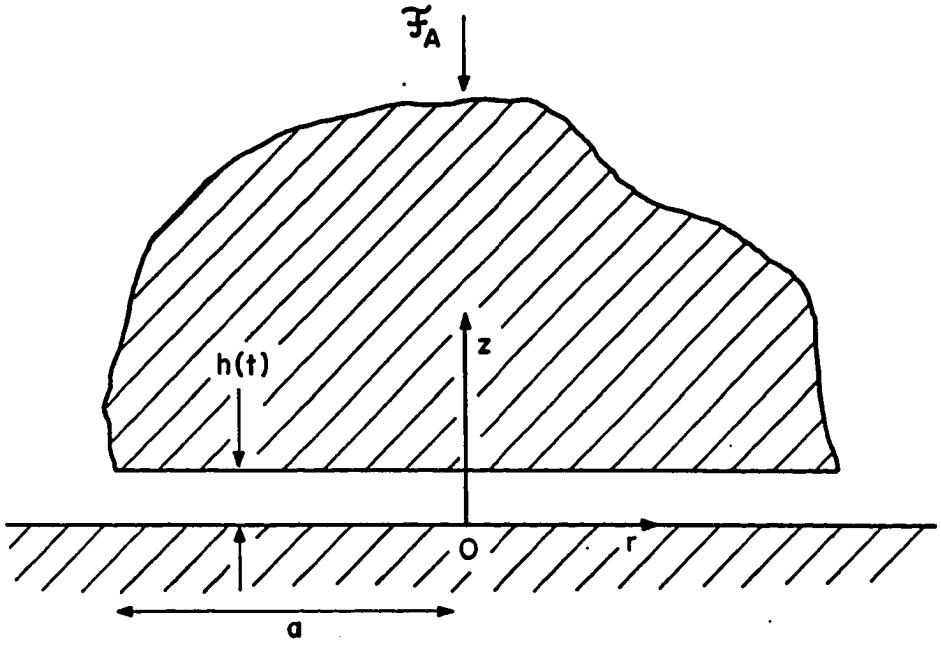

Figure 4.1. The geometry and coordinate system for a flat body near a plane.

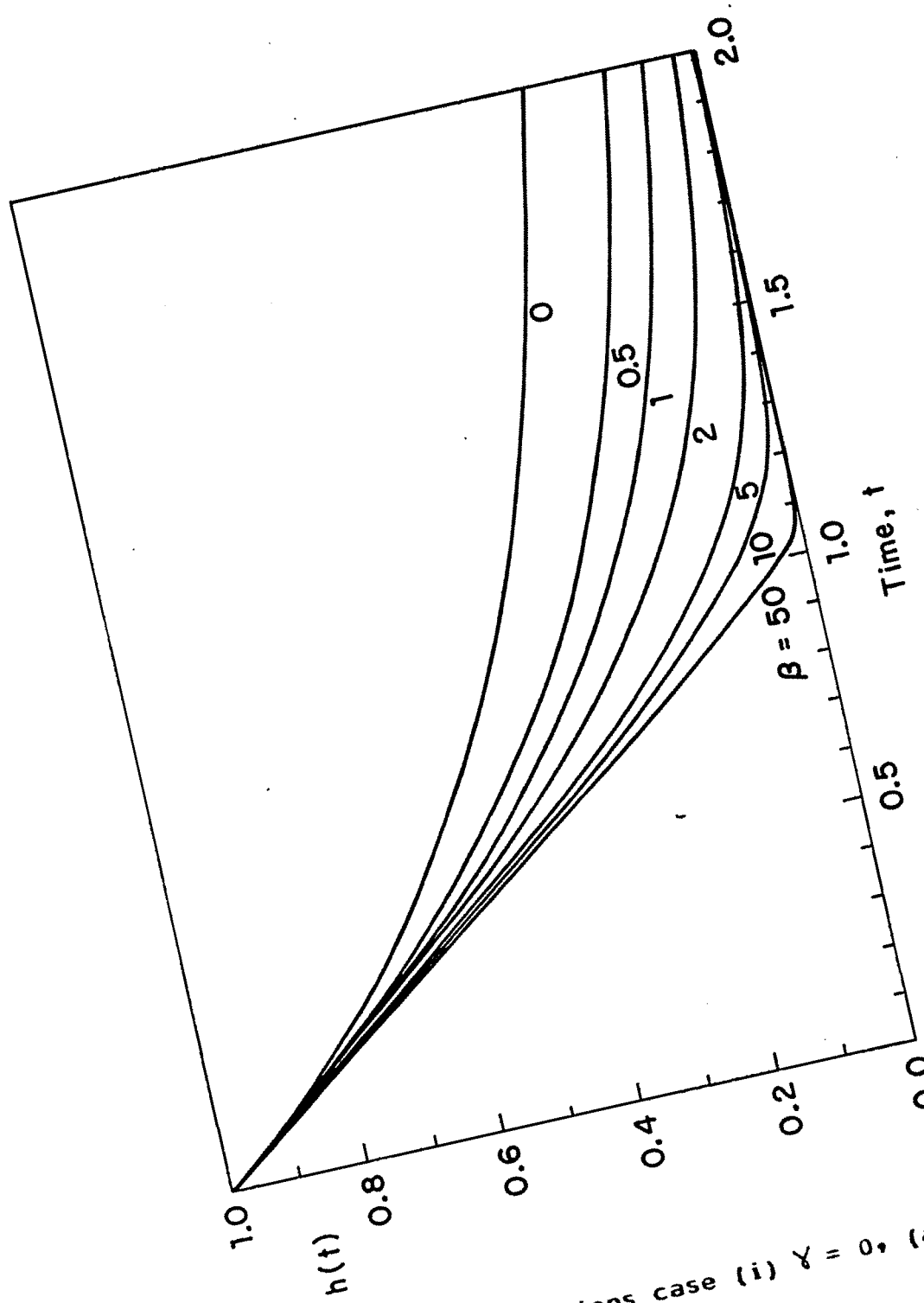

Figure 4.2. Inviscid solutions case (i) $\gamma = 0$, (a) $h(t)$

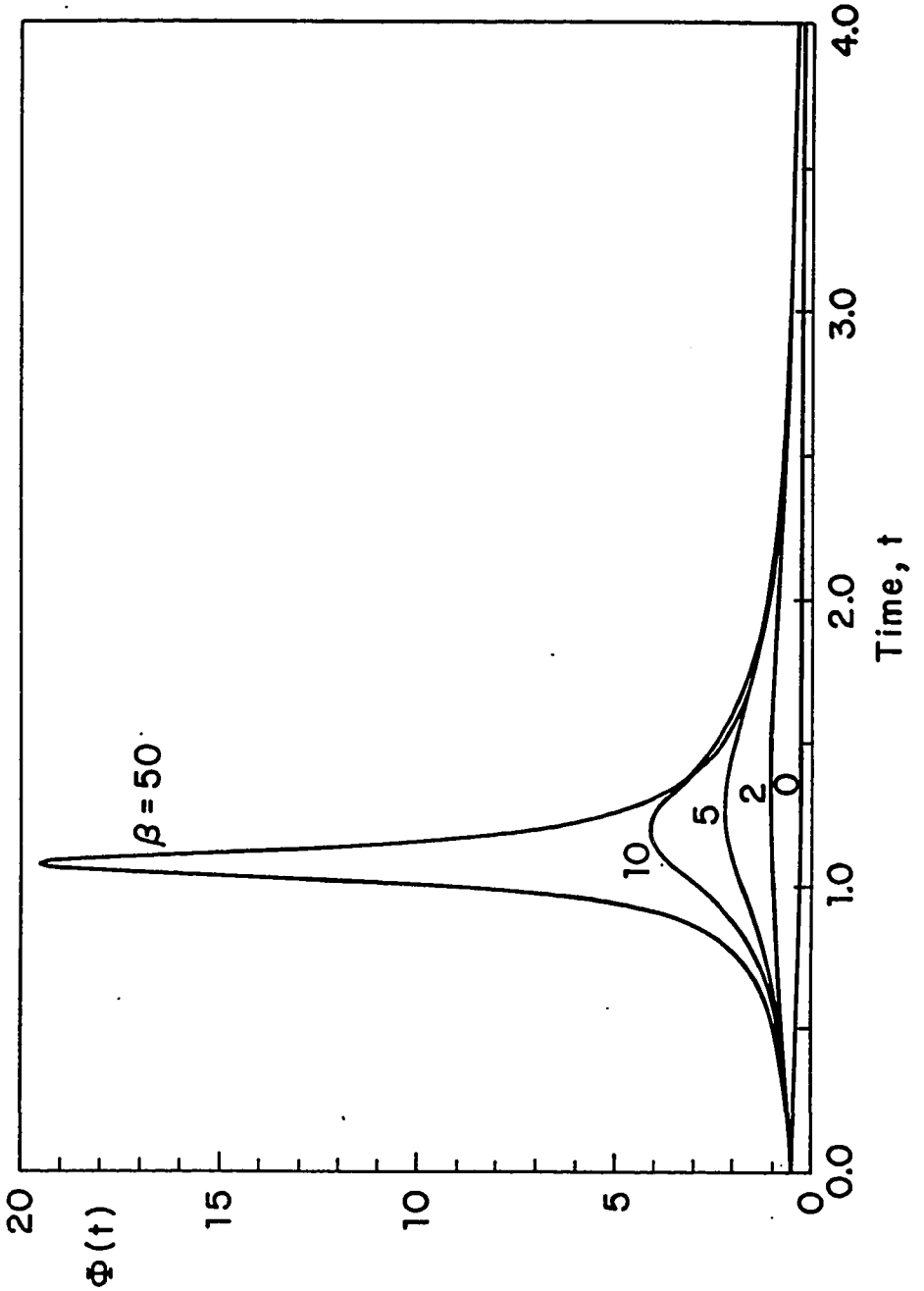

Figure 4.2. Inviscid solutions case (i) $\gamma = 0$, (b) $\Phi(t)$

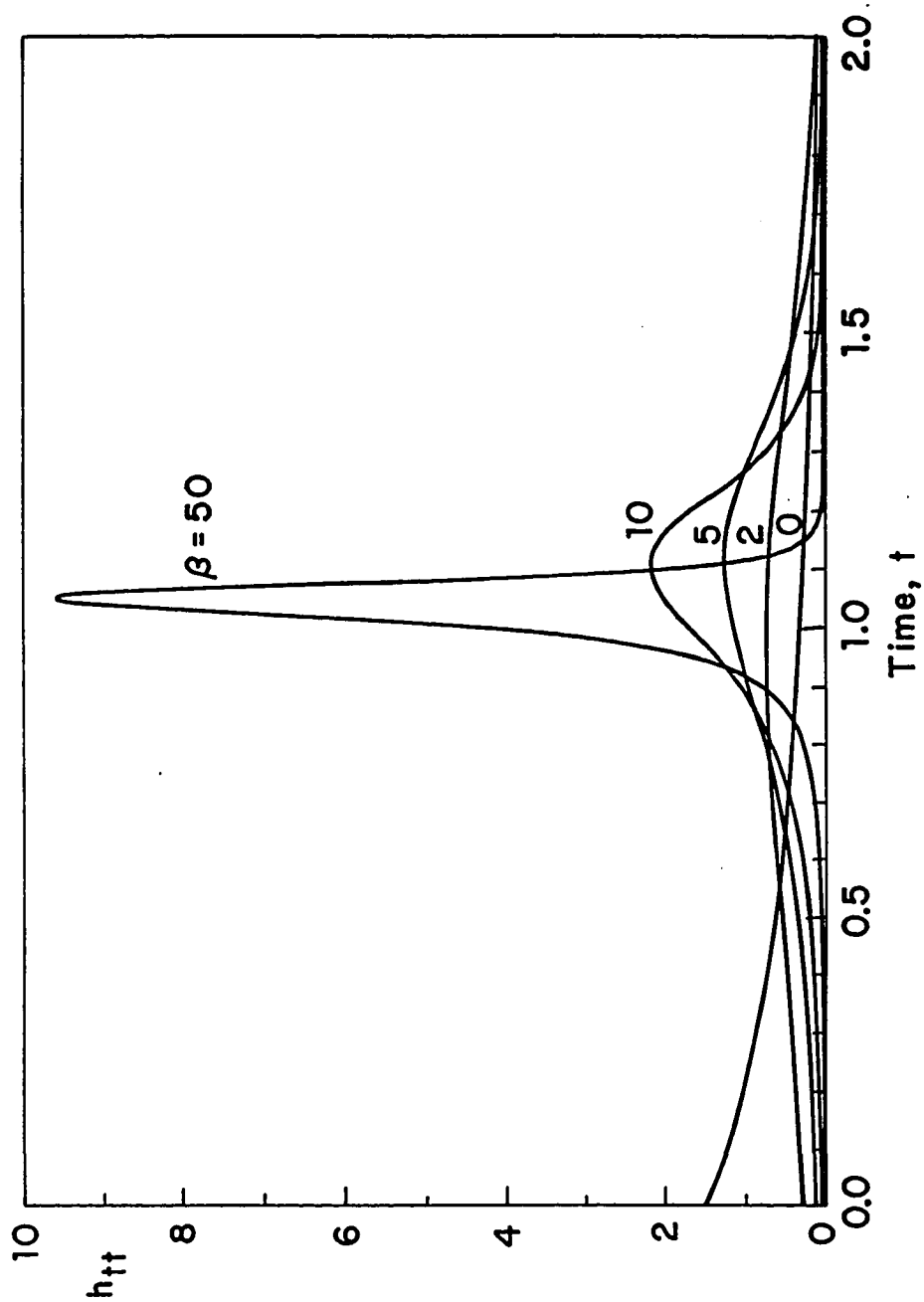

Figure 4.2. Inviscid solutions case (i) $\gamma = 0$, (c) h_{tt}.

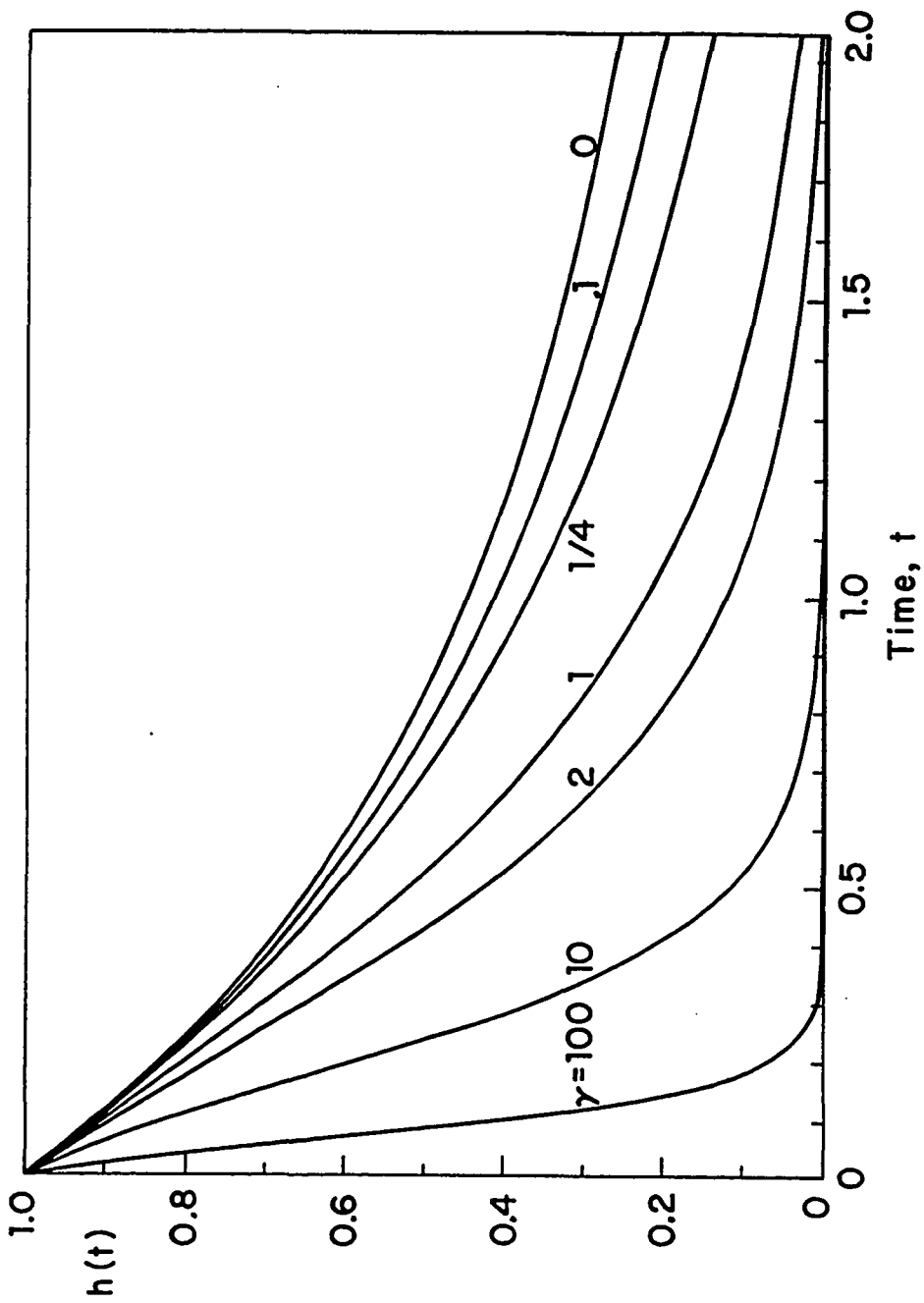

Figure 4.3. Inviscid solutions case (ii) $\beta = 0$, (a) h(t).

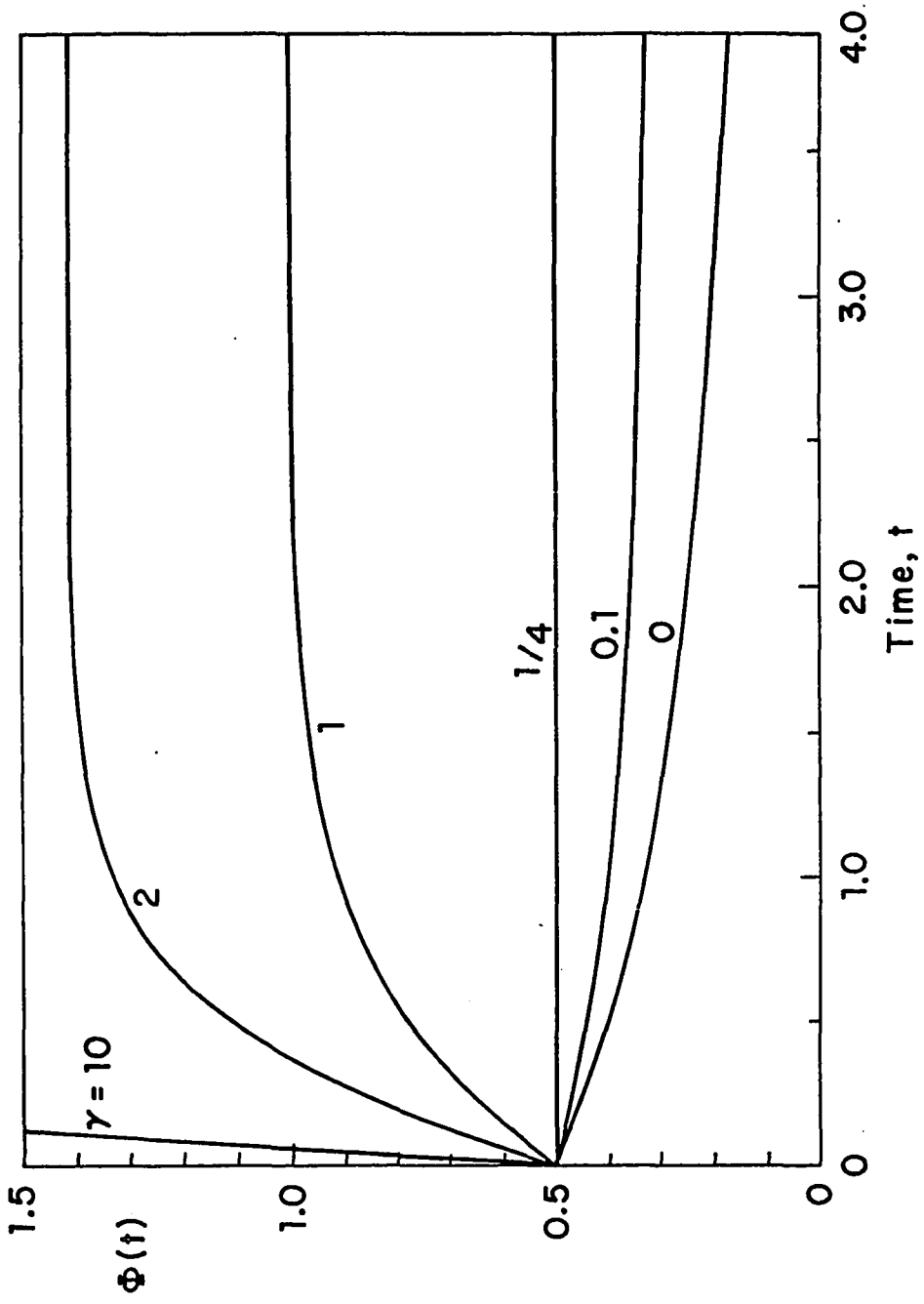

Figure 4.3. Inviscid solutions case (ii) $\beta = 0$, (b) $\Phi(t)$.

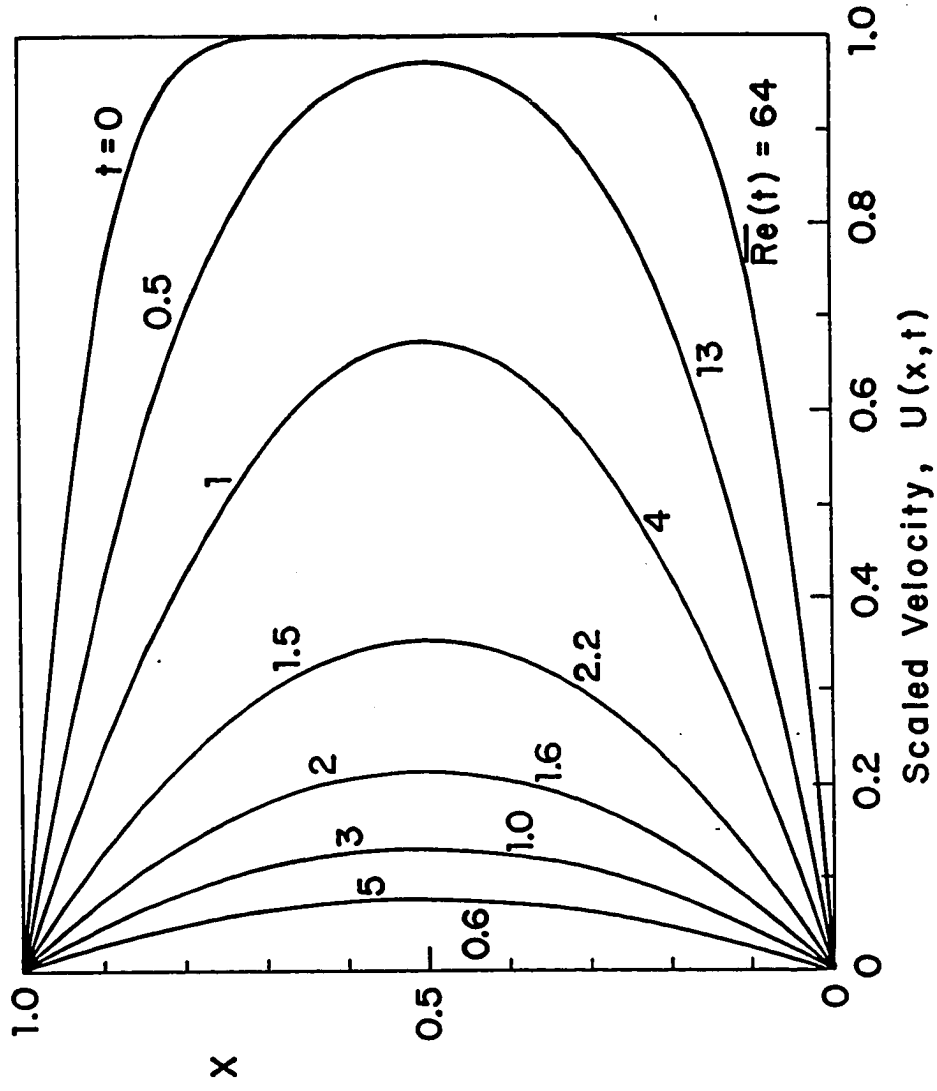

Figure 4.4. Velocity profiles for the numerical solution of the draining problem.

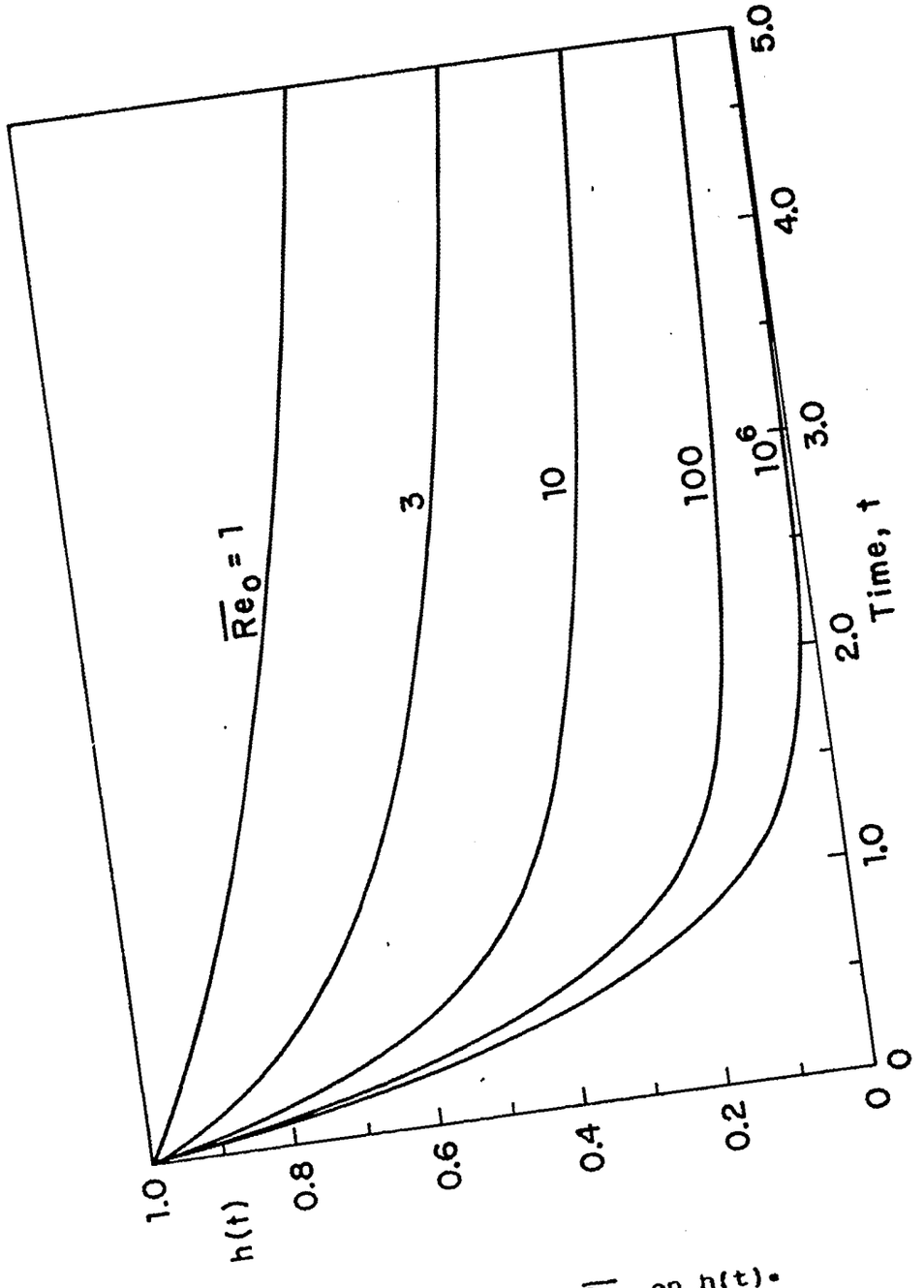

Figure 4.5(a). The effect of $\overline{Re}_o$ on h(t).

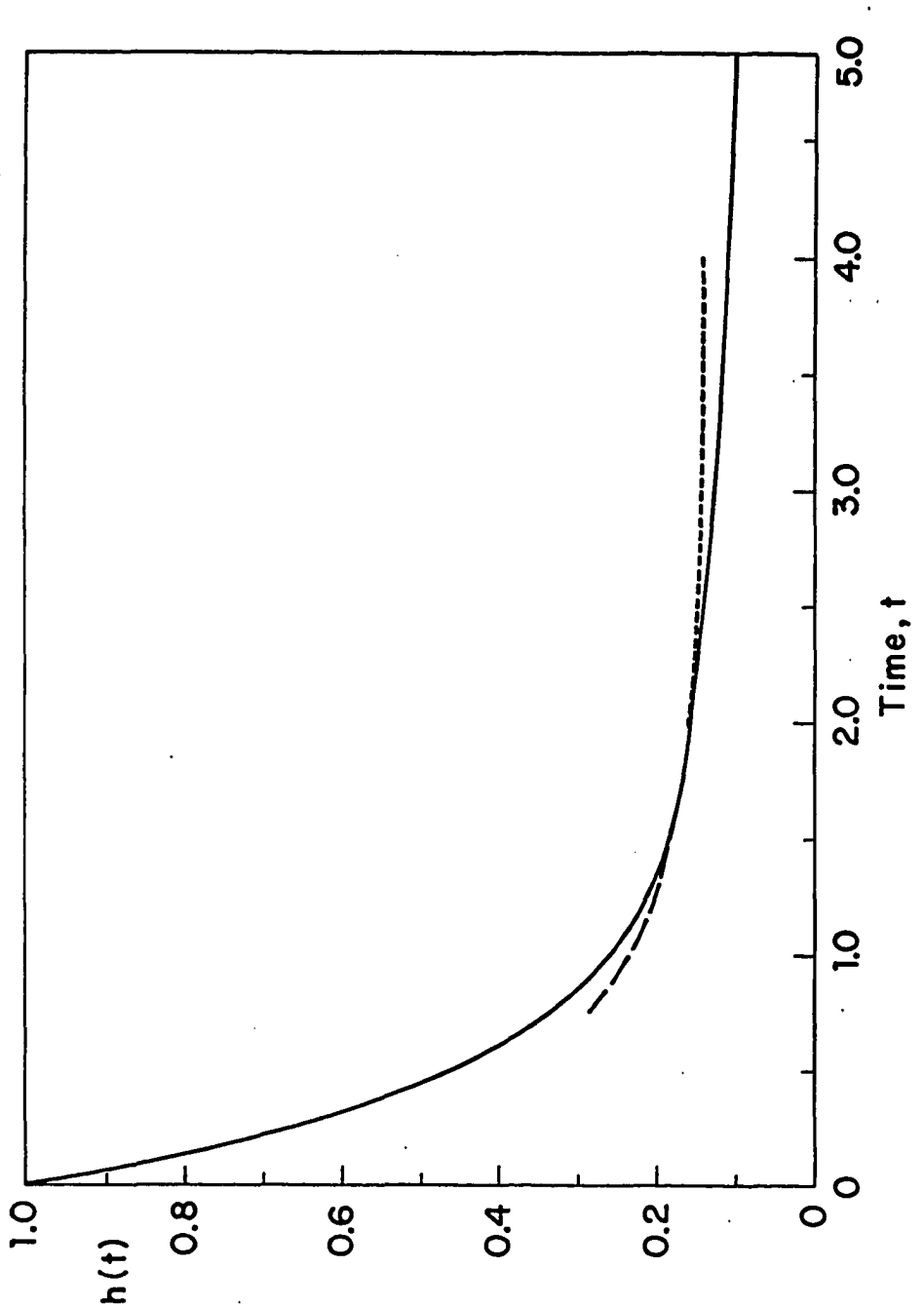

Figure 4.5(b). Solutions (a) .... , (b) ____ , (c) ----
showing overlap of the regions of validity for $\overline{Re}_o = 64$.

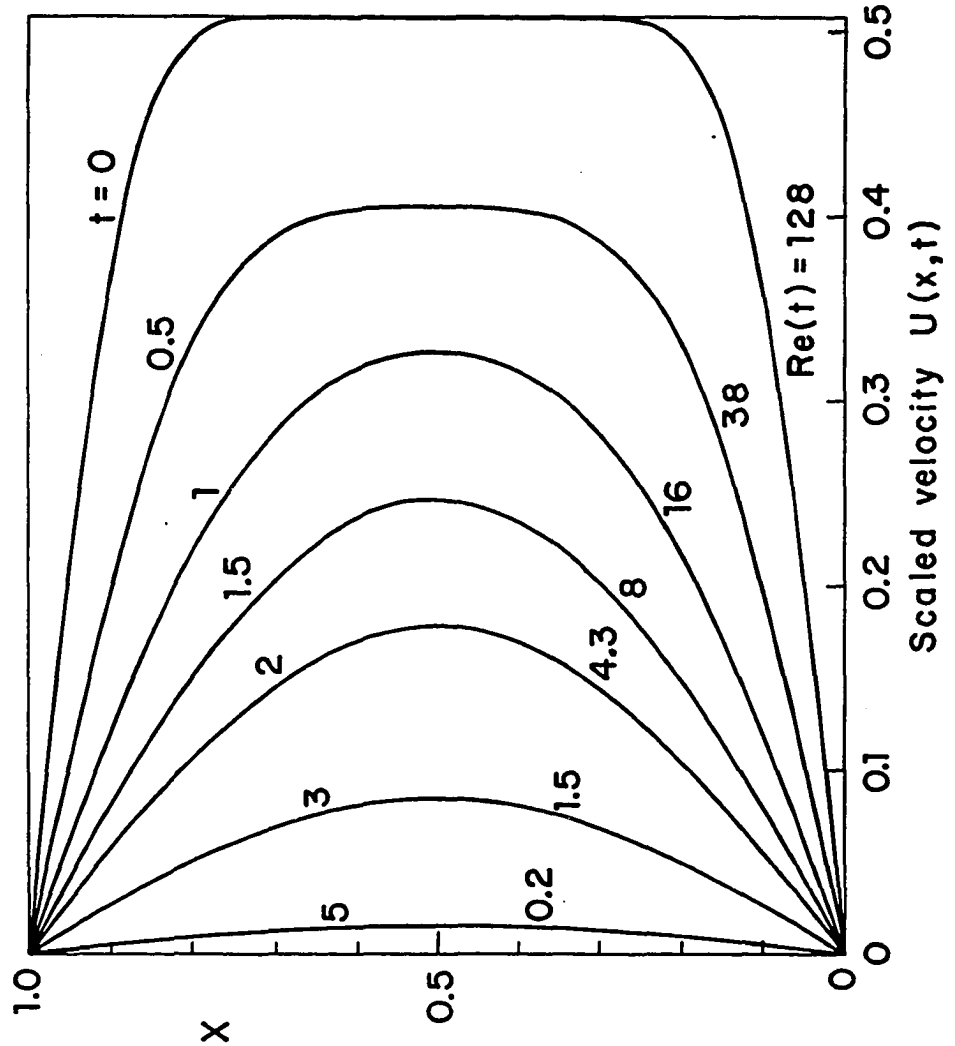

Figure 4.6. Velocity profiles for the numerical solution of the arrest problem.

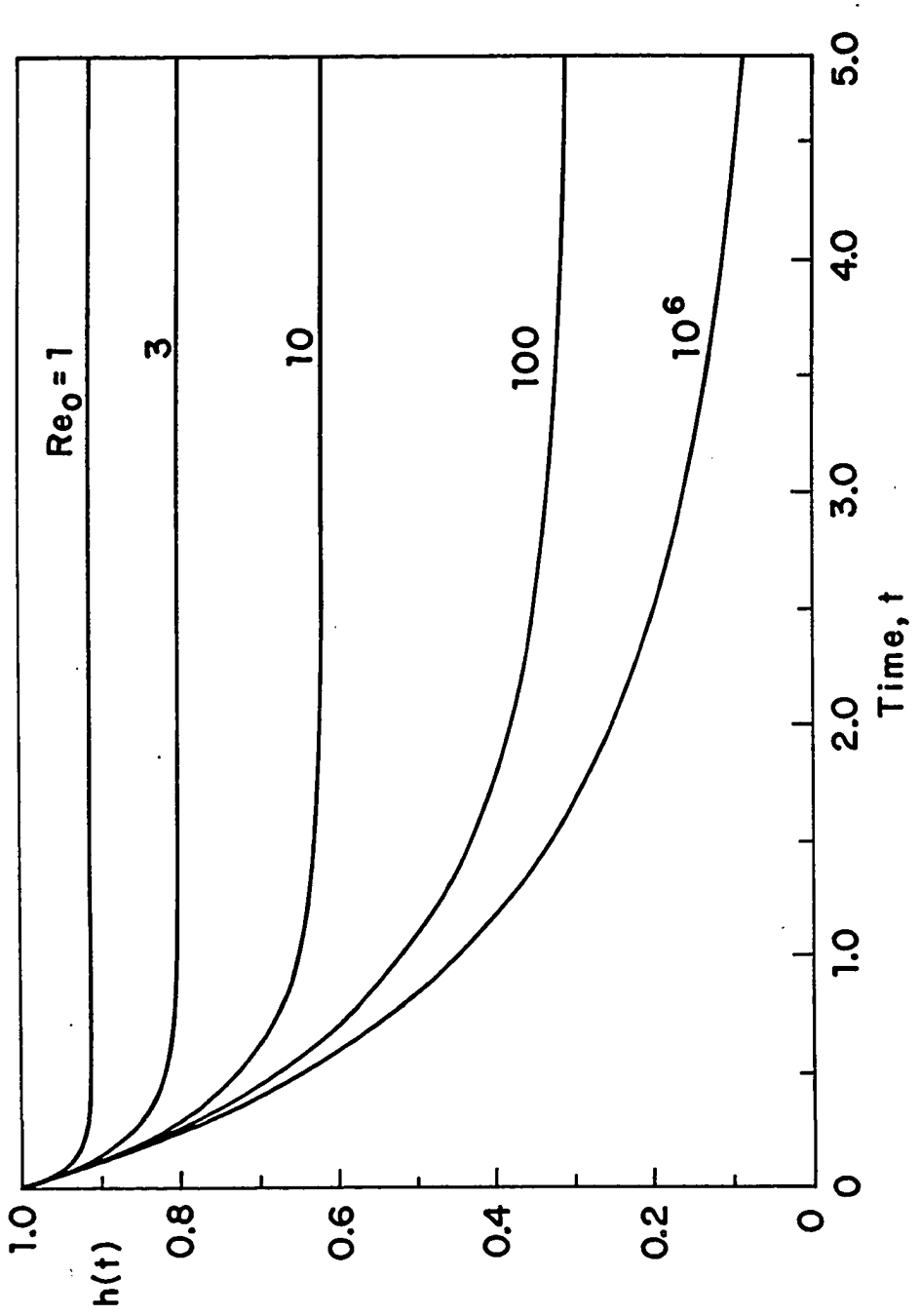

Figure 4.7(a). The effect of Re_o on the arrest process.

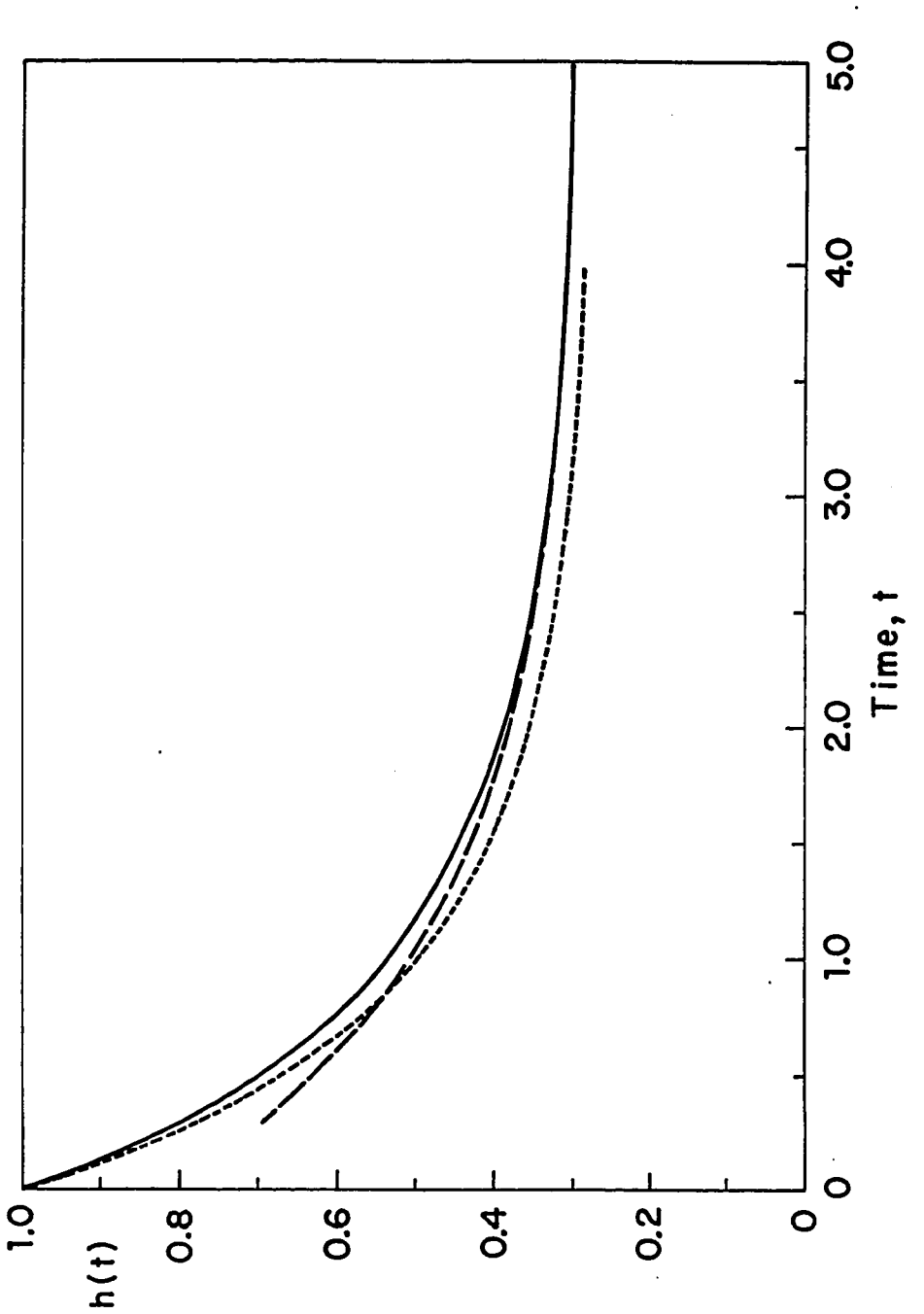

Figure 4.7(b). Solutions (a) .... , (b) ____ , (c) ----
showing overlap of the regions of validity for Re_0 = 128.

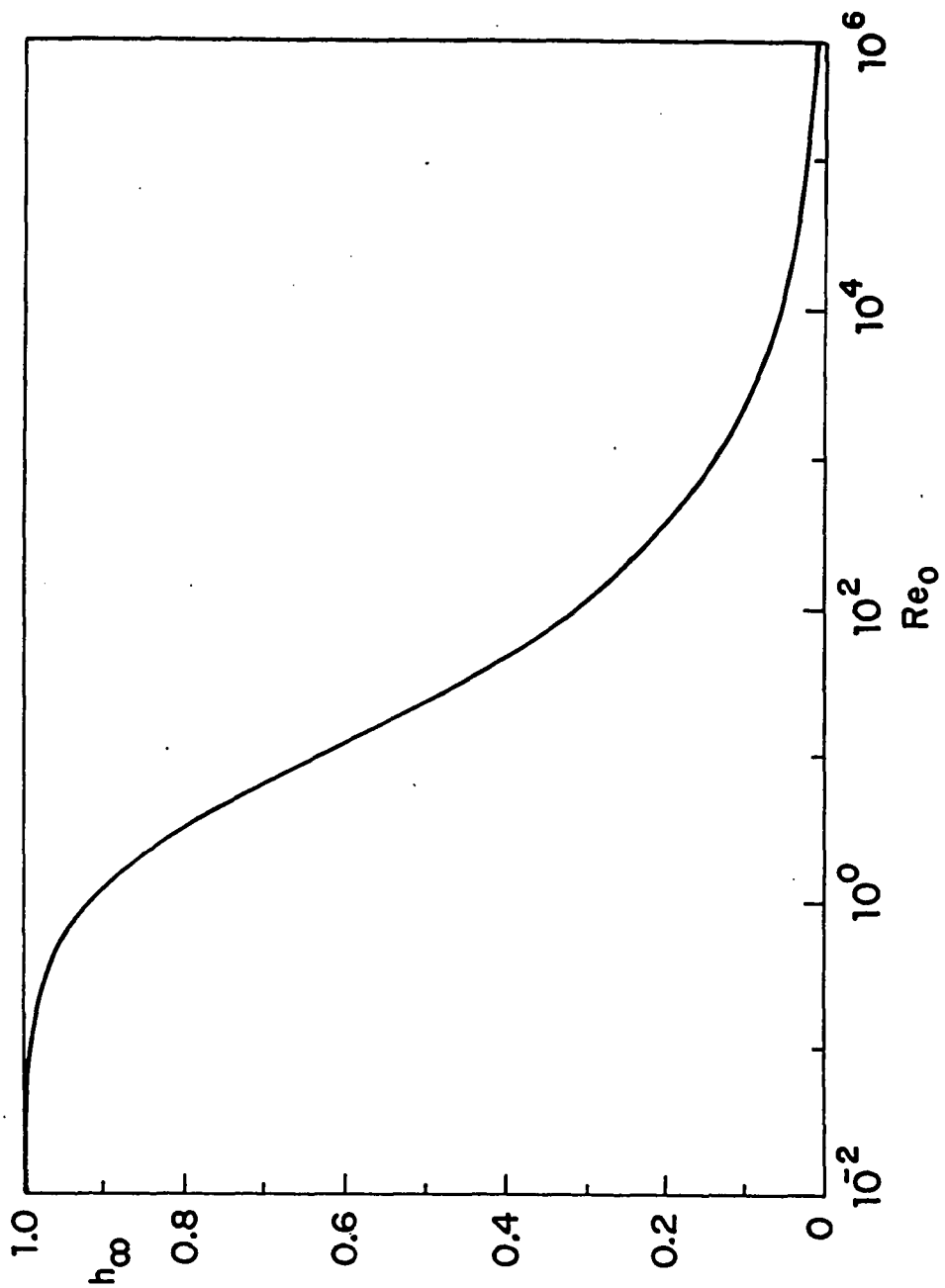

Figure 4.8. The ultimate gap height h_∞ as a function of Re_o.

CHAPTER 5. VISCOUS DRAINING FOR A DISC DROPPED FROM REST NEAR A PLANE

5.1 INTRODUCTION

In this chapter, we consider the motion of a flat-bottomed body falling from rest towards a parallel plane surface. The equations of motion are the same as in Chapter 4, but now we focus attention on the transience of the solution by starting the body from rest near the wall. In this case, a slightly different approach will be used to bring out the important features of the problem.

The non-dimensionalization of the governing equations for the motion of the object and of the intervening fluid shows that there are three important characteristic timescales. The viscous diffusion timescale is $t_d = h_o^2/\nu$, where h_o is the initial gap height and ν is the kinematic viscosity of the fluid. The inertial timescale is $t_i = (\pi\rho a^4/4W)^{\frac{1}{2}}$, where ρ is the density of the fluid, a is the radius of the disc and W is the net force acting on the object when the system is at rest: $W = (m-m_b)g + F$ where m is the mass of the object, m_b is the mass of the fluid displaced by the object and F is the external force. The third timescale is $t_g = (mh_o/W)^{\frac{1}{2}}$; when there is no external force and buoyancy is negligible, $W = mg$ and t_g reduces to $(h_o/g)^{\frac{1}{2}}$, which is the gravitational timescale for an object

falling a distance h in a vacuum. The characteristic diffusion time for the viscous boundary layers on the top and bottom boundaries to spread throughout the gap is t_d, t_i is the timescale for the fluid layer to drain in the absence of viscosity and t_g characterizes the time that it would take the object to fall in the absence of hydrodynamic forces. A fourth timescale which is not independent of the others is the viscous flow time, $t_v = t_i^2/t_d = \pi\mu a^4/4Wh_o^2$. This characterizes the time for the fluid to drain in the absence of inertia. The above definition of t_i gives rise to a characteristic inertial settling velocity $V = h_o/t_i = 2(h_o/a)(W/\pi\rho a^2)^{\frac{1}{2}}$. The ratios of the three characteristic timescales define the two fundamental dimensionless groups:

$$Re = \frac{t_d}{t_i} = \frac{h_o V}{\nu}, \qquad \beta = \frac{t_g^2}{t_i^2} = \frac{4h_o m}{\pi\rho a^4} \tag{5.1}$$

The first group is the Reynolds number based on the characteristic inertial settling velocity defined above and the second group is the ratio of the squares of the gravitational and inertial settling times. Since the mass of fluid in the gap is $m_f = \pi\rho a^2 h_o$, β can also be written as $4(h_o/a)^2(m/m_f)$, which is particularly convenient for defining the regimes of motion.

Then the equations governing the flow are:

$$F_{zt} + F_z^2 - 2FF_{zz} - \frac{t_c}{t_i}\frac{1}{Re}F_{zzz} = \beta h_{tt} + \frac{t_c^2}{t_i^2} \tag{5.2}$$

with on $z=0$: $F = 0$, $F_z = 0$ (5.3)

$$\text{on } z = h(t): \quad F = -\tfrac{1}{2}h_t, \quad F_z = 0 \tag{5.4}$$

$$\text{when } t = 0: \quad F = 0, \quad h = 1, \quad h_t = 0 \tag{5.5}$$

In equation (5.2) t_c is the characteristic timescale used to define the dimensionless variables. The choice of t_c depends on the timescale of interest; the most obvious choice is to use t_i (as in Chapter 4), but we shall see that interesting behaviour occurs on other timescales.

In all applications, we shall assume that the ratio h_0/a is sufficiently small for the edge effects near r = a to be confined to a small part of the total gap area and therefore to be unimportant in determining both the velocity and pressure distributions in the intervening fluid space. Even with this limitation, a rather surprising diversity of behaviour can be anticipated when the object is dropped from rest, determined by the relative ordering of the three basic timescales as expressed in the magnitudes of the dimensionless numbers β and Re just defined. For a small piston applied to a microchip, Re is of the order of 0.1, whereas for a book released 1 cm above a desk top Re is of the order of 10^3 to 10^4. The physically realizable range of β depends strongly on the working fluid. for a liquid, m/m_f is typically of the order of 1 to 10 and therefore, if $h_0/a < 0.1$, β will be small compared to unity in most situations. On the other hand, for air typical values of this mass ratio will be 10^3 or larger. For a sheet of paper

dropped from a height of 1 cm, β will be of order unity, whereas for a pane of glass or a book dropped from this height, β will be of the order of 10^2.

The foregoing estimates are intended to provide some feeling for the regimes of behaviour. When $t_g >> t_i$ or $\beta >> 1$, the primary force balance is between the net force on the object and its rate of change of momentum. The velocities and accelerations in the fluid gap will not be sufficient to generate a significant hydrodynamic pressure on the underside of the object, and it will fall as though it were in a vacuum until the gap becomes very narrow. In the other limit $t_g << t_i$ or $\beta << 1$, the net weight of the object is instantly supported almost entirely by the hydrodynamic pressure on its underside with the result that the object experiences very small accelerations compared with gravity. The contrast is easily illustrated by dropping a book and a piece of paper on a table, where only the latter exhibits a slow, hovering descent.

In this chapter, we are interested primarily in the effect of the applied force, so we will consider the case of zero β. We discuss three different limiting cases of the problem, then go on to the full numerical solution. The first limit considered is that of low Reynolds number, where it will be shown that the static initial condition results in a small modification to the classical lubrication theory;

the body appears to have come from a slightly higher starting position. The next limit to be considered is that of small time. We shall see how the flow is developed from rest, and the results will be used to start the longer time solutions which follow. The third limit studied is that of large Re. The boundary layer equations cannot be treated analytically because of the constraint of the initial condition, so an integral equation technique is used to give a high-accuracy approximation to the flow. Finally, the full numerical solution will be presented and compared to the limiting results.

5.2 LOW REYNOLDS NUMBER SOLUTION

The standard lubrication theory calls for a balance between the viscous and radial pressure gradient terms in (5.2). This balance is achieved if t_c is chosen to be $t_v = t_i/Re$. Introducing a new dimensionless time $T = t/t_v$ and stream function $f = Ft_v/h_o$, one obtains

$$f_{zzz} + 1 = Re^2 (f_{zT} + f_z^2 - 2ff_{zz}) \qquad (5.6)$$

The required solution is an expansion to be asymptotic for fixed t as $Re \to 0$, in the form

$$f(z,T;Re) \sim f_0(z,h(T)) + Re^2 f_2(z,h,h_T) + O(Re^4) \qquad (5.7)$$

$$h(T;Re) \sim h_0(T) + Re^2 h_2(T) + O(Re^4) \qquad (5.8)$$

Relation (5.7) is substituted into (5.6) and the boundary conditions (5.3) and (5.4). The result of the substitution must be valid for any small Re, so that the coefficients of each power of Re form independent equations. At zero order, one obtains

$$f_{ozzz} + 1 = 0 \tag{5.9}$$

with boundary conditions

$$\text{on } z=0: \quad f_o = 0, \quad f_{oz} = 0 \tag{5.10}$$

$$\text{on } z=h(T): \quad f_{oz} = 0 \tag{5.11}$$

The solution of (5.9)-(5.11) gives the lubrication-theory result

$$f_o = \tfrac{1}{4}hz^2 - \tfrac{1}{6}z^3 \tag{5.12}$$

which is a parabolic radial-velocity profile $u = \frac{1}{2}rz(h-z)$. At second order, one finds

$$f_{2zzz} = f_{ozT} + f_{oz}^2 - 2f_o f_{ozz} = \tfrac{1}{12}(6zh_T + 2z^3h - z^4) \tag{5.13}$$

with boundary conditions

$$\text{on } z=0: \quad f_2 = 0, \quad f_{2z} = 0 \tag{5.14}$$

$$\text{on } z=h(T): \quad f_{2z} = 0 \tag{5.15}$$

Equations (5.13)-(5.15) have the solution

$$f_2 = \frac{1}{5040}\left[105\, h_T (z^4 - 2z^2h^2) - 2z^7 + 7z^6 h - 14 z^2 h^5\right] \qquad (5.16)$$

Initial condition (5.5) cannot be satisfied, showing that an "inner" expansion will be required on a shorter timescale which must be matched to (5.7) and (5.8). This is dealt with in the next paragraph. Substituting (5.8), (5.12) and (5.16) into boundary condition (5.4) and separating in powers of Re^2 one obtains two equations for h_0 and h_2:

$$h_{0T} = -\frac{1}{6} h_0^3 \qquad (5.17)$$

$$h_{2T} + \frac{1}{2} h_0^3 h_2 = \frac{1}{24} h_0^4 h_{0T} + \frac{18}{5040} h_0^7 \qquad (5.18)$$

Equation (5.17) has the general solution

$$h_0 = \left(\frac{3}{T + C_0}\right)^{\frac{1}{2}} \qquad (5.19)$$

which can be used to find the general solution to (5.18)

$$h_2 = C_1 \left(\frac{3}{T+C_0}\right)^{\frac{3}{2}} + \frac{17}{1680}\left(\frac{3}{T+C_0}\right)^{\frac{5}{2}} \qquad (5.20)$$

The initial conditions (5.5) cannot be used to find the constants C_0 and C_1 since the velocity profiles obtained from (5.12) and (5.16) do not satisfy the correct initial condition as mentioned above.

The appropriate timescale for the inner expansion is $t_d = Re\, t_i$. Taking this value for t_c in (5.2) and using τ for the dimensionless short time and G for the dimensionless inner stream function, one obtains

$$G_{z\tau} + G_z^2 - 2\, G G_{zz} - G_{zzz} = Re^2 \qquad (5.21)$$

τ and G are related to T and f by $\tau = T/Re^2$, $G = Re^2 f$. The solution is required to be asymptotic for fixed τ as $Re \to 0$ and of the form

$$G(z,\tau;Re) \sim Re^2 G_2(z,\tau) + O(Re^4) \tag{5.22}$$

$$h(\tau;Re) \sim 1 + Re^2 H_2(\tau) + O(Re^4) \tag{5.23}$$

Relations (5.22) and (5.23) are first substituted into (5.21), (5.3) and (5.5). To lowest order in Re^2 one gets

$$G_{2zz\tau} - G_{2zzzz} = 1 \tag{5.24}$$

$$\text{on } z=0: \quad G_2 = 0, \quad G_{2z} = 0 \tag{5.25}$$

$$\text{when } t=0: \quad G_2 = 0, \quad H_2 = 0 \tag{5.26}$$

Boundary conditions (5.4) are now expanded in Taylor series about z = 1 and the coefficients of the powers of Re^2 are equated. This gives

$$G_2 = -\tfrac{1}{2} H_{2\tau}, \quad G_{2z} = 0. \quad \text{on } z = 1 \tag{5.27}$$

Equations (5.24), (5.25) and (5.26) have a separable solution

$$G_2 = \tfrac{1}{4}z^2 - \tfrac{1}{6}z^3 - \sum_{n\,\text{odd}} \frac{4}{n^4\pi^4}(1-\cos n\pi z)\, e^{-n^2\pi^2\tau} \tag{5.28}$$

Substituting (5.28) in (5.27), one obtains

$$H_2 = -\tfrac{1}{6}\tau + \sum_{n\,\text{odd}} \frac{16}{n^6\pi^6}\left(1 - e^{-n^2\pi^2\tau}\right) \tag{5.29}$$

The two solutions (5.8) and (5.23) for h are both valid on the intermediate timescale with variable $s = Re^{2\alpha} T$ provided $0 < \alpha < 1$. The solutions are matched by expressing each in terms of the variable s and requiring that the coefficients of each power of Re^2 be equal. This gives the values

$$C_0 = 3, \qquad C_1 = \frac{11}{1680} \tag{5.30}$$

Summarizing these results, one has on the long timescale

$$h \sim (1+\tfrac{1}{3}T)^{-\frac{1}{2}} + Re^2 \tfrac{1}{1680}\left[11(1+\tfrac{1}{3}T)^{-\frac{3}{2}} + 17(1+\tfrac{1}{3}T)^{-\frac{5}{2}}\right] + O(Re^4) \tag{5.31}$$

$$h_T \sim -\tfrac{1}{6}(1+\tfrac{1}{3}T)^{-\frac{3}{2}} - Re^2 \tfrac{1}{10080}\left[33(1+\tfrac{1}{3}T)^{-\frac{5}{2}} + 85(1+\tfrac{1}{3}T)^{-\frac{7}{2}}\right] + O(Re^4) \tag{5.32}$$

On the short timescale $\tau = T/Re^2$,

$$h \sim 1 - Re^2 \tfrac{1}{6}\left[\tau - \sum'_{n\,odd} \frac{96}{n^6\pi^6}\left(1 - e^{-n^2\pi^2\tau}\right)\right] + O(Re^4) \tag{5.33}$$

$$h_\tau \sim -Re^2 \tfrac{1}{6}\left[1 - \sum'_{n\,odd} \frac{96}{n^4\pi^4} e^{-n^2\pi^2\tau}\right] + O(Re^4) \tag{5.34}$$

The long-timescale solution satisfies the initial condition on h with error $O(Re^2)$ even though the stream function does not satisfy the initial condition. This means that the long-timescale solution is valid almost from t = 0 for small values of Re. This is shown in figure 5.1, which shows the time-dependence of h for different values of Re. Since the dimensionless times T and τ used above differ by a factor of Re^2, it is convenient to use the intermediate timescale $\tilde{t} = t/t_i = T/Re = \tau Re$ to plot the results (5.31)–(5.34), noting also that $h_T = (1/Re)h_{\tilde{t}}$. Figures 5.1

and 5.2 then show the results scaled with inertial time $t_i = (\pi\rho a^4/4W)^{\frac{1}{2}}$, length h_0 and inertial velocity $V = h_0/t_i$.

Figure 5.1 shows that the long-time expansion (5.31) is accurate for all time for Reynolds numbers up to unity. It gives a slight overshoot of the initial value of h by an amount $\frac{1}{60}Re^2$. For larger Reynolds numbers, the expansion (5.33) must be used for t up to about 0.5 to account for the inertial resistance of the fluid to its initial acceleration. The matched expansions are quite accurate for Reynolds numbers up to 10, even though they were derived for $Re \ll 1$. This is because of the large denominator in the second term of (5.31) and because one only needs to use values of τ up to about $\frac{1}{2}Re$ in (5.33). Figure 6 shows that the matching of the expansions for body velocity (5.32) and (5.34) are less accurate than those for gap height (5.31) and (5.33) because each expansion is a monotonic function of time, one increasing for short times and the other decreasing for large times, giving rise to curves with opposite slopes. One would expect the true velocity curve to have a smooth peak somewhat below the intersection of the two expansions.

In all the cases studied the initial acceleration of the object causes an acceleration of the fluid in the gap. For the inviscid limit this is an acceleration of a one-dimensional profile whereas for the low Reynolds number

limit this is an acceleration to a quasi-steady profile that changes with Re. For early times the lowest order solution for the radial velocity profile obtained from the stream function solution (5.28) is the same as the start-up flow in a parallel-wall channel in which a constant pressure gradient has been applied at $t = 0$. At larger times the radial velocity profile to $O(Re)$ is obtained from solutions (5.12) and (5.16) and is a function of the instantaneous gap width and Re. These profiles are shown as a function of Re at fixed h in the upper half of the diagram, figure 5.3(a), and as a function of h (or equivalently t) at a fixed Re in the lower half of the diagram, figure 5.3(b). One observes that as either Re or h approaches zero the profile becomes parabolic.

The long-time asymptotic decay of the motion is fundamentally different in the low-Re and the inviscid limits. In the low-Re limit the inertial terms rapidly damp out due to viscosity, and the pressure field on the underside of the disc is due to a quasi-steady pressure viscous-force balance. In the inviscid limit the radial velocity approaches a constant value at any r and a quasi-steady state Bernoulli pressure distribution is established on the underside of the disc. The fascinating observation is that this pressure distribution is the same in both limits, being a simple parabolic function of r.

5.3 SMALL TIME SOLUTION

An asymptotic solution can be found for the short period after the release of the body when it remains close to its original position. This solution is useful in starting the longer-time solutions in the following sections and is an interesting exercise in asymptotic analysis. To reveal the behaviour for short times, t_c is chosen to be ϵt_i with ϵ a small constant. New symbols are introduced for the dimensionless variables: τ for time and G for stream function. The boundary and initial conditions are unchanged and (5.2) is re-written as

$$G_{z\tau} + G_z^2 - 2GG_{zz} = \epsilon \frac{1}{Re} G_{zzz} + \epsilon^2 \tag{5.35}$$

The required solution must be asymptotic for fixed z and Re as $\epsilon \to 0$. A suitable form is

$$G(z,\tau;\epsilon) \sim \epsilon^2 G_4(z,\tau) + \epsilon^{5/2} G_5(z,\tau) \tag{5.36}$$

Equations for G_4 and G_5 are found by substituting (5.36) into (5.35)

$$G_{4z\tau} = 1 \tag{5.37}$$

$$G_{5z\tau} = 0 \tag{5.38}$$

Equations (5.37) and (5.38) have solutions

$$G_4 = z\tau + a_4(\tau) + b_4(z) \tag{5.39}$$

$$G_5 = a_5(\tau) + b_5(z) \tag{5.40}$$

where a_4, b_4, a_5 and b_5 are unknown functions. Initial condition (5.5) requires that $b_4 = b_5 = 0$, but the boundary conditions (5.3) and (5.4) cannot be satisfied by (5.39) and (5.40). Therefore, boundary layers must be present near $z = 0$ and 1, so inner expansions must be used. To examine the boundary layer near $z = 0$, z is replaced by a new independent variable $\zeta = z/\epsilon^{1/2}$ and G is replaced by $g = G/\epsilon^{5/2}$. Equation (5.35) takes the form

$$g_{\zeta\tau} - \frac{1}{Re} g_{\zeta\zeta\zeta} - 1 = \epsilon^2 (2g_{\zeta\zeta} - g_\zeta^2) \qquad (5.41)$$

The solution to (5.41) must be asymptotic for fixed ζ and Re as $\epsilon \to 0$, in the form

$$g(\zeta, \tau; \epsilon) \sim g_0(\zeta, \tau) + O(\epsilon^{1/2}) \qquad (5.42)$$

This expansion (5.42) is substituted into (5.41) to give an equation for g_0.

$$g_{0\zeta\tau} - \frac{1}{Re} g_{0\zeta\zeta\zeta} - 1 = 0 \qquad (5.43)$$

Note that (5.43) is the same as the start-up problem for undirectional flow in a channel under the action of a constant applied pressure gradient. The boundary and initial conditions for g_0 are:

$$\text{on } \zeta = 0: \; g_0 = 0, \; g_{0\zeta} = 0; \; \text{when } t = 0; \; g_0 = 0 \qquad (5.44)$$

Equations (5.43) and (5.44) have a solution in similarity form

$$g_0 = \zeta\tau + \frac{8}{Re^{\frac{1}{2}}} \tau^{\frac{3}{2}} \left\{ i^3 \operatorname{erfc}\left[\frac{\zeta}{2}\left(\frac{Re}{\tau}\right)^{1/2}\right] - \frac{1}{6\pi^{1/2}} \right\} \qquad (5.45)$$

where $i^3\text{erfc}$ is the third repeated integral of the complementary error function, which takes the value $1/6\pi^{1/2}$ for zero argument.

It is expected that G will be of order ϵ^2 everywhere, so boundary condition (5.4) suggests that h will be of the form

$$h(\tau;\epsilon) \sim 1 + \epsilon^2 h_4(\tau) + \epsilon^{5/2} h_5(\tau) + O(\epsilon^3) \qquad (5.46)$$

Relation (5.46) indicates that the upper boundary will move very little from its initial position during the timescale of interest. Accordingly, boundary conditions (5.4) can be expanded in Taylor series about z = 1 and the appropriate boundary-layer variable is $\xi = (1-z)/\epsilon^{1/2}$.

Equation (5.35) is rewritten in terms of ξ and a scaled stream function $\tilde{g} = G/\epsilon^{5/2}$ to give

$$\tilde{g}_{\xi\tau} - \frac{1}{Re}\tilde{g}_{\xi\xi\xi} = -1 - \epsilon^2(2\tilde{g}\tilde{g}_{\xi\xi} - \tilde{g}_\xi^2) \qquad (5.47)$$

The required solution to (5.47) is asymptotic for fixed ξ and Re as $\epsilon \to 0$ in the form

$$\tilde{g}(\xi,\tau;\epsilon) \sim \epsilon^{-1/2}\tilde{g}_{-1}(\xi,\tau) + \tilde{g}_0(\xi,\tau) + O(\epsilon^{1/2}) \qquad (5.48)$$

Equation (5.48) is inserted into (5.47) to give equations for $\tilde{g}_{-1}$ and $\tilde{g}_0$:

$$\tilde{g}_{-1\xi\tau} - \frac{1}{Re}\tilde{g}_{-1\xi\xi\xi} = 0 \qquad (5.49)$$

$$\tilde{g}_{0\xi\tau} - \frac{1}{Re}\tilde{g}_{0\xi\xi\xi} + 1 = 0 \qquad (5.50)$$

with boundary and initial condition derived from (5.4) and (5.5)

$$\text{on } \zeta=0:\ \tilde{g}_{-1\zeta}=0,\ \tilde{g}_{-1}=-\tfrac{1}{2}h_{4\tau};\ \text{when } \tau=0:\ \tilde{g}_{-1}=0 \qquad (5.51)$$

$$\text{on } \zeta=0:\ \tilde{g}_{0\zeta}=0,\ \tilde{g}_{0}=-\tfrac{1}{2}h_{5\tau};\ \text{when } \tau=0:\ \tilde{g}_{0}=0 \qquad (5.52)$$

Equations (5.49) to (5.52) are solved to find

$$\tilde{g}_{-1}=-\tfrac{1}{2}h_{4\tau} \qquad (5.53)$$

$$\tilde{g}_{0}=-\tfrac{1}{2}h_{5\tau}-\zeta\tau-\frac{8}{Re^{1/2}}\tau^{3/2}\left\{i^{3}\operatorname{erfc}\left[\tfrac{\zeta}{2}\left(\frac{Re}{\tau}\right)^{\frac{1}{2}}\right]-\frac{1}{6\pi^{1/2}}\right\} \qquad (5.54)$$

Equations (5.36), (5.42) and (5.48) are matched on intermediate spatial scales to give equation for a_4, a_5, b_4, b_5, h_4 and h_5. These are:

$$a_4(\tau)=0,\quad a_5(\tau)=-\frac{4}{3\pi^{1/2}}\tau^{3/2}Re^{-1/2} \qquad (5.55)$$

$$b_4(\tau)=0,\quad b_5(\tau)=0 \qquad (5.56)$$

$$h_{4\tau}=-2\tau,\quad h_{5\tau}=-2a_5+\frac{8}{3\pi^{1/2}}\tau^{3/2}Re^{-1/2} \qquad (5.57)$$

Equations (5.57) with initial condition (5.5) have solutions

$$h_4=-\tau^2 \qquad (5.58)$$

$$h_5=\frac{32}{15\pi^{1/2}}\tau^{5/2}Re^{-1/2} \qquad (5.59)$$

Finally, we have a uniform asymptotic expansion for G,

$$G\sim\epsilon^2\zeta\tau-8\epsilon^{5/2}\tau^{3/2}Re^{-1/2}\left\{\frac{1}{6\pi^{1/2}}-i^3\operatorname{erfc}\left(\frac{\zeta}{2}\left(\frac{Re}{\epsilon\tau}\right)^{1/2}\right)\right. \qquad (5.60)$$
$$\left.+i^3\operatorname{erfc}\left(\frac{1-\zeta}{2}\left(\frac{Re}{\epsilon\tau}\right)^{1/2}\right)\right\}+O(\epsilon^3)$$

and
$$h\sim 1-\epsilon^2\tau^2+\frac{32}{15\pi^{1/2}}Re^{-1/2}\epsilon^{5/2}\tau^{5/2}+O(\epsilon^3) \qquad (5.61)$$

Equations (5.35), (5.41) and (5.47) show that no more terms will be generated until $O(\epsilon^4)$, so the remainder terms in (5.60) and (5.61) can be reduced. Since ϵ was artificially introduced into the problem, it can be removed by using a different timescale to express the results. If t_c is chosen to be t_i, as will be the case in the rest of this chapter, the expansions are expressed in their most useful form:

$$F \sim zt - 8t^{3/2}Re^{-1/2}\left[\frac{1}{6\pi^{1/2}} - i^3\operatorname{erfc}\left(\frac{z}{2}\left(\frac{Re}{t}\right)^{1/2}\right) + i^3\operatorname{erfc}\left(\frac{1-z}{2}\left(\frac{Re}{t}\right)^{1/2}\right)\right] + O(t^3) \qquad (5.62)$$

$$h \sim 1 - t^2 + \frac{32}{15\pi^{1/2}}Re^{-1/2}t^{5/2} + O(t^4) \qquad (5.63)$$

These expansions are valid whenever $t \ll 1$ and $t \ll Re$. The velocity profile is

$$\frac{u}{r} \sim t\left\{1 - 4i^2\operatorname{erfc}\left(\frac{z}{2}\sqrt{\frac{Re}{t}}\right) - 4i^2\operatorname{erfc}\left(\frac{1-z}{2}\sqrt{\frac{Re}{t}}\right)\right\} + O(t^3) \qquad (5.64)$$

Expansion (5.64) shows a uniform constant acceleration in the inviscid core with boundary layers whose thickness grows as $(t/Re)^{1/2}$. For small Re the above expansions quickly become invalid as the boundary layers merge and viscous effects dominate the flow. For large Reynolds numbers the boundary layers persist for a long time but the expansions break down when nonlinear effects become important and the acceleration is no longer constant. The effect of Re first enters in terms of $O(\epsilon^{5/2})$ in (5.61) and (5.63) and describes the radial outflow in the top and bottom start-up boundary layers for a uniformly accelerated core.

5.4 SOLUTION FOR LARGE RE

When the Reynolds number is large, the flow is governed by the inertia of the fluid except for thin boundary layers near the top and bottom walls. Thus, it is appropriate to choose the characteristic inertial time $t_c = t_i$ in (5.2) This gives

$$F_{zt} + F_z^2 - 2FF_{zz} - \frac{1}{Re} F_{zzz} = 1 \qquad (5.65)$$

Equations (5.65) and (5.4) must be satisfied in the inviscid core. In this region the reduced stream function F takes the simpler form

$$F = z\,\Phi(t) + \Theta(t) \qquad (5.66)$$

where the first term describes an inviscid stagnation-point flow and the second term, as we shall soon show, the displacement effect of the boundary layers. Substituting (5.66) in (5.65), one obtains

$$\Phi^2 + \Phi_t = 1 \qquad (5.67)$$

Φ and Θ satisfy the initial conditions

$$\Phi = 0,\ \Theta = 0, \text{ when } t = 0 \qquad (5.68)$$

The solution for Φ is:

$$\Phi = \tanh t \qquad (5.69)$$

This is the same as the solution in the inviscid limit given by Weinbaum, Lawrence & Kuang (1985). Boundary

conditions (5.3) and (5.4) cannot be satisfied by (5.66), so it is necessary to consider boundary layers near $z = 0$ and $z = h(t)$. The radial velocity outside the boundary layers is determined by the radial pressure gradient alone and is simply $u = r \tanh t$. It is unaffected by the presence of the boundary layers, so the analysis will be valid until the boundary layers overlap.

To analyze the boundary layer near $z = 0$, new variables $\zeta = zRe^{1/2}$ and $f = FRe^{1/2}$ are introduced. Equation (5.65) becomes the boundary-layer equation

$$f_{\zeta t} + f_\zeta^2 - 2ff_{\zeta\zeta} - f_{\zeta\zeta\zeta} = 1 \tag{5.70}$$

which has initial and boundary conditions

$$f = 0 \quad \text{when } t = 0 \tag{5.71}$$

$$f = 0, \quad f_\zeta = 0 \quad \text{on } \zeta = 0 \tag{5.72}$$

$$f \sim \zeta\Phi - Re^{1/2}\Theta \quad \text{as } \zeta \to \infty \tag{5.73}$$

In (5.66), Θ is the correction to the inviscid vertical velocity due to the displacement effect of the boundary layers. To illustrate this, the boundary layer displacement thickness δ^* is introduced:

$$\delta^*(t) = Re^{-1/2}\int_0^\infty \left(1 - \frac{f_\zeta}{\Phi}\right)d\zeta = Re^{-1/2}\Delta^* \tag{5.74}$$

in which f_ζ and Φ respectively represent the radial velocity in the boundary layer and core, and Δ^* is of order unity. Equation (5.74) is integrated directly and (5.73) is used to obtain

$$\delta^*(t) = \frac{\Theta(t)}{\Phi(t)} \quad \text{or} \quad \Theta(t) = \delta^*(t)\,\Phi(t) \tag{5.75}$$

Then in terms of δ^*, the stream function in the inviscid core is

$$F = (z-\delta^*)\,\Phi, \tag{5.76}$$

and the limiting condition on the boundary-layer equation (5.73) becomes

$$f \sim (\zeta-\Delta^*)\,\Phi \quad \text{as} \quad \zeta \to \infty \tag{5.77}$$

The flow is clearly symmetrical about the plane $z = \frac{1}{2}h$, so the boundary layer equations on the top surface $z = h$ can be cast in the same form as (5.70), (5.71), (5.72) and (5.77). To acnieve this, new variables $\tilde{\zeta} = Re^{1/2}(h-z)$ and $\tilde{f} = Re^{1/2}(\Phi h - F - 2\Theta)$, are introduced and substituted into (5.65), (5.4) and (5.5). The resulting equations are then separated in powers of Re to give the same set of boundary-layer equations, but with $\tilde{f}$ and $\tilde{\zeta}$ replacing f and ζ. However a new equation is also produced from (5.4) and (5.76),

$$h_t + 2h\Phi - 4\Theta = 0 \tag{5.78}$$

Using initial condition (5.5), one can solve equation (5.78) exactly to give

$$h = \frac{1}{\cosh^2 t} + Re^{-\frac{1}{2}} h_1(t) \qquad (5.79)$$

in which $h_1(t)$ is the correction to the inviscid result due to the displacement effect of the boundary layers. It satisfies the equations

$$h_{1t} + 2(h_1 - 2\delta^*)\Phi = 0 \qquad (5.80)$$

$$h_1 = 0 \quad \text{when } t=0 \qquad (5.81)$$

Equations (5.66), (5.70)-(5.72), (5.77) and (5.79)-(5.81) represent a solution which is exact whenever there are distinct boundary layers in the flow. The solution only breaks down when the boundary layers begin to overlap. $\delta^*(t)$ represents the correction to the inviscid solution developed in Weinbaum, Lawrence & Kuang (1985). It is determined by solving (5.69)-(5.72) and (5.77) and can then be used in (5.80) to calculate the correction to the gap height, $h_1(t)$. It is possible to solve (5.70) numerically, but this is complicated by the presence of the time derivative and is tantamount to a solution of the full Navier-Stokes equation which will be undertaken in section 5.5 below. To gain from a boundary layer analysis we must simplify the equation, so we will find an approximate solution using a time-dependent momentum integral method.

Equation (5.70) is reduced to an ordinary differential equation by integrating through the boundary layer and assuming a particular form of the velocity profile. A new variable, $\delta(t) = Re^{\frac{1}{2}}\Delta(t)$ is introduced to represent the outer edge of the boundary layer. Equation (5.70) is integrated over ζ from 0 to Δ to give

$$[F(\Delta)]_t - \Delta_t f_\zeta(\Delta) + 3\int_0^\Delta f_\zeta^2\, d\zeta - 2f_\zeta(\Delta)f(\Delta) - f_{\zeta\zeta\zeta}(\Delta) + f_{\zeta\zeta\zeta}(0) - \Delta = 0 \quad (5.82)$$

A biquadratic radial velocity profile is chosen ($u = rf_\zeta$) where the velocity and its gradient are matched at $\zeta = k\Delta$. A simple cubic or quartic profile is not sufficiently general to describe the behaviour at early time:

$$f = a_0 + a_1\zeta + a_2\zeta^2 + a_3\zeta^3, \qquad 0 \le \zeta \le k\Delta \quad (5.83)$$

$$f = b_0 + b_1\zeta + b_2\zeta^2 + b_3\zeta^3, \qquad k\Delta \le \zeta \le \Delta \quad (5.84)$$

The a_i and b_i and δ are functions of t, and k is a constant to be chosen at a later stage in the analysis. The boundary conditions to be satisfied by (5.83), (5.84) are :

$$\text{on } \zeta = 0: \quad f = 0,\ f_\zeta = 0,\ f_{\zeta\zeta\zeta} = -1 \quad (5.85)$$

$$\text{on } \zeta = \Delta: \quad f_\zeta = \Phi,\ f_{\zeta\zeta} = 0 \quad (5.86)$$

$$\text{on } \zeta = k\Delta: \quad f,\ f_\zeta,\ f_{\zeta\zeta} \text{ are continuous} \quad (5.87)$$

The first two of equations (5.85) are the original boundary conditions; the third is derived by setting $\zeta = 0$ in (5.70). Equations (5.86) constitute the definition of the outer edge of the boundary layer and (5.87) are desirable smoothness properties of the velocity profile. Equations (5.83)-(5.87) are solved to find the coefficients a_i and b_i in terms of the still unknown k and $\Delta(t)$. The details of this and the following algebra are to be found in Kuang (1984). The coefficients are determined to be :

$$a_0 = 0, \quad a_1 = 0, \quad a_2 = \frac{k\Delta^2 + 2\Phi}{2\Delta(1+k)}, \quad a_3 = -\frac{1}{6} \tag{5.88}$$

$$b_0 = \frac{-k^3\Delta(\Delta^2 - 2\Phi)}{6(1-k^2)}, \quad b_1 = \frac{k^2(\frac{1}{2}\Delta^2 - \Phi)}{(1-k^2)}, \quad b_2 = \frac{\Phi - \frac{1}{2}k^2\Delta^2}{\Delta(1-k^2)}, \quad b_3 = \frac{k^2\Delta^2 - 2\Phi}{6\Delta^2(1-k^2)} \tag{5.89}$$

Equations (5.83), (5.84), (5.88) and (5.89) describe a family of velocity profiles which, once k is chosen, will have a single parameter, $\Lambda(t) = \Delta^2/\Phi$. These equations are substituted into (5.82) and after a great deal of algebraic manipulation an equation for Λ is derived:

$$\Lambda_t = \frac{-1 + \Lambda[\frac{1}{2} + d_1\Phi_t + d_2\Phi^2] + \Lambda^2[-\frac{1}{8}k^2\Phi_t + d_3\Phi^2] + \Lambda^3 d_4\Phi^2}{\Phi(\frac{1}{8}k^2\Lambda + d_5)} \tag{5.90}$$

where $d_1, \ldots, d_5$ are constants depending only on the choice of k. If a simple cubic or quartic profile had been used one would obtain in place of (5.90) an equation with no real roots for Λ at $t = 0$.

$$d_1 = \frac{1}{4}(k^2 - k - 1), \qquad d_2 = -\frac{1}{3}(k^2 - 2k - 2) + \frac{2}{5}\frac{2k^3 - k^2 - 4k - 2}{1+k} \tag{5.91}$$

$$d_3 = \frac{1}{6}k^2 - \frac{1}{20}k^2\frac{k^3 - 3k^2 + 8k + 4}{1+k} \tag{5.92}$$

$$d_4 = \frac{1}{40} k^4 \frac{k-3}{1+k}, \qquad d_5 = -\frac{1}{12}(k^2-5k-5) \tag{5.93}$$

Before an attempt is made to solve (5.90), it is useful to consider the range of values for Λ. The shear stress must be positive in the boundary layer, which requires that $f_{\eta\eta} > 0$ everywhere. This is true only for values of Λ between $\Lambda_{min} = -2/k$ and $\Lambda_{max} = 2/k$, so Λ is bounded. Furthermore, Λ must be positive since Φ is always positive. Thirdly, there is a value Λ_b for which the denominator of (5.90) vanishes and the profile changes discontinuously. This non-physical behaviour is not permissible and occurs when

$$\Lambda = \Lambda_b = \frac{2}{3k^2}(k^2-5k-5) \tag{5.94}$$

We can also use (5.90) to find the initial and final values for Λ. For very large time, the flow in the boundary layer will be that for a quasi-steady stagnation point, since Φ from (5.69) approaches unity and Λ will approach a steady value Λ_∞ which satisfies

$$d_4 \Lambda_\infty^3 + d_3 \Lambda_\infty^2 + d_2 \Lambda_\infty - 1 = 0 \tag{5.95}$$

When $t = 0$, the denominator of (5.90) vanishes since Φ is zero. Since Λ should not be singular, the numerator must also vanish. One can show that the vanishing of the numerator requires that Λ have the initial value Λ_0, with

$$\Lambda_0 = \frac{1}{k^2}\left\{(1-k+k^2) \pm \left[(1-k+k^2)^2 - 8k^2\right]^{1/2}\right\} \tag{5.96}$$

using the fact that $\Phi \sim t$ at very short time. Equation (5.96) can be used to find a suitable value for k since the analytic solution is available for the first part of the motion from section 5.2. Equations (5.62) and (5.77) imply that when t is small $\Delta^* = (4/3\pi^{\frac{1}{2}})t^{\frac{1}{2}}$. For the assumed velocity profile (5.83), (5.84), the scaled displacement thickness is

$$\Delta^* = \Delta \frac{(1+k+k^2)-\frac{1}{2}k^2\Lambda}{3(1+k)} \tag{5.97}$$

From the definition of Λ, $\Delta = \Lambda^{\frac{1}{2}}\Phi^{\frac{1}{2}}$ and so, when t is small,

$$\Delta \sim \Lambda_0^{\frac{1}{2}} t^{\frac{1}{2}} \tag{5.98}$$

Equation (5.98) is substituted into (5.97) to give for small t

$$\Delta^* = c^* t^{\frac{1}{2}} \tag{5.99}$$

with
$$c^* = \Lambda_0^{\frac{1}{2}} \frac{(1+k+k^2)-\frac{1}{2}k^2\Lambda_0}{3(1+k)} \tag{5.100}$$

For each value of k, (5.96) and (5.100) give two values of c^* (one for each root of Λ_0), as shown in figure 5.4. There are no real solutions for c^* if k is chosen larger than 0.2819. This means that, for larger k, the velocity profile (5.83), (5.84) is not an adequate representation of the true solution and leads to physically unrealizable results. For k smaller than this limit, values of c^* between $\frac{2}{3}$ and $\frac{2\sqrt{2}}{3}$ are physically possible. However, if we wish to obtain limiting behaviour for δ^* at very short

times, which is the same as the analytic solution in section 5.2, then c^* must be $4/3\pi^{1/4}$. This corresponds to the value of k = 0.2397 which is on the lower branch of the curve using the negative sign in (5.96). With this value of k, equations (5.94)-(5.96) give

$$\Lambda_0 = 6.275, \quad \Lambda_\infty = 3.032, \quad \Lambda_b = 15.05 \qquad (5.101)$$

The shape of the velocity profile is shown in figure 5.5 for these values of Λ and for $\Lambda = 0$. It is clear that very little change in the profile occurs between the values Λ_0 and Λ_∞. The small-time profile (5.64) is drawn on a corresponding scale and we see that it is modelled quite closely by the curve for Λ_0.

Equation (5.90) is relatively easy to integrate numerically to find $\Lambda(t)$, $\delta(t)$ and $\delta^*(t)$, which are shown in figure 5.6. Λ decays monotonically from Λ_0 to Λ_∞ and is well within the physical bounds defined above. δ and δ^* do not increase monotonically, but increase to maxima just after t = 1 and then decay slightly to their steady values. The steady value of δ^* is 0.5665 Re , which compares well with the exact numerical solution for steady stagnation-point flow obtained by Frössling (1940) $\delta^* = 0.5685 Re^{-\frac{1}{2}}$. The decline in δ and δ^* can be explained by regarding the end of the boundary-layer development as a quasi-steady stagnation-point flow. For the steady flow the boundary layer thickness is inversely proportional to the square root

of the core velocity. Thus, as the velocity increases slowly toward the steady value, the boundary-layer thickness decreases slightly. The steady value of δ, $1.741Re^{-\frac{1}{2}}$, can be used to estimate the limit of validity of the solution. When Re is sufficiently large, the steady-state boundary-layer will develop before the limit is reached and h(t) is accurately approximated by $1/\cosh^2 t$. The limit is reached when $h = 2\delta \approx 3.5Re^{-\frac{1}{2}}$; this gives the limit of validity $t_{max} \approx \frac{1}{4}\log Re$.

Equations (5.80) and (5.81) are integrated numerically using the solution for δ^*. The displacement correction to the inviscid solution to the gap height h_i is shown in figure 5.7 together with the total height for various Reynolds numbers. These solutions have the limit of validity derived above; after the limit is passed the height tends to a constant non-zero value, which is not physically possible. However, for $Re > 10^4$, the body falls through more than 98% of the initial height before the limit is reached, so the approximate solution describes the important part of the motion.

It will be shown that the solutions are very accurate compared with the exact numerical solution until the limit derived above is reached. The two important features of the solution which give rise to this accuracy are the use of the analytically derived form of δ^* when t is small and the fact

that the radial velocity component in the inviscid core is independent of the displacement effect of the top and bottom boundary layers.

5.5 NUMERICAL SOLUTION

The boundary conditions (5.4) at the moving boundary $z = h$ are inconvenient to apply in a numerical solution so a new independent variable $x = z/h(t)$ is introduced. The characteristic inertial time t_i is used for non-dimensionalization, since it is the time most commonly used in the previous sections. For brevity, the velocity $U = (1/h)F_x$ is introduced and (5.2) becomes

$$U_t + U^2 - \frac{2FU_x}{h} - \frac{xh_tU_x}{h} - \frac{U_{xx}}{Reh^2} - 1 = 0 \qquad (5.102)$$

Equation (5.102) contains a new term arising from the time-dependence of the x-coordinate. The boundary conditions become:

$$F = 0, \quad U = 0 \quad \text{on} \quad x = 0 \qquad (5.103)$$

$$F = -\tfrac{1}{2}h_t, \quad U = 0 \quad \text{on} \quad x = 1 \qquad (5.104)$$

The flow is symmetrical about $x = \frac{1}{2}$, so the equation need be solved only in the region $0 \leqslant x \leqslant \frac{1}{2}$ and (5.104) can be replaced by

$$F = -\tfrac{1}{4}h_t, \quad U_x = 0 \quad \text{on} \quad x = \tfrac{1}{2} \qquad (5.105)$$

Equations (5.102), (5.103) and (5.105) are solved using an implicit central difference numerical scheme. For small to moderate Re, the boundary layer development is so rapid that no special consideration is needed. For larger Re, the detailed structure of the boundary layer is important for a considerable part of the motion. However, a simplifying feature is that when the boundary layer must be modelled, the core flow need not be since it is a simple plug flow. In either case, the small time solutions (5.62)-(5.64) are used to start the numerical procedure. Because of the diffusive nature of the solution, a rather small time step is needed for the integration to be stable. For all Reynolds numbers, the velocity profile eventually becomes nearly parabolic and then fewer points are needed in the discretization of the x-direction. In the limit of parabolic flow, the central difference scheme is exact and only two points are needed to apply the boundary conditions. The error in these numerical solutions is estimated to be 0.1% up to t = 4. The solutions for $h(t)$, $h_t(t)$ and $\delta^*(t)$ are shown in figures 5.7, 5.8 and 5.9.

Figure 5.9 shows that the integral boundary layer solution predicts δ^* very accurately up to the time when the boundary layers meet. The limit of validity of the integral solution t_{max} is predicted accurately for $Re > 10^3$, but over predicted for smaller Re because then the boundary layers' development is not completed before they meet. The

predictions of the displacement correction to h and h_t shown in figures 5.7 and 5.8 are accurate well beyond t_{max}, because the total flow does not change very much until well after the boundary layers meet. The figures indicate that the integral boundary layer method gives satisfactory results for almost all of the motion for Re larger than 1000. For smaller Re, the boundary layers meet when the height is still relatively large and the interaction is important. The figures also confirm that the small Re solution derived in section 5.2 retains some accuracy up to a Reynolds number of 10.

The development of the velocity profile is shown in figure 5.10 for Re = 10 and Re = 1000. For the larger Reynolds number, the profile shows a boundary layer almost until the peak velocity is achieved. The boundary layers merge between t = 1.5 and 2.0 and then the viscous forces slow down the flow, with the profile moving towards a parabola. For the smaller Reynolds number, the viscous effects become important well before the peak velocity is achieved. The acceleration of the viscous flow is much slower and a lower maximum velocity is achieved.

5.6 DISCUSSION

This chapter began with a discussion of the timescales in the problem and we are now in a position to resume that discussion. Figure 5.11 shows the times for the draining of 50% and 95% of the fluid filled gap as a function of Reynolds number for zero β. The time for h to fall to 5% of its original value will be referred to as the draining time. We see that this is nearly constant for $Re > 10^3$, when the fluid motion is largely inviscid throughout the draining time. For smaller Re, viscous effects become important during the draining time and the time taken varies inversely with Re. This figure is plotted using a dimensionless time based on t_i. The results are more illuminating when put in dimensional form, with dimensional draining time T. For zero β we have two limiting cases. For large Re ($>10^3$), $T = 2.18t_i$, so the draining time is indeed characterized by the inertial time t_i. For small Re (<10), $T = 1197t_v$, so the draining time depends only on t_v, but it is a very large multiple of t_v. This explains why the low Reynolds number analysis is valid even for Reynolds numbers up to 10. The results of all the limiting cases presented in this chapter can be treated in this way and are summarized in table 5.1. The limit $Re \to 0$, $\beta \to \infty$ is not treated in this chapter since only pathological physical interpretations could be found. The results in this limit depend on the product $Re\beta$. The table confirms the interpretations of the three

Limit	Ordering of timescales	Draining time T
$Re \to \infty$, $\beta \to 0$	$t_g \ll t_i \ll t_d$	$2.18 t_i$
$Re \to \infty$, $\beta \to \infty$	$t_i \ll t_d$, $t_i \ll t_g$	$1.38 t_g$
$Re \to 0$, $\beta \to 0$	$t_d \ll t_i$, $t_g \ll t_i$	$1197 t_v$

Table 5.1. Summary of results for dimensional draining time T in limiting cases.

characteristic times of the problem and the limits in which they are important. The draining time is determined by the dominant force resisting the motion. If the fluid inertia is dominant, the draining time is characterized by t_i. If the viscous forces are dominant, the important timescale is t_v, but the draining time is a large multiple of t_v. This is because t_v is based on the initial configuration and the velocity decreases as the gap narrows. If the body inertia is dominant, the draining time is characterized by t_g.

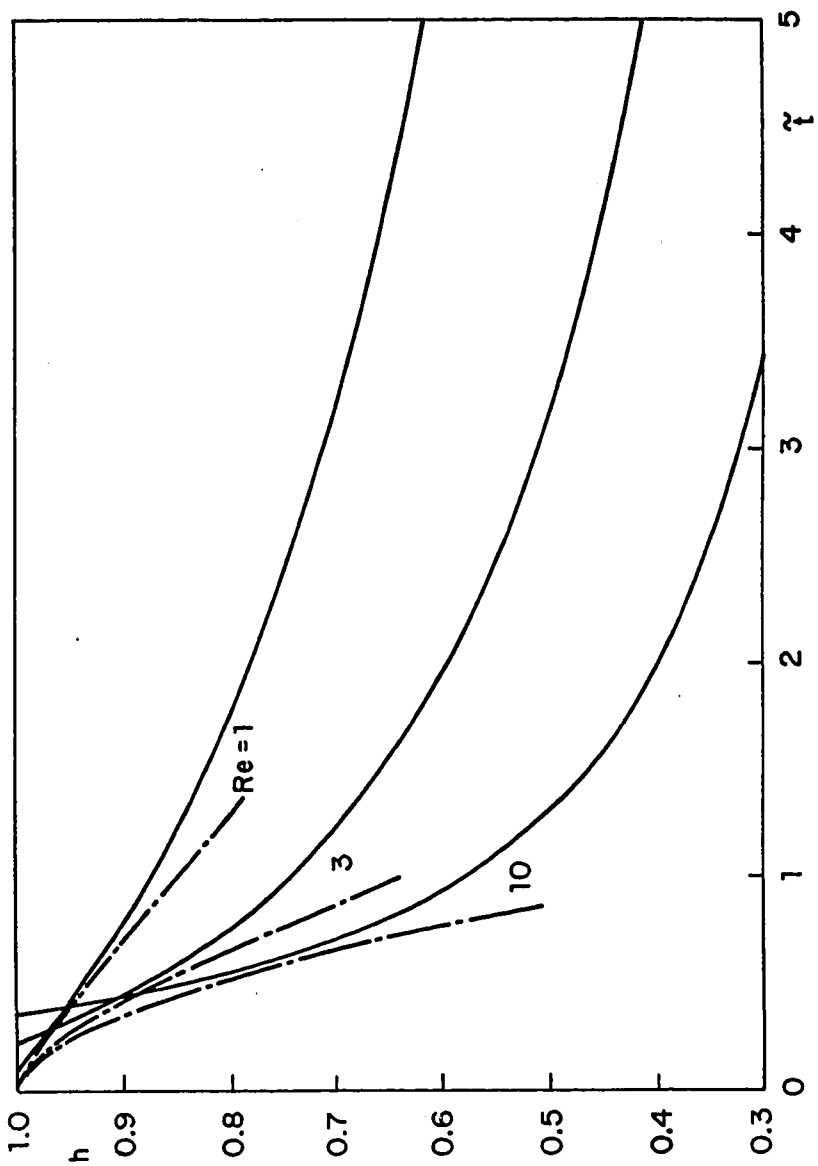

Figure 5.1. Time-dependence of h for small Reynolds numbers ($\beta = 0$ limit): -.-.- , small t asymptotic expansion (5.33); _____ , large t asymptotic expansion (5.31).

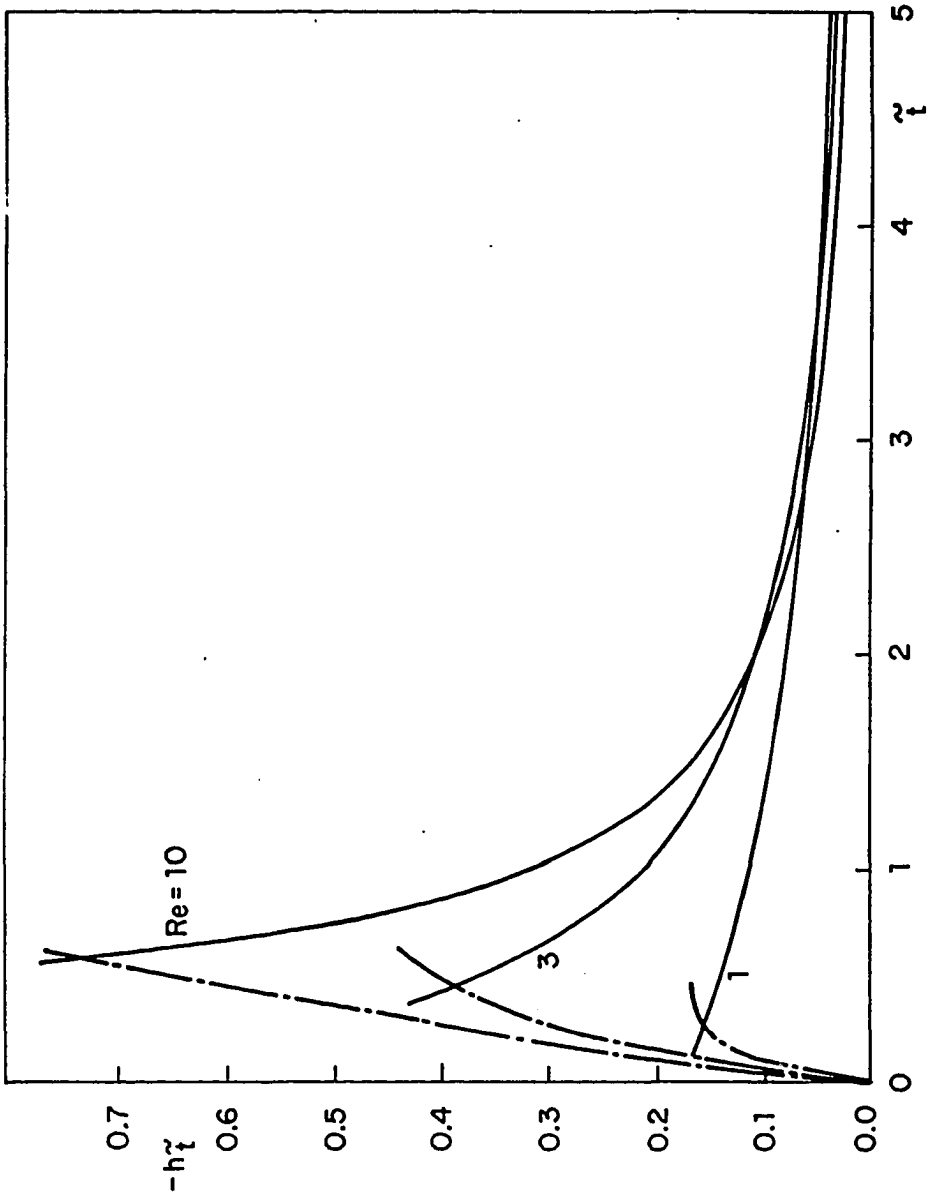

Figure 5.2. Time-dependence of disc velocity for small Re ($\beta = 0$ limit): -.-.- , small t asymptotic expansion (5.34); ——— , large t asymptotic expansion (5.32).

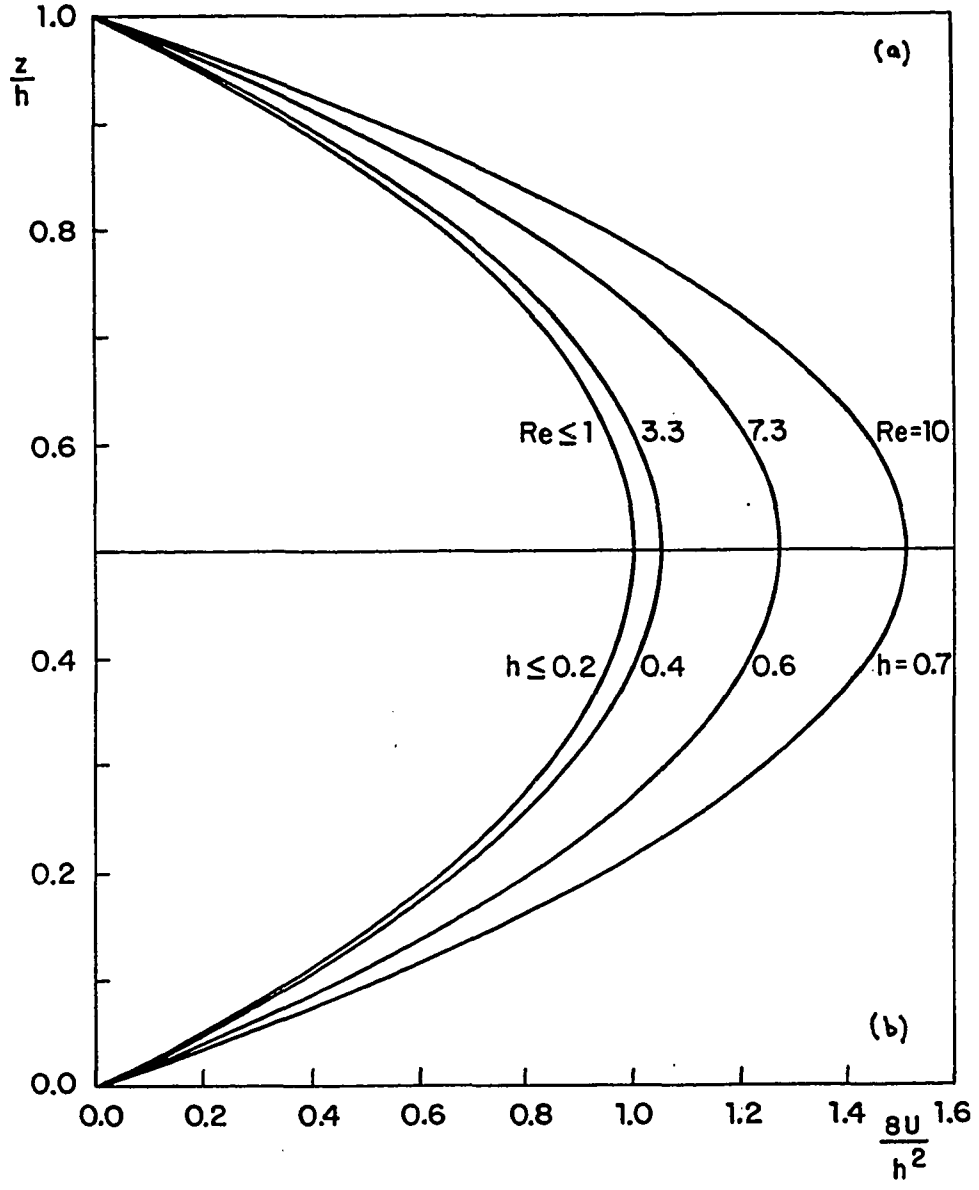

Figure 5.3. Velocity profiles in the limit $\beta = 0$ for small Re, (a) the dependence on Re at given h = 0.7. (b) the dependence on h for given Re = 10.

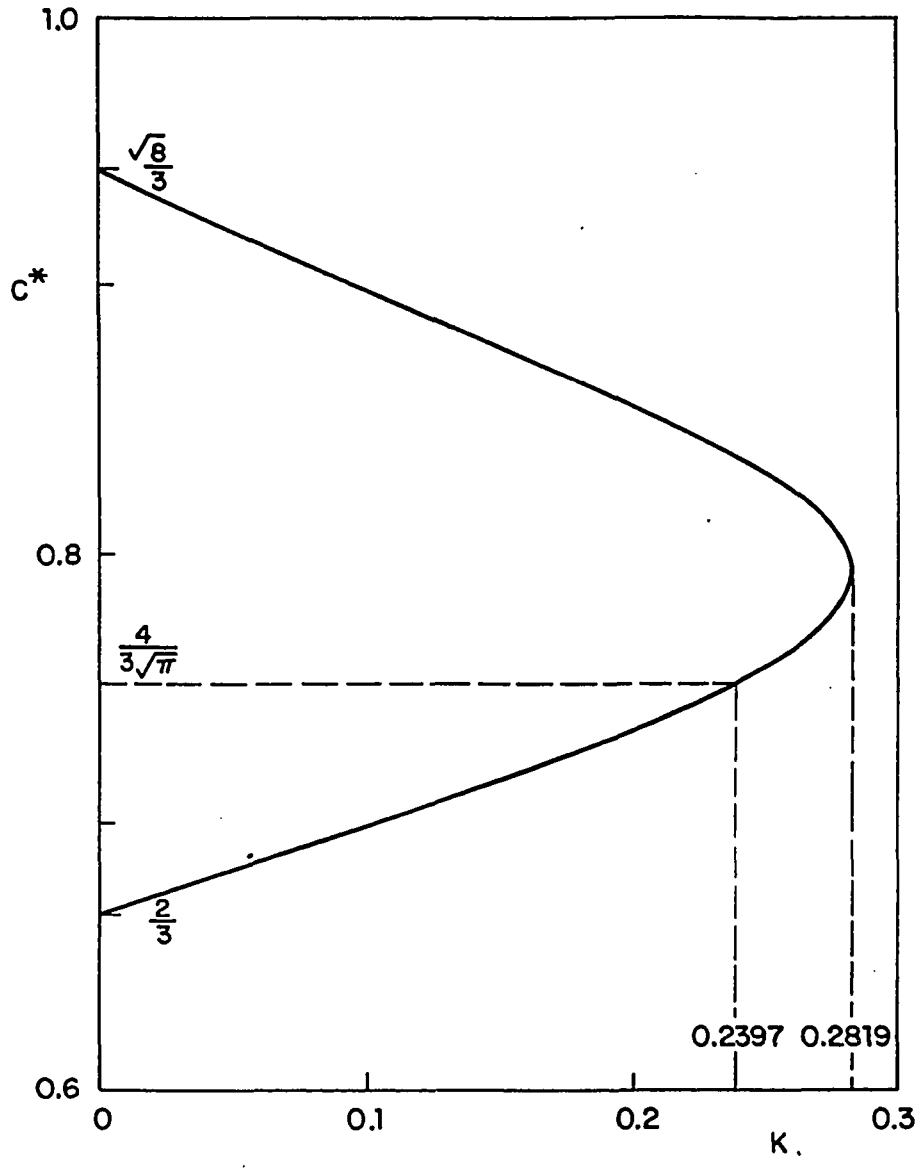

Figure 5.4.Variation of the coefficient c^* with choice of k.

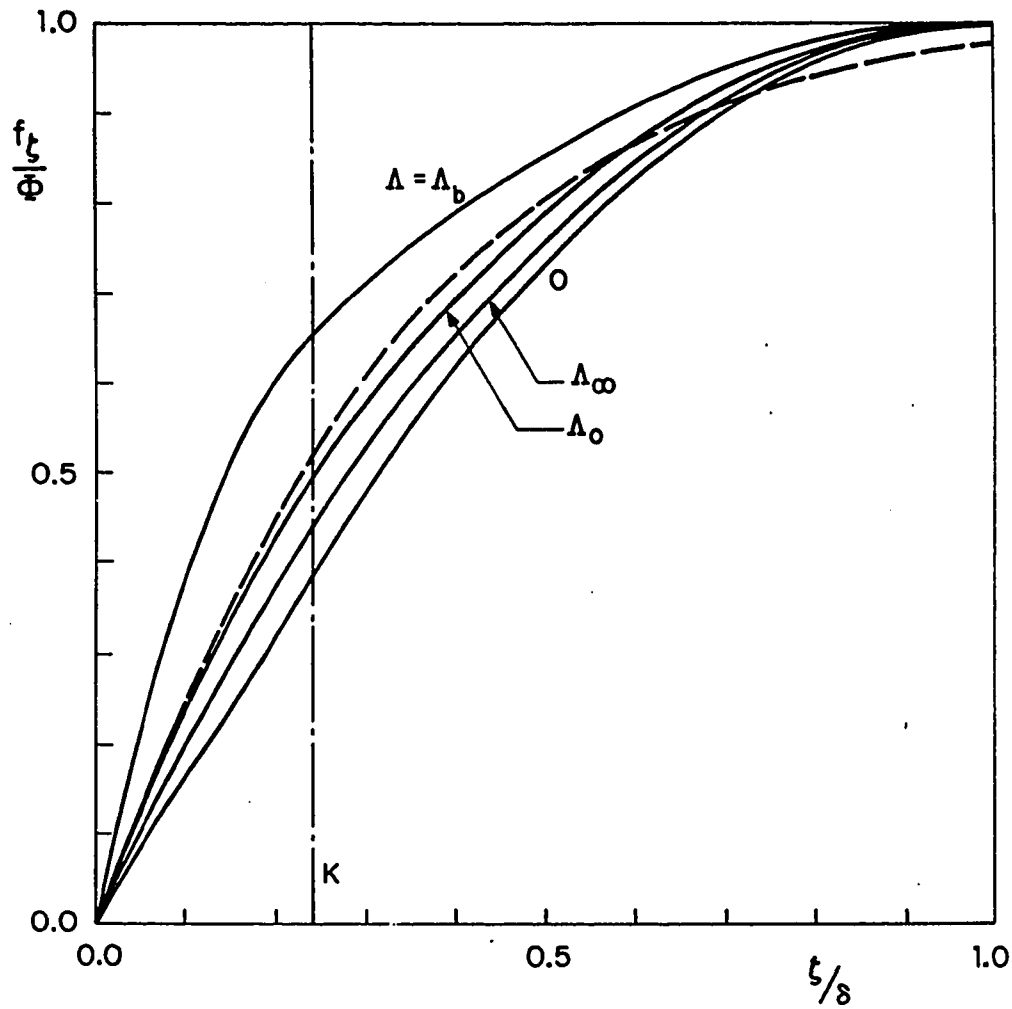

Figure 5.5. Velocity profiles in the boundary layer: ——— , biquadratic profiles used in integral solution (5.83), (5.84), (k = 0.2397, Λ_0 = 6.2745, Λ_∞ = 3.0315, Λ_b = 15.05); – – – – – , analytic solution for small t (5.64).

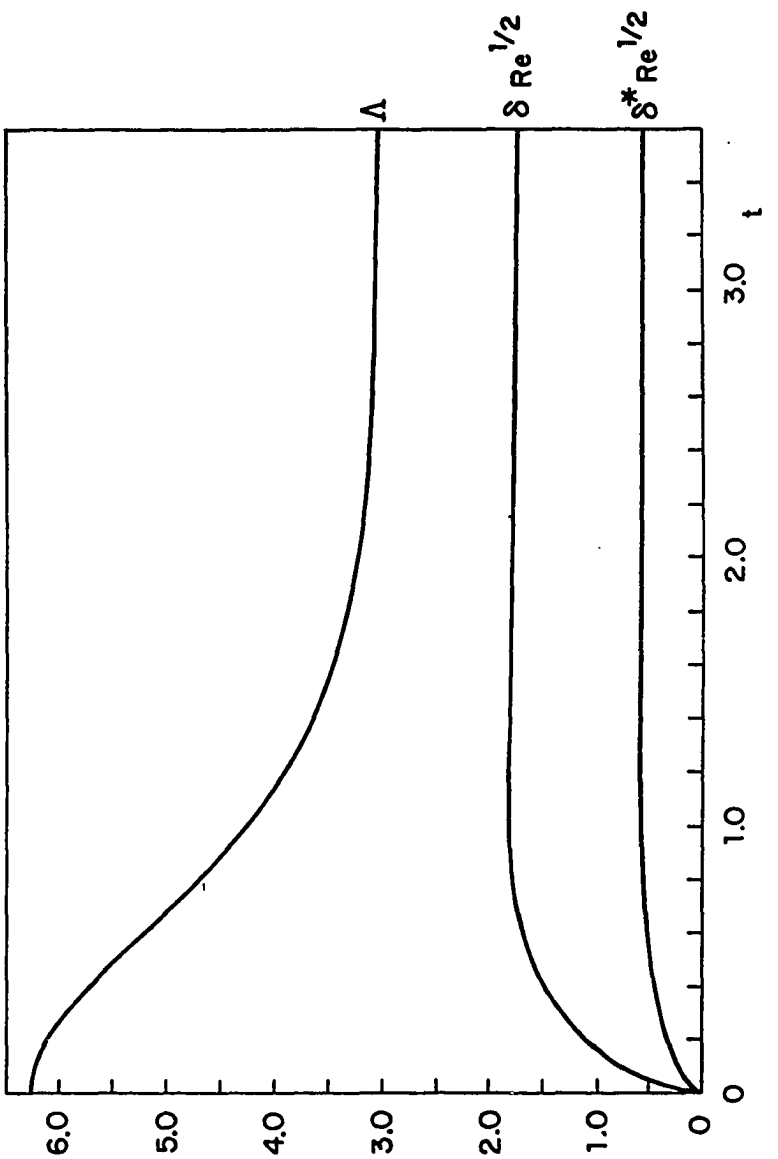

Figure 5.6. Numerical solution of (5.90) for $\Lambda(t)$, $\delta(t)$ and $\delta^*(t)$.

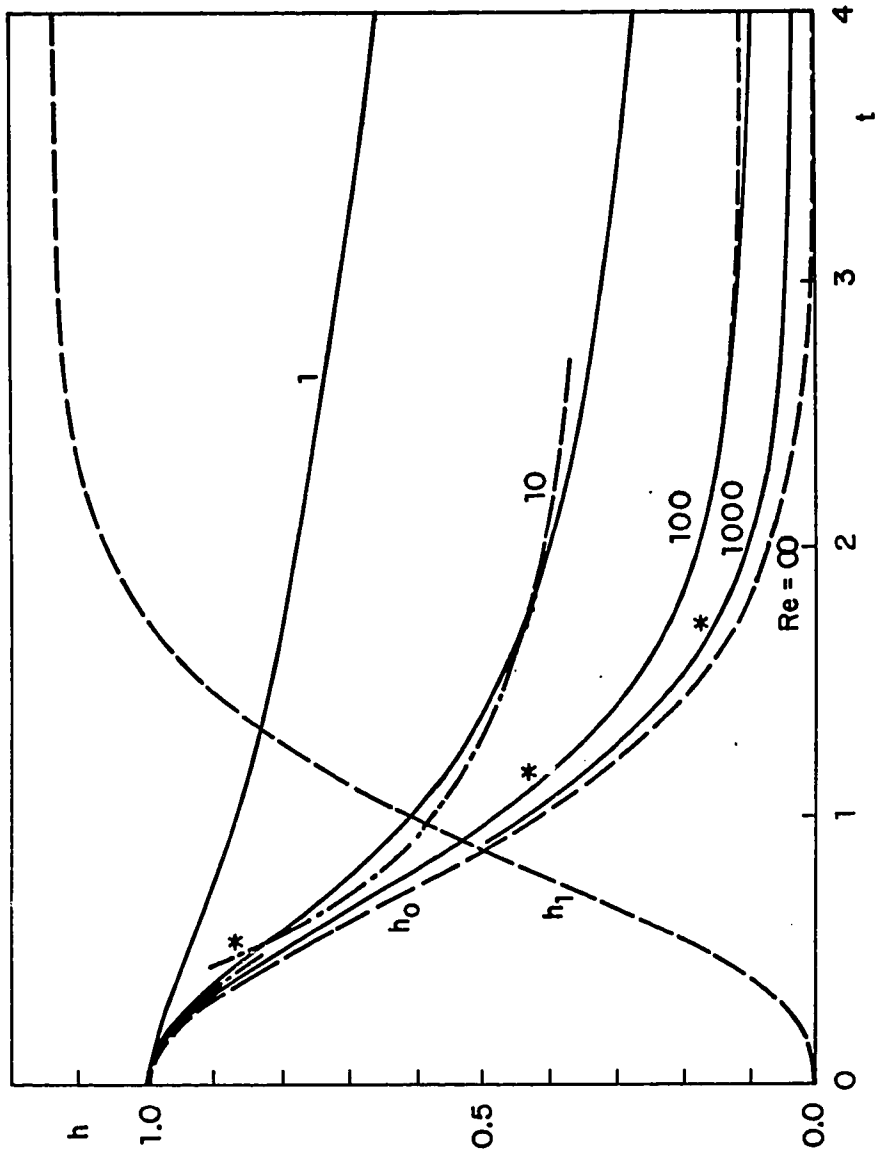

Figure 5.7. Solutions for the gap height h(t): ____ , numerical solution; ---- , integral boundary layer solution for large Re (h_0, h_1 also shown); *, predicted limit of validity of large Re solution; -•-•- , matched asymptotic solution for small Re.

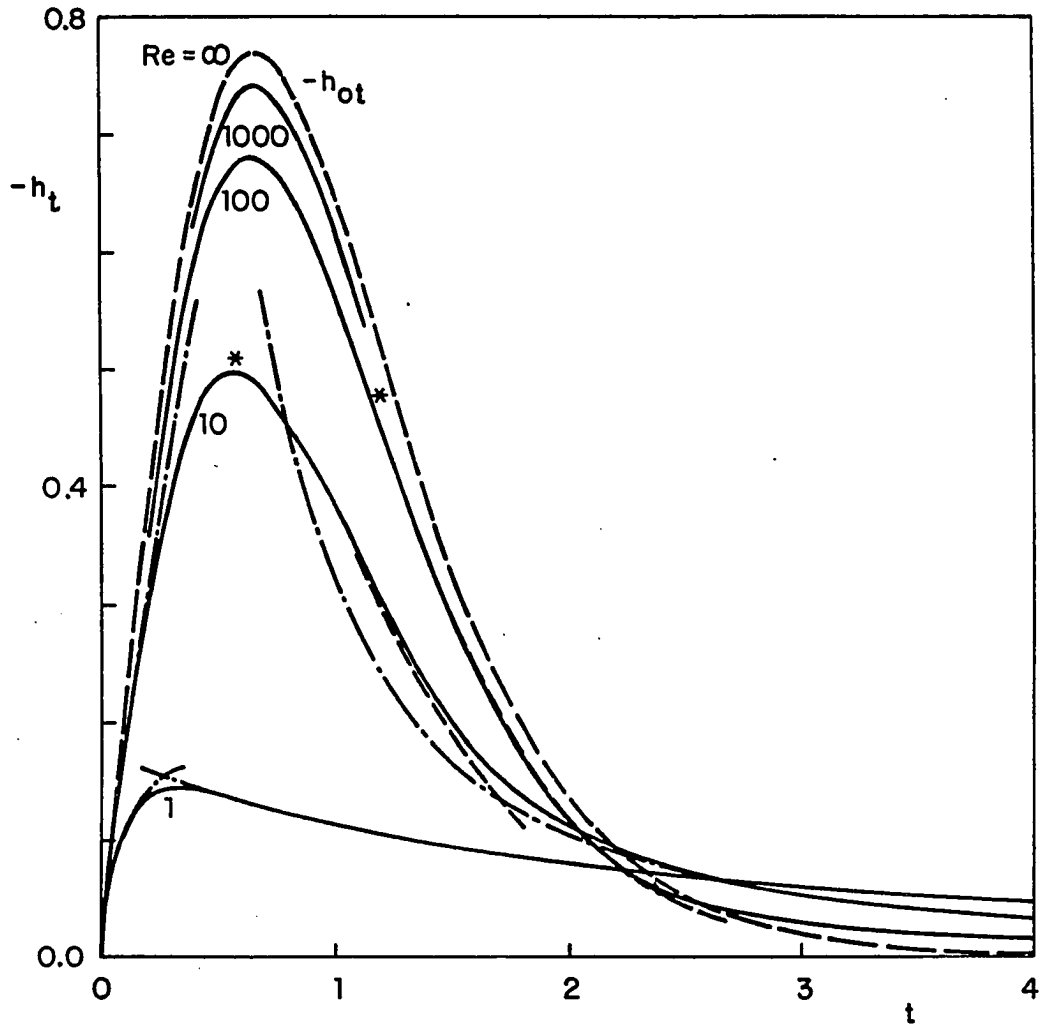

Figure 5.8. Solutions for the disc velocity $h_t(t)$: ____ , numerical solution; ---- , integral boundary layer solution for large Re; *, predicted limit of validity of integral solution; -.-.- , matched asymptotic solution for small Re.

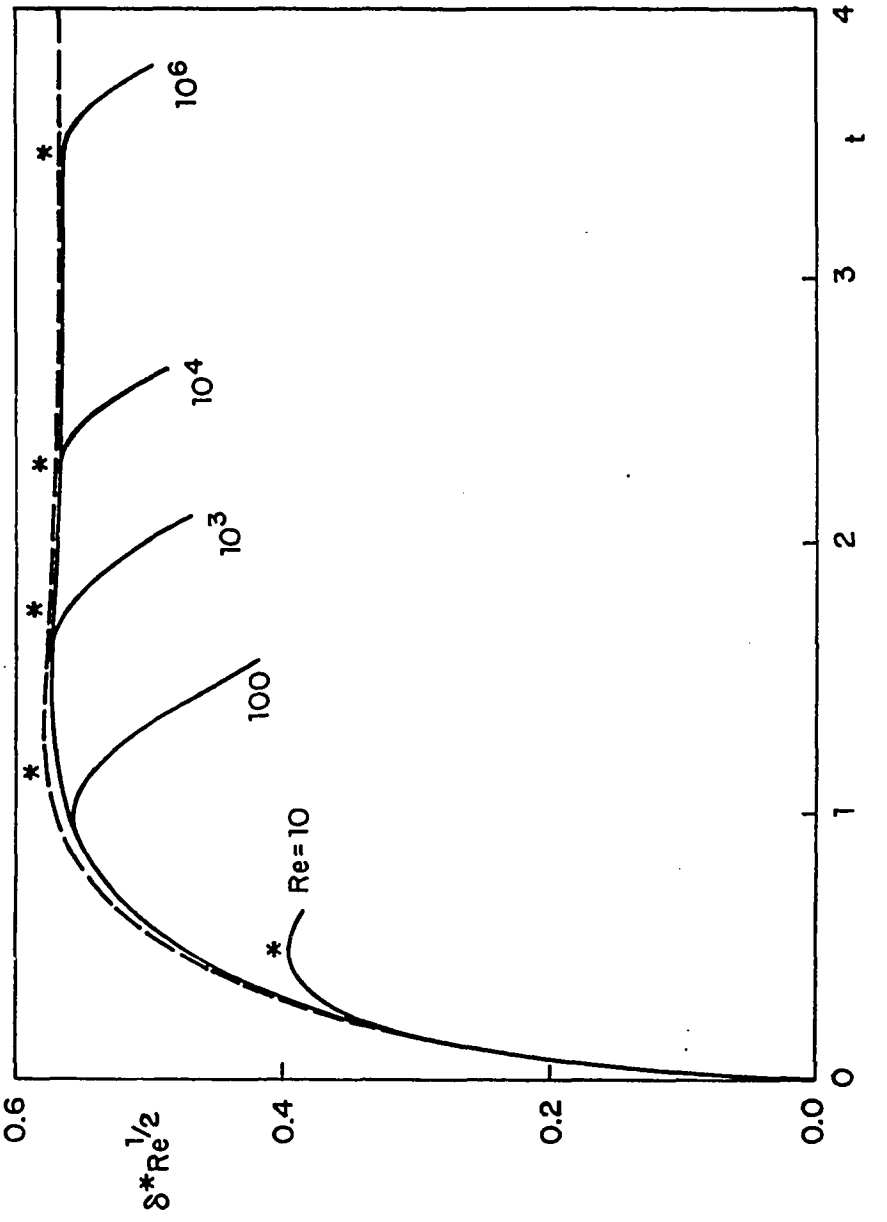

Figure 5.9. Scaled boundary layer displacement thickness $\delta^*(t)Re^{1/2}$ for large Reynolds numbers: ____ , numerical solution; ---- , integral boundary layer solution; *, predicted limit of validity of integral solution.

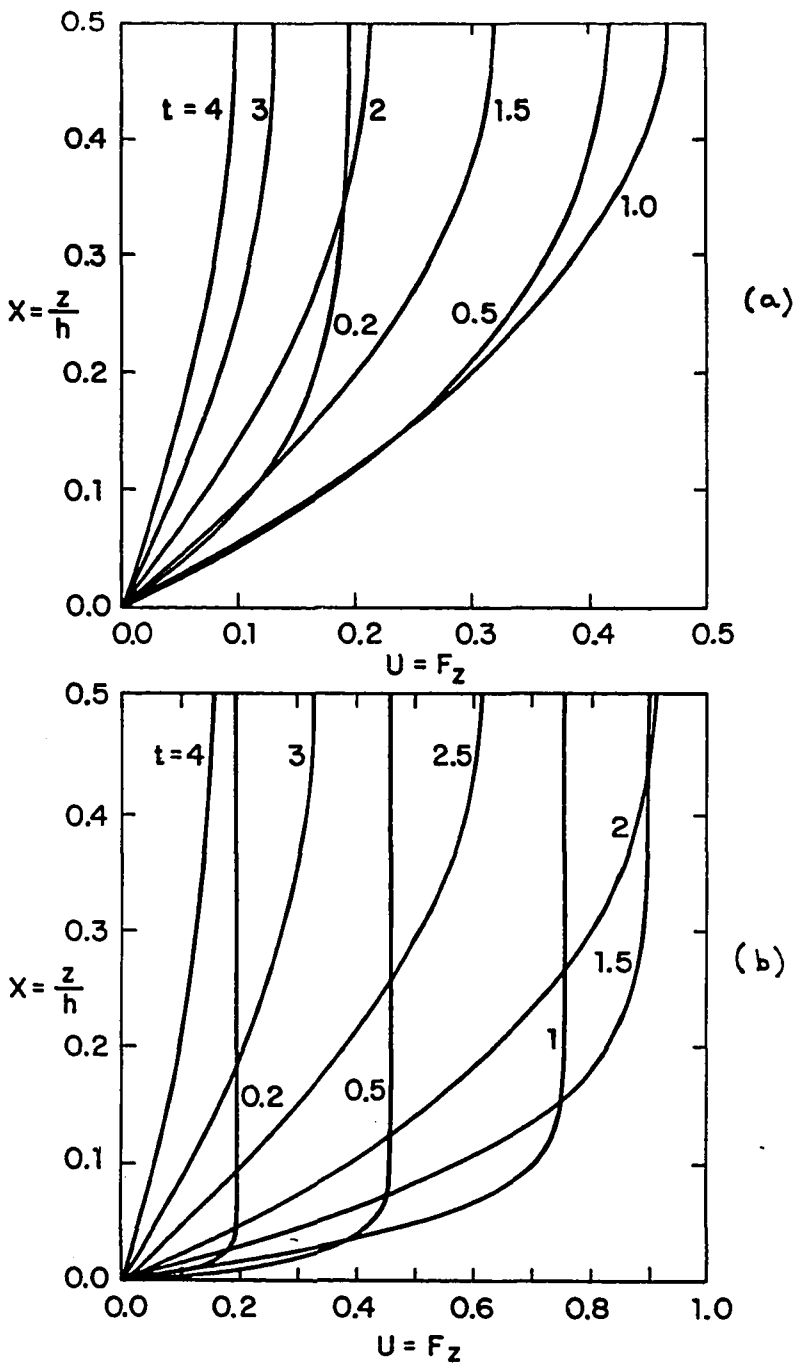

Figure 5.10. Development of radial velocity profile with time: (a) Re = 10; (b) Re = 1000. Note that the velocity scale in (a) is twice that in (b).

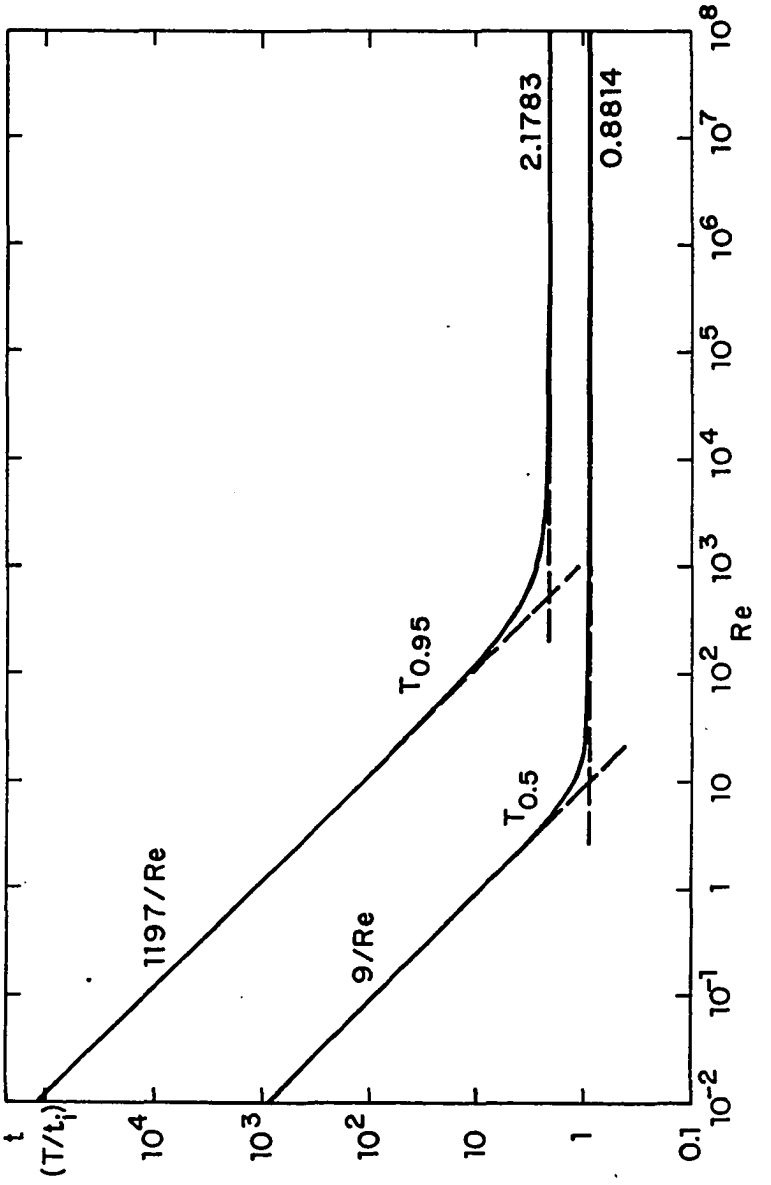

Figure 5.11. Draining times: T_f is the time for a fraction f of the fluid to drain from the gap.

CHAPTER 6. RELATED AND FUTURE WORK

6.1 INTRODUCTION

The work presented in Chapters 2 to 5 has broken new ground and has led to the development of some very interesting related problems. The original goal was to develop a theoretical understanding of an arbitrary hydrodynamic collision. In this problem two particles of arbitrary shape interact hydrodynamically and elastically. A general solution is still very far from being attained, but some progress has been made. In the present chapter, two paths which lead towards the general goal will be explored, each one emanating from a part of the main work of the dissertation. Firstly, the linearised equations of Chapter 3 will be adapted to deal with the slow time-dependent interaction of a rigid spherical particle with a rigid plane. A solution procedure will be proposed to circumvent the nonlinearity introduced by the time-dependent geometry. Secondly, the nonlinear equations of Chapters 4 and 5 will be modified to incorporate a simple model of elastic deformation. The parallel-plane geometry will be retained and a simple set of governing equations will be derived.

Other offshoots of the work described in this dissertation are being studied or are being considered for

development. These include the study of sideways linearized motion of a spheroid, leading to a possible generalization of Kim's (1985) work. Kim studied the quasi-steady interactive settling of a pair of equal spheroidal particles and it would be interesting to see the effect of the linear inertia terms on his solutions. Furthermore, a study has already begun to find the effects of elastic deformation in the collision approach of a convex body with a planar surface in the inviscid limit, with the objective of relating the magnitude of the elastic recoil to the storage of elastic energy from the build-up of pressure in the fluid gap.

6.2 SPHERE MOVING TOWARDS A PLANE IN LINEAR FLOW

The problem of a sphere falling through a fluid onto a plane surface is a very basic one and has often been studied (Brenner 1961, Wakiya 1961, Jeffrey & Chen 1977, Cox & Brenner 1967, etc.) However, the fully time-dependent case has not been studied. Wakiya (1961) used the method of reflections to find the effect of a distant wall on the time-dependent motion of a sphere, and Happel & Brenner (1965) noted that: "This solution is of interest in that no other treatment of unsteady flow in the presence of boundaries appears to be available." Later Cox & Brenner (1967) studied the inertial effects in the near collision

interaction of a sphere with a boundary. Jeffrey & Chen (1977) found the virtual mass of a sphere moving towards a plane wall through inviscid fluid and concluded: "It seems, therefore, that an unsteady analysis of the motion of the sphere is needed to settle exactly how it moves near the wall." The analysis of this problem seems, therefore, to be worthwhile and a solution procedure will be described below.

Whilst the steady Stokes equations and Laplace's equation are separable in the bispherical coordinate system, the unsteady Stokes equations are not. Thus, a more general technique such as the boundary integral method or multipole collocation method must be used. Ganatos, Weinbaum & Pfeffer (1980) showed that a multipole technique works very well for the problem of quasi-steady Stokes flow generated by a sphere moving between two plane walls, and their results may be used as a model for the present problem. Two coordinate systems are used and the geometry is shown in figure 6.1. Two cases will be discussed; (a) the sphere oscillates with small displacements about a fixed position, and (b) the sphere falls (slowly) towards the plane.

(a) oscillating sphere

In this case the problem is fully linear provided that the displacement of the sphere is small compared to its diameter and the gap height. The boundary condition on the

moving sphere may be linearized and applied at the average position of the boundary. The equations and boundary conditions to be solved are:

$$\psi = \psi^P + \psi^D \quad \text{with} \quad E^2\psi^P = 0 \quad \text{and} \quad (E^2 - c^2)\psi^D = 0 \tag{6.1}$$

$$\text{on } r=1: \quad \psi = -\tfrac{1}{2}\sin^2\theta, \quad \psi_r = -\sin^2\theta \tag{6.2}$$

$$\text{on } \varpi=0: \quad \psi = 0, \quad \psi_\varpi = 0 \tag{6.3}$$

$$\text{on } z=0: \quad \psi = 0, \quad \psi_z = 0 \tag{6.4}$$

The solution to (6.1)-(6.4) is given in mixed coordinates by:

$$\psi = \psi_s + \psi_w \tag{6.5}$$

where ψ_s is a series of Basset's spherical harmonics from (2.80), (2.81), representing the disturbance due to the sphere and ψ_w is a Fourier-Bessel integral of cylindrical harmonics which represents the disturbance due to the wall. These solutions are:

$$\psi_s = \sum_0^\infty \left[A_n r^{-n+1} + B_n R_n^{(-)}(r)\right] \mathcal{J}_n(\cos\theta) \tag{6.6}$$

$$\psi_w = \int_0^\infty \left[A(\alpha)e^{-\alpha z} + B(\alpha)e^{-\beta z}\right] \varpi J_1(\alpha\varpi)\, d\alpha \tag{6.7}$$

with

$$\beta^2 = \alpha^2 + c^2 \quad \text{and} \quad \mathrm{Re}\{\beta\} > 0 \tag{6.8}$$

The procedure of Ganatos, Weinbaum & Pfeffer (1980) is to satisfy (6.4) identically by writing (6.6) in cylindrical

coordinates and inverting the Hankel transform along the wall to determine the functions $A(\alpha)$, $B(\alpha)$ in terms of the coefficients A_n and B_n. The boundary conditions on the sphere (6.2) are then satisfied at a set of discrete points and the series are truncated to give a finite system of linear algebraic equations for A_n and B_n. The equations form a square matrix which is inverted to find the coefficients. The force on the wall may be found by integration of the normal stress (pressure); then the force on the sphere is found by adding the force on the wall to the far field terms. The problem of the oscillating sphere is not really important in itself, but gives insight into the more general problem described below, in which the velocity varies in an arbitrary way. It is also quite likely that this simpler problem may be used as the basis of an approximation to the solution of the more difficult problem.

(b) falling sphere

When the sphere falls towards the plane, the geometry of the problem is time-dependent and the boundary condition (6.10) cannot be linearized; thus the problem is nonlinear. The problem of part (a) is not a Laplace transform of the current problem and so cannot be inverted to find the force on the sphere in arbitrary motion. The memory integral (Basset force) in such an inversion would contain

accelerations that occured at different positions, so the resistance coefficient is implicitly time-dependent. However, the problem is not intractable if its linearity is exploited to the full before applying the nonlinear boundary conditions. The equations and boundary conditions for the problem are:

$$\nu E^4 \Psi - E^2 \Psi_t = 0 \tag{6.9}$$

with on $\varpi = \varpi_0(z,t)$: $\Psi = -\frac{1}{2}\varpi^2 W(t)$, $\Psi_n = -\varpi \varpi_n W$ (6.10)

$$\text{on } \varpi = 0: \quad \Psi = 0, \quad \Psi_{\varpi} = 0 \tag{6.11}$$

$$\text{on } z = 0: \quad \Psi = 0, \quad \Psi_z = 0 \tag{6.12}$$

where $$\varpi_0(z,t) = \varpi_0(z - d(t)) = \left[a^2 - (z-d)^2\right]^{1/2} \tag{6.13}$$

and $$d(t) = d_0 + \int_0^t W(t')dt' \tag{6.14}$$

Now we separate the disturbances due to the two boundaries before taking the Laplace transform.

So $$\Psi = \Psi_s + \Psi_w \tag{6.15}$$

where Ψ_s and Ψ_w satisfy (6.9) and (6.11), but the other conditions are relaxed. The problem for Ψ_s may now be re-written in the time-dependent coordinate system which is fixed in the sphere, since the acceleration of the frame of reference has no direct effect on the stream function. Thus, we can take Laplace transforms of the two individual problems, resulting in the same pair of proolems as were

solved in part (a). Thus the Laplace transforms of Ψ_s and Ψ_w are given by (6.6) and (6.7).

The transform for Ψ_s may be inverted to give

$$\Psi_s = \sum_0^\infty [a_n(t)\, r^{-n+1} + b_n(t) * r_n^{(-1)}(r,t)]\, S_n(\cos\theta) \qquad (6.16)$$

with $$r_n^{(-)}(r,t) = r^n \left(\frac{1}{r}\frac{d}{dr}\right)^{n-1}\frac{1}{r} f_1(r,t) \qquad (6.17)$$

In equation (6.16), $a_n(t)$, $b_n(t)$ and $f_1(r,t)$ are the inverse Laplace transforms of A_n, B_n and e^{-cr} respectively, and * is the convolution operator. The inverse transform of e^{-cr} may be found explicitly to give

$$f_1(r,t) = \frac{r}{2\sqrt{\pi}}\, e^{-r^2/4t}\, t^{-3/2} \qquad (6.18)$$

so that $$r_n^{(-)}(r,t) = -r^n \left(\frac{-1}{2t}\right)^n \frac{1}{\sqrt{\pi t}}\, e^{-r^2/4t} \qquad (6.19)$$

The transform ψ_w may be inverted to give:

$$\Psi_w = \int_0^\infty [a(\alpha,t)\, e^{-\alpha z} + b(\alpha,t) * f_2(\alpha,z,t)]\, \varpi J_1(\alpha\varpi)\, d\alpha \qquad (6.20)$$

in which $a(\alpha,t)$, $b(\alpha,t)$ and f_2 are the inverse Laplace transforms of $A(\alpha)$, $B(\alpha)$ and $e^{-\beta z}$ respectively, and f_2 may be found explicitly to be:

$$f_2(\alpha,z,t) = \frac{z}{2\sqrt{\pi}}\, e^{-z^2/4t}\, t^{-3/2}\, e^{-\alpha^2 t} \qquad (6.21)$$

Finally, we have:

$$\Psi_s = \sum_0^\infty \left\{ r^n \left(-\tfrac{1}{2}\right)^{n-1} \frac{1}{2\sqrt{\pi}} \int_0^t b_n(t-\tau)\, \tau^{-1/2}\, \tau^{-n}\, e^{-r^2/4\tau}\, d\tau + r^{-n+1} a_n(t) \right\} S_n(\cos\theta) \qquad (6.22)$$

$$\Psi_w = \int_0^\infty \left\{ a(\alpha,t) e^{-\alpha z} + \int_0^t b(\alpha,t-\tau) \frac{z}{2\sqrt{\pi}}\, e^{-z^2/4\tau}\, \tau^{-3/2}\, e^{-\alpha^2\tau}\, d\tau \right\} \varpi J_1(\alpha\varpi)\, d\alpha \qquad (6.23)$$

Now the solution procedure is the same as in (a). We express (6.22) in the cylindrical coordinate system by use of the time-dependent coordinate transformation. The boundary condition on the wall is satisfied by inverting the Hankel transform along the wall to get $a(\alpha,t)$, $b(\alpha,t)$ in terms of $a_n(t)$, $b_n(t)$. Finally, the boundary condition on the sphere is satisfied at a set of discrete points, and the force on the sphere is calculated. In this way, the solution procedure explicitly includes the effect of the time-varying geometry on the fall of the sphere.

The force determines the acceleration of the sphere which may be integrated numerically to give the velocity. The procedure should be started with the sphere at some distance from the plane, either at rest or falling with its terminal velocity. The above calculation must be repeated at each time-step to find the subsequent velocity of the sphere.

6.3 ELASTIC RECOIL IN THE NONLINEAR ARREST PROBLEM

Real impact problems are complicated by the elastic deformation of the boundaries which may lead to recoil of the body. Davis, Serayssol & Hinch (1985) discussed the motion of an elastic body in the lubrication limit. Their viscosity dominated analysis predicted damped oscillations in some cases. We can learn a little by incorporating

elasticity into the model of Chapters 4 & 5 where the bottom of the body is represented by a circular disc.

It may be the case that elastic deformations do not significantly alter the geometry of contact; at any rate, we have seen that the parallel wall configuration leads to such great simplifications that it may be enlightening to consider it as a mathematical model, even though it may be an imperfect representation of a real collision. The radial pressure distribution (4.19) is parabolic and this will lead to an indenting of the body and plane near the point of contact. When the pressure peak is very large, a significant proportion of the kinetic energy of the motion may be stored as elastic potential energy, which will be released to give a strong recoil. On the other hand, if the fluid has large inertia, the energy of the flow will be lost with the fluid that escapes from the gap. Thirdly, if there is significant viscosity, the energy will be dissipated during the arrest and any rebound will be muted.

We shall consider an average elastic displacement q(t) defined by $\mathcal{F}_A = -Kq$, K being a constant depending on the elastic properties of the body and wall. Equations (4.21) and (4.22) are replaced by:

$$-Kq = m(h+q)_{tt} + \mathcal{F}_A \tag{6.24}$$

$$\nu F_{zzz} + 2FF_{zz} - F_z^2 - F_{zt} = \frac{4}{\pi\rho a^4}(Kq) \tag{6.25}$$

closure of the system of equations is again provided by the boundary condition

$$\text{on } z = h(t): \qquad h_t = -2F \tag{6.26}$$

Thus q(t) is a third dependent variable and introduces a third equation. Equations (6.24) and (6.25) are formal since κ and q have not been properly defined. However, they constitute an exact description of the mechanical system of figure 5.2. In this idealized system, the mass m is attached to a massless rigid disc via a spring with elastic constant k. The natural length of the spring is L and its extension is q. Only the fluid between the disc and the plane contributes to the hydrodynamic force $\mathcal{F}_H$.

We introduce a new dimensionless parameter $\varkappa$, defined by:

$$\varkappa = \frac{4k}{\pi\rho w_0^2}\left(\frac{h_0}{a}\right)^2 \tag{6.27}$$

Then in dimensionless terms we have:

$$F_{zt} + F_z^2 - 2FF_{zz} - \frac{1}{Re_0}F_{zzz} = -\varkappa q = \beta(h+q)_{tt} + \gamma \tag{6.28}$$

The interactions between the terms of (6.28) are clearer in the inviscid case, $Re_0 \to \infty$, when $F = z\Phi(t)$ and we have a fourth-order system of simple ordinary differential equations.

$$\Phi' = -\varkappa(y-h) - \Phi^2 \tag{6.29}$$

$$h' = -2\Phi h \tag{6.30}$$

$$y' = Y \tag{6.31}$$

$$Y' = \frac{1}{\beta}\left[-\kappa(y-h) - \gamma\right] \tag{6.32}$$

when $t = 0$: $\quad h = 1,\ y = 1,\ Y = -1,\ \Phi = \frac{1}{2}$ (6.33)

In the above, we have substituted $y = h+q$ and $y_t = Y$ to simplify the equations and have assumed that the initial deflection is zero. The three parameters β, γ and κ may take any values. However, we are particularly interested in recoil for which γ has little importance, so it is only necessary to consider the case $\gamma = 0$. This should give a good qualitative indication of the amount of recoil one can expect. The main drawback is, of course, that the deflection and Φ may depend quite strongly on the radial coordinate; for accurate results a one-dimensional model should be used, resulting in partial differential equations for $\Phi(r,t)$, $n(r,t)$ and $y(r,t)$. A further complication is that (4.22) was derived for the body approaching the plane and may not be valid when the direction of motion is reversed, since the external pressure drop Δp of (4.17) may not be negligible in that case.

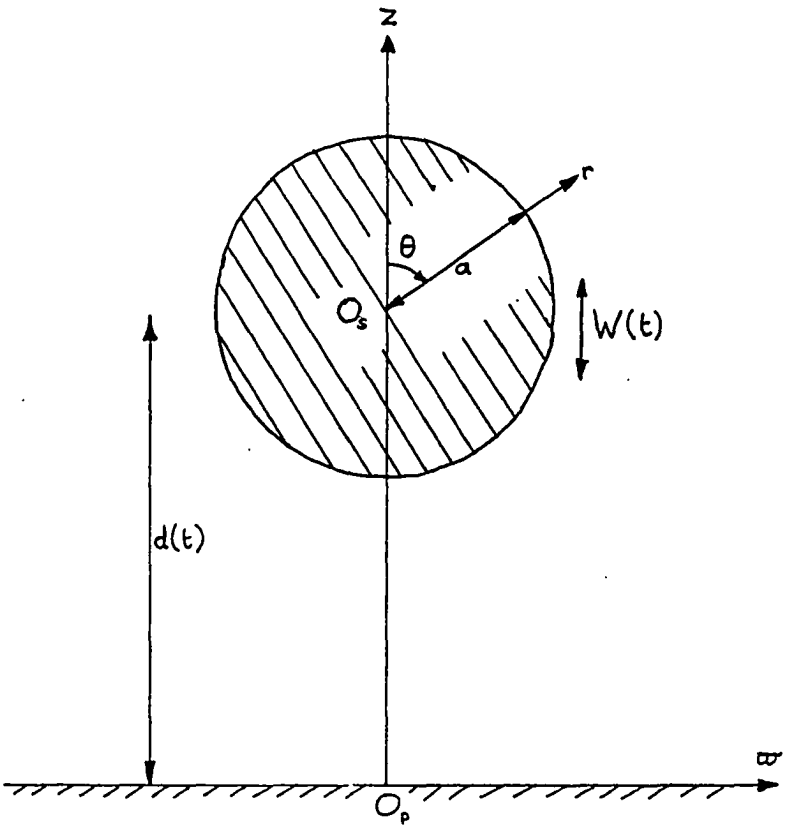

Figure 6.1. The geometry and mixed coordinates for a sphere moving near a plane.

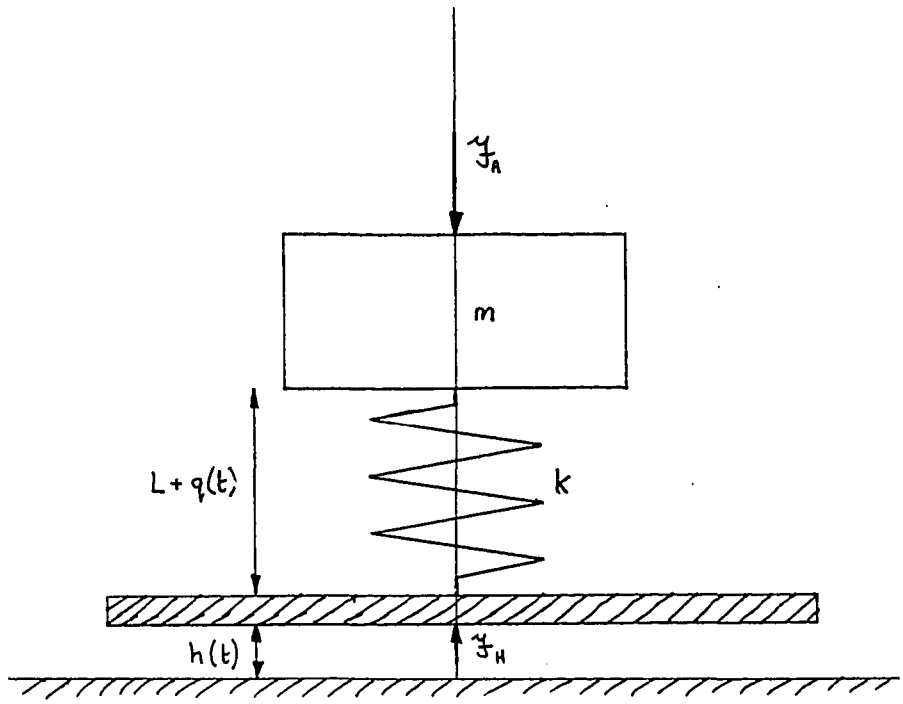

Figure 6.2. The mechanical system represented by equations (6.24) and (6.25).

APPENDIX. CALCULATIONS AND SPECIAL FUNCTIONS

A.1 SPHEROIDAL WAVE FUNCTIONS

To find the force on the oscillating spheroid of Chapter 3, we must invert the pair of matrix equations (3.133) and (3.134). We need to calculate the ratio $DR_{in}^{(3)}(c,ix_0)/R_{in}^{(3)}(c,ix_0)$. Although the differential equations encountered most closely resemble those of Stratton et al (1955), the book by Flammer (1957) is more complete and so his notation will be followed. Abramowitz & Stegun (1965) has been used to cross-check some of the more complicated equations.

The simplest representation of $R_{in}^{(3)}(c,z)$ is given in terms of spherical Hankel functions of the first kind, $h_n^{(1)}(z)$:

$$R_{in}^{(3)}(c,z) = \frac{1}{\sum_{0}^{\infty\prime} d_r^{in}(c)(r+1)(r+2)} \left(\frac{z^2-1}{z^2}\right)^{1/2} \sum_{r=0}^{\infty\prime} i^{r+1-n} d_r^{in}(c)(r+1)(r+2) h_{1+r}^{(1)}(cz) \qquad (A.1)$$

To calculate $DR_{in}^{(3)}(c,z)$ we proceed as follows.

$$D\left(\frac{z^2-1}{z^2}\right)^{1/2} h_{1+r}^{(1)}(cz) = \frac{d}{dz}\left(z-\frac{1}{z}\right) h_{r+1}^{(1)}(cz) \qquad (A.2)$$

$$= \left(1+\frac{1}{z^2}\right) h_{r+1}^{(1)}(cz) + c\left(z-\frac{1}{z}\right) h_{r+1}^{(1)\prime}(cz) \qquad (A.3)$$

Now Abramowitz & Stegun (1965) give the differentiation formula

$$\frac{d}{dz} h_n^{(1)}(z) = h_{n-1}^{(1)}(z) - \frac{n+1}{z} h_n^{(1)}(z) \qquad (A.4)$$

So $$h_{r+1}^{(1)\prime}(cz) = h_r^{(1)}(cz) - \frac{r+2}{cz} h_{r+1}^{(1)}(cz) \quad (A.5)$$

Thus $$D\left(\frac{z^2-1}{z^2}\right)^{\frac{1}{2}} h_{1+r}^{(1)}(cz) = c(z-\tfrac{1}{z}) h_r^{(1)}(cz) + \left[1+\tfrac{1}{z^2}-(r+2)(1-\tfrac{1}{z^2})\right] h_{r+1}^{(1)}(cz) \quad (A.6)$$

$$= \tfrac{1}{z^2}\left\{cz(z^2-1)h_r^{(1)}(cz) + [r+3-(r+1)z^2] h_{r+1}^{(1)}(cz)\right. \quad (A.7)$$

So $$DR_{in}^{(3)}(c,z) = \frac{1}{\sum_0^{n\prime\prime} d_r^{in}(c)(r+1)(r+2)} \tfrac{1}{z^2} \sum_0^{n\prime\prime} i^{r+1-n} d_r^{in}(c)(r+1)(r+2)\left\{cz(z^2-1)h_r^{(1)}(cz)\right. \quad (A.8)$$
$$\left. + [r+3-(r+1)z^2] h_{r+1}^{(1)}(cz)\right\}$$

The Hankel functions are calculated from (Abramowitz & Stegun 1965)

$$h_n^{(1)}(z) = i^{-n-1} z^{-1} e^{iz} \sum_0^{n} \frac{(n+k)!}{k!\,(n-k)!\,(-2iz)^k} \quad (A.9)$$

Although the equations (A.1), (A.8), (A.9) are relatively simple, the sums converge only when $|x_0| > 0.5$. This limits the usefulness of these results to bodies which do not differ greatly from spheres. These results then were used only as a check on other calculations. Good agreement was found with the approximate solution of Section 3.3(c) for a nearly spherical body in the range $0.9 < b/a < 1.1$

A more robust method of calculation is required, and this is found by converting the radial wave function to angular ones via the following definitions.

$$R_{in}^{(3)}(c,z) = R_{in}^{(1)}(c,z) + i R_{in}^{(2)}(c,z) \quad (A.10)$$

$$S_{in}(c,z) = \mathcal{K}_{in}^{(1)}(c) R_{in}^{(1)}(c,z) \quad (A.11)$$

$$S_{in}^{(2)}(c,z) = \mathcal{K}_{in}^{(2)}(c) R_{in}^{(2)}(c,z) \quad (A.12)$$

Thus we have

$$R_{in}^{(3)}(c,z) = \frac{1}{\mathcal{N}_{in}^{(1)}} S_{in}(c,z) + \frac{i}{\mathcal{N}_{in}^{(2)}} S_{in}^{(2)}(c,z) \qquad (A.13)$$

The joining factors $\mathcal{N}_{in}^{(i)}(c)$ are given (for n odd) by:

$$\mathcal{N}_{in}^{(1)}(c) \frac{3(n+1)! \sum_0^{\infty\prime} d_r^{in}(c)(r+1)(r+2) \frac{(r+1)!}{(\frac{r+1}{2})!}}{2^{n+1} d_0^{in}(c)\, c\, (\frac{n-1}{2})!\,(\frac{n+1}{2})!} \qquad (A.14)$$

$$\mathcal{N}_{in}^{(1)}(c) = \frac{2^n}{(n+1)!} (\tfrac{n-1}{2})!\,(\tfrac{n+1}{2})!\, d_{-2}^{in}(c) \sum_0^{\infty\prime} d_r^{in}(c)(r+1)(r+2) \qquad (A.15)$$

As in Chapter 3, the angle wave function of the first kind is given in terms of Legendre polynomials,

$$S_{in}(c,z) = \sum_0^{\infty\prime} d_r^{in}(c) P_{r+1}^1(z) \qquad (A.16)$$

The angle wave function of the second kind is given as a doubly infinite sum of Legendre functions,

$$S_{in}^{(2)}(c,z) = \sum_{r=-2}^{\infty\prime} d_r^{in}(c) Q_{r+1}^1(z) + \sum_{r=4}^{\infty\prime} d_{p|r}^{in} P_{r-2}^1(z) \qquad (A.17)$$

Note that in (3.126), (3.127), etc. a special definition of $P_n^1(y)$ is used for real argument in the range $-1 < y < 1$. Now, the argument may take any complex value, so a more general definition will be used for calculating the Legendre functions in section A.3 below. The coefficients d_{-2}^{in}, $d_{p|r}^{in}$ are simply related to the d_r^{in} and will be discussed in the next section (section A.2). The derivative $DR_{in}^{(3)}$ is also needed; it is given by:

$$DR_{in}^{(3)} = \frac{1}{\mathcal{N}_{in}^{(1)}} DS_{in}(c,z) + \frac{i}{\mathcal{N}_{in}^{(2)}} DS_{in}^{(2)}(c,z) \qquad (A.18)$$

with
$$DS_{in}(c,z) = \sum_{r=0}^{\infty\prime} d_r^{in}(c) DP_{r+1}^1(z) \qquad (A.19)$$

and
$$DS_{in}^{(2)}(c,z) = \sum_{r=-2}^{\infty\prime} d_r^{in}(c) DQ_{r+1}^1(z) + \sum_{r=4}^{\infty\prime} d_{p|r}^{in} DP_{r-2}^1(z) \qquad (A.20)$$

It is worthy of note that (A.17) is derived from

$$S_{1n}^{(1)} = \sum_{r=-\infty}^{\infty}{}' d_r^{1n}(c) Q_{r+1}^1(z) \qquad (A.21)$$

in which for $r = -4, -6, \ldots$, $d_r^{1n}(c)$ is zero and $Q_{r+1}^1(z)$ is infinite. A limiting process is used to derive (A.17), and $d_{p|r}^{1n}$ is defined by:

$$d_{p|r}^{1n} = \lim_{\rho \to 0} \left(\frac{1}{\rho} d_{-r+p}^{1n} \right) \qquad (A.22)$$

A.2 THE COEFFICIENTS $d_r^{1n}(c)$

The coefficients needed are $d_r^{1n}(c)$, $r = -2, 0, 2, 4, \ldots$ and $d_{p|r}^{1n}(c)$, $r = 4, 6, 8, \ldots$ for odd values of n only. When c is zero, d_{n-1}^{1n} is unity and all the other coefficients are zero, since the spheroidal wave functions reduce to Legendre functions. For non-zero c, we expect d_{n-1}^{1n} to be the largest, with adjacent coefficients becoming non-zero.

The first step in the procedure is to find the eigenvalue $\lambda_{1n}(c)$. We start with a power series approximation valid for small c and then make iterative improvements. The power series is

$$\lambda_{1n}^{(1)}(c) = \sum_{k=0}^{3} l_{2k}^{1n} c^{2k} \qquad (A.23)$$

with coefficients

$$l_0^{1n} = n(n+1) \qquad (A.24)$$

$$l_2^{in} = \tfrac{1}{2}\left[1 - \frac{3}{(2n-1)(2n+3)}\right] \tag{A.25}$$

$$l_4^{in} = \tfrac{1}{2}\left[\frac{(n-2)(n-1)n(n+1)}{(2n-3)(2n-1)^3(2n+1)} - \frac{n(n+1)(n+2)(n+3)}{(2n+1)(2n+3)^3(2n+5)}\right] \tag{A.26}$$

$$l_6^{in} = 3\left[\frac{n(n+1)(n+2)(n+3)}{(2n-1)(2n+1)(2n+3)^5(2n+5)(2n+7)} - \frac{(n-2)(n-1)n(n+1)}{(2n-5)(2n-3)(2n-1)^5(2n+1)(2n+3)}\right] \tag{A.27}$$

The estimate is improved using the following scheme.

$$\lambda_{in}^{(j+1)} = \lambda_{in}^{(j)} + \delta\lambda_{in}^{(j)} \tag{A.28}$$

$$\delta\lambda_{in}^{(j)} = \frac{\left[U_1(\lambda_{in}^{(j)}) + U_2(\lambda_{in}^{(j)})\right] \Big/ \left[\frac{(\bar{N}'_{n+1})^2}{\beta'_{n+1}} + \frac{(\bar{N}'_{n+1})^2(\bar{N}'_{n+3})^2}{\beta'_{n+1}\beta'_{n+3}} + \cdots\right]}{\left[1 + \beta'_{n-1}/(N'_{n-1})^2 + \beta'_{n-1}\beta'_{n-3}/(N'_{n-1})^2(N'_{n-3})^2 + \cdots\right]} \tag{A.29}$$

with $$U_2(\lambda_{in}) = -\bar{N}'_{n+1} = \frac{-\beta'_{n+1}}{\gamma'_{n+1} - \lambda_{in} - \beta'_{n+3}/(\gamma'_{n+3} - \lambda_{in} - \cdots)} \tag{A.30}$$

$$U_1(\lambda_{in}) = N'_{n+1} = \gamma'_{n-1} - \lambda_{in} - \frac{\beta'_{n-1}}{\gamma'_{n-2} - \lambda_{in} - \beta'_{n-3}/(\gamma'_{n-3} - \lambda_{in} - \cdots)} \tag{A.31}$$

In (A.29) the first sum is finite, the second is infinite. The continued fraction (A.30) is infinite, while (A.31) terminates. The numerical coefficients are defined by:

$$N'_{r+2} = \gamma'_r - \lambda_{in} - \frac{\beta'_r}{N'_r}, \quad r \geq 2 \tag{A.32a}$$

$$N'_2 = \gamma'_0 - \lambda_{in} \tag{A.32b}$$

$$\bar{N}'_r = \beta'_r / (\gamma'_r - \lambda_{in} - \bar{N}'_{r+2}), r \geq 2 \tag{A.33}$$

$$\gamma'_r = (1+r)(2+r) + \tfrac{1}{2}c^2\left[1 - \frac{3}{(2r+1)(2r+5)}\right], \quad r \geq 0 \tag{A.34}$$

$$\beta'_r = (r-1)r(r+1)(r+2)c^4/(2r-1)(2r+1)^2(2r+3), \quad r \geq 2 \tag{A.35}$$

The N'_r and $\bar{N}'_r$ are ostensibly the same series, but $\bar{N}'_r$ diverges downwards, starting at an assumed value for a large $r = R$, $\bar{N}'_R = c^4/16R^2$, and N'_r diverges upwards starting from N'_2. Since the largest value is $N'_{n+1} = \bar{N}'_{n+1}$, the series N'_r is good for $r = 2, 4, \ldots, n+1$ and the series $\bar{N}'_r$ is good for

$r = n+1, n+3, \ldots, R$. For all the following calculations, $R = 100$ was used.

The iteration for λ_{1n} converges very rapidly to the correct value provided that $c < 10$. For larger values of c, asymptotic expansions are available for λ_{1n}, but the series (A.16), (A.17) for the wave functions become cumbersome since many of the $d_r^{1n}(c)$ become important. The very nature of the functions is different for large values of c, as discussed by Flammer, and it is more sensible to use a different approach such as that of section 3.3(b).

Once the eigenvalues and N-coeffients are known, it is possible to calculate the $d_r^{1n}(c)$. Since d_{n-1}^{1n} is the largest, we set it equal to unity for the time being. Then the other values are calculated as follows.

For $r = 2, 4, \ldots, (n-1)$, we have:

$$d_{r-2}^{1n} = \frac{-d_r^{1n}(r+2)(r+1)c^2}{N_r^1(2r+1)(2r+3)} \qquad (A.36)$$

For $r = (n+1), (n+3), \ldots, R$ we have:

$$d_r^{1n} = -\overline{N}_r^1 d_{r-2}^{1n} \frac{(2r+1)(2r+3)}{(r+2)(r+1)c^2} \qquad (A.37)$$

The d_r^{1n} are normalized so that

$$S_{1n}(c,0) = P_n^1(0) = \frac{(-1)^{\frac{n-1}{2}}(n+1)!}{2^n\left(\frac{n-1}{2}\right)!\left(\frac{n+1}{2}\right)!} \qquad (A.38)$$

We put $(d_r^{1n})^* = \eta\, d_r^{1n}$, then

$$\eta = \frac{(-1)^{\frac{n-1}{2}}(n+1)!}{2^{n-1}\left(\frac{n-1}{2}\right)!\left(\frac{n+1}{2}\right)!} \Bigg/ \sum_{r=0}^{\infty\,\prime} \frac{(-1)^{r/2}(r+2)!}{2^r\left(\frac{r}{2}\right)!\left(\frac{r+2}{2}\right)!} d_r^{1n} \qquad (A.39)$$

Next we calculate d^{in}_{-2} and $d^{in}_{\rho lr}$ which essentially continue the series of values to negative r. The recurrence relation is the same as before, but Flammer (1957) uses different notation and so shall we. Introduce

$$A^1_r(c) = \frac{(2+r)(1+r)c^2}{(2r+1)(2r+3)} \qquad (A.40)$$

$$B^1_r(c) = \gamma^1_r - \lambda_{1n}(c) \qquad (A.41)$$

$$C^1_r(c) = \beta^1_{r+2}/A^1_{r+2} = \frac{(r+1)(r+2)c^2}{(2r+3)(2r+5)} \qquad (A.42)$$

in which r may take negative values. (Note that $A^1_{-2} = C^1_{-2} = 0$). We define

$$M^{in}_r = d^{in}_{\rho lr} / d^{in}_{\rho lr-2}, \quad r = 6, 8, \ldots, R \qquad (A.43)$$

then $$M^{in}_r = \frac{-A^1_{-r+2}}{B^{in}_{-r} + C^1_{-r-2} M^{in}_{r+2}} \qquad (A.44)$$

and $$\frac{d^{in}_{-2}}{d^{in}_0} = -\frac{A^1_0}{B^{in}_{-2}} \qquad (A.45)$$

and $$\frac{d^{in}_{\rho l4}}{d^{in}_{-2}} = \frac{-\lim_{\rho\to 0}\left(\frac{1}{\rho}A^1_{-2+\rho}\right)}{B^{in}_{-4} + C^1_{-6} M^{in}_6} = \frac{\frac{1}{3}c^2}{B^{in}_{-4} + C^1_{-6} M^{in}_6} \qquad (A.46)$$

We start with $M^{in}_R = -c^2/4R^2$ and work back to M^{in}_6 using (A.44). Then we use (A.45) to get d^{in}_{-2} from d^{in}_0, then (A.46) to get $d^{in}_{\rho l4}$ and (A.43) to find the other $d^{in}_{\rho lr}$.

A.3 LEGENDRE FUNCTIONS

We need to calculate the functions $P^1_n(z)$, $Q^1_n(z)$, $DP^1_n(z)$ and $DQ^1_n(z)$ for n = 1, 2, 3, ... as well as $Q^1_{-1}(z)$ and $DQ^1_{-1}(z)$. First we consider $DP^1_n(z)$.

$$DP_n^1(z) = \frac{d}{dz}(z^2-1)^{\frac{1}{2}} P_n^1(z) = (z^2-1)^{\frac{1}{2}} P_n^{1\prime}(z) + \frac{z}{(z^2-1)^{1/2}} P_n^1(z) \qquad (A.47)$$

Abramowitz & Stegun (1965) give the formula

$$(z^2-1)\frac{d}{dz} P_n^1(z) = n(n+1)(z^2-1)^{\frac{1}{2}} P_n(z) - z P_n^1(z) \qquad (A.48)$$

So we have $$D P_n^1(z) = n(n+1)P_n(z) \qquad (A.49)$$

Similarly,

$$D Q_n^1(z) = n(n+1)Q_n(z) \qquad (A.50)$$

The P_n are the easiest to calculate so we begin with them. They obey the recurrence relation

$$(n+1)P_{n+1}(z) = (2n+1)z P_n(z) - n P_{n-1}(z) \qquad (A.51)$$

We begin with

$$P_0(z)=1, \quad P_1(z)=z, \quad P_2(z)=\tfrac{1}{2}(3z^2-1), \text{ etc.} \qquad (A.52)$$

and then use (A.51) to calculate the $P_n(z)$ as far as they are needed. The recurrence relation gives good results for all n and z. Next the $P_n^1(z)$ are found from the relation

$$P_n^1(z) = n(z^2-1)^{-1/2}\left[z P_n(z) - P_{n-1}(z)\right] \qquad (A.53)$$

The Q_n may be calculated in exactly the same way as the P_n if $|z| < 1$, starting with

$$Q_0(z)=\tfrac{1}{2}\log\left(\tfrac{z+1}{z-1}\right), \quad Q_1(z)=\tfrac{z}{2}\log\left(\tfrac{z+1}{z-1}\right)-1, \quad Q_2(z)=\tfrac{1}{4}(3z^2-1)\log\left(\tfrac{z+1}{z-1}\right)-\tfrac{3z}{2} \qquad (A.54)$$

and using the recurrence relation (A.51). However, the results are not good if $|z| > 1$, since then Q_n decreases as n increases, whereas (A.51) yields a diverging sequence. The simple solution is to use (A.51) backwards. We follow Herndon (1961) and define $R_{n-1} = Q_{n-1}/Q_{n-2}$.

Then $$R_{n-1} = \frac{n-1}{(2n-1)z - nR_n} \qquad (A.55)$$

The limiting value for large n is

$$R_n \longrightarrow z - \sqrt{z^2-1} \qquad (A.56)$$

We choose a large value of n, e.g. 100, and work back to R_1. Then we begin with Q_0 and multiply up to get Q_n. As above, the Q_n' are found from the Q_n using recurrence relation (A.53).

The evaluation of Q_{-1}' and DQ_{-1}' requires special care since (A.51) cannot be used to find $Q_{-1}(z)$. We use the recurrence relation for the $Q_n'(z)$:

$$n\,Q_{n-2}' = (2n-1)z\,Q_{n-1}' - (n-1)Q_n' \qquad (A.57)$$

Then (A.57) gives

$$Q_{-1}'(z) = z\,Q_0'(z) \qquad (A.58)$$

Now $Q_0'(z)$ is found from Rodriguez' formula,

$$Q_0'(z) = (z^2-1)^{1/2}\frac{d}{dz}Q_0(z) = -(z^2-1)^{-1/2} \qquad (A.59)$$

So $$Q_{-1}'(z) = -z(z^2-1)^{-1/2} \qquad (A.60)$$

And finally,

$$DQ^1_{-1}(z) = \frac{d}{dz}(z^2-1)^{1/2} Q^1_{-1}(z) = -1 \qquad \text{(A.61)}$$

A.4 MATRIX TRUNCATION AND INVERSION

The matrix coefficients in equations (3.13), (3.13) are non-zero only for odd values of n and m. Thus we can pack the matrix by introducing

$$a_m = \begin{cases} A_{2m-1}\,; & m = 1,2,\ldots,M \\ B_{2(m-M)-1} & m = M+1,\ldots,2M \end{cases} \qquad \text{(A.62)}$$

where M is the order of truncation. We define

$$\mathcal{D}_m = \begin{cases} \frac{1}{2}(1+x_0^2)^{1/2} / Q^1_1(ix_0) \\ x_0 / DQ^1_1(ix_0) \\ 0 \end{cases} \qquad \text{(A.63)}$$

$$\mathcal{C}_{mn} = \begin{cases} \delta_{mn}\,, & 1 \le m,n \le M \\ d^{1,2(n-M)-1}_{2m-2}(c) / Q^1_{2m-1}(ix_0), & 1 \le m \le M,\ M+1 \le n \le 2M \\ \delta_{m-M,n}\,, & M+1 \le m \le 2M,\ 1 \le n \le 2M \\ \left[d^{1,2(n-M)-1}_{2(m-M)-2}(c) / DQ^1_{2(m-M)-1}(ix_0) \right] \dfrac{DR_{1,2(n-M)-1}(c,ix_0)}{R_{1,2(n-M)-1}(c,ix_0)}\,, & M+1 \le m,n \le 2M \end{cases} \qquad \text{(A.64)}$$

Then we have the simple matrix equation,

$$\mathcal{C}_{mn}\, a_n = \mathcal{D}_m \qquad \text{(A.65)}$$

We are interested only in $A_1 = a_1$ which contributes to the force. The correct order of truncation is found by iteration beginning with M = 2. At each step, the force calculated with truncation M is compared with that found at truncation M-1, until the desired degree of accuracy is obtained. For small values of c and nearly spherical bodies, M = 3 is adequate, whilst for long bodies and large values of c, values of M up to 15 are required. The matrix inversion was performed using a high accuracy iterative routine for complex linear algebraic equations.

BIBLIOGRAPHY

ABRAMOWITZ, M. & STEGUN, I.A. 1965 Handbook of Mathematical Functions, Dover, New York.

ADAMCZYK, Z. ADAMCZYK, M. & VAN DE VEN, T.G.M. 1983 Resistance coefficient of a solid sphere approaching plane and curved boundaries. J. Coll. Interface. Sci. 96, 204.

ALDER, B.J. & WAINWRIGHT, T.E. 1967 Velocity autocorrelations for hard spheres. Phys. Rev. Lett. 18, 988.

ALDER, B.J. & WAINWRIGHT, T.E. 1970 Decay of velocity autocorrelation. Phys. Rev. A 1, 18.

AOI, T. 1955a The steady flow of viscous fluid past a fixed spheroidal obstacle at small Reynolds numbers. J. Phys. Soc. Jap. 10, 119.

AOI, T. 1955b On spheroidal functions. J. Phys. Soc. Jap. 10, 130.

ARMINSKI, L. & WEINBAUM, S. 1979 Effect of waveform and duration of impulse on the solution to the Basset-Langevin equation. Phys. Fluids 22, 404.

BASSET A.B. 1888 A Treatise on Hydrodynamics, Volume II Deighton, Bell & Co., Cambridge.

BATCHELOR, G.K. 1951 Note on a class of solutions of the Navier-Stokes equations representing steady rotationally symmetric flow. Quart. J. Mech. Appl. Math. 4, 29.

BATCHELOR, G.K. 1954 The skin friction on infinite cylinders moving parallel to their length. Quart. J. Mech. Appl. Math. 7, 179.

BATCHELOR, G.K. 1967 An Introduction to Fluid Dynamics, Camb. Univ. Press, Cambridge.

BEDEAUX, D. & MAZUR, P. 1974 Brownian motion and fluctuating hydrodynamics. Physica 76, 247.

BRENNER, H. 1961 The slow motion of a sphere through a viscous fluid towards a plane surface. Chem. Eng. Sci. 16, 242.

CHEN, S.S., WAMBSGANSS, M.W., & JENDRZEJCZYK, J.A. 1976 Added mass and damping of a vibrating rod in confined viscous fluids. J. Appl. Mech. 43, 325.

CHRISTENSEN, H. 1962 The oil film in a closing gap. Proc. Roy. Soc. Lond. A 265, 312.

COX, R.G. & BRENNER, H. 1967 The slow motion of a sphere through a viscous fluid towards a plane surface - II Small gap widths including inertial effects. Chem. Eng. Sci. 22, 1753.

DAGAN, Z., WEINBAUM, S. & PFEFFER, R. 1982 An infinite-series solution for the creeping motion through an orifice of finite length. J. Fluid Mech. 115, 505

DAVIS, R.H. SERAYSSOL, J.-M. & HINCH, E.J. 1986 The elastohydrodynamic collision of two spheres. J. Fluid Mech. to appear.

FELDERHOF, B.U. 1976a Force density induced on a sphere in linear hydrodynamics. I. Fixed sphere, stick boundary conditions. Physica 84A, 557.

FELDERHOF, B.U. 1976b Force density induced on a sphere in linear hydrodynamics. II. Moving sphere, mixed boundary conditions. Physica 84A, 569.

FLAMMER, C. 1957 Spheroidal Wave Functions, Stamford Univ. Press, California.

FRÖSSLING, N. 1940 Verdunstung, Warmeübertragung und Geschwindigkeitsverteilung bei zweidimensionaler und rotationssymmetrischer laminarer Grentschichströmung. Lunds. Univ. Arsskr. N.F. Avd. 2, 35 No. 4.

GANATOS, P., WEINBAUM, S. & PFEFFER, R. 1980 A strong interaction theory for the creeping motion of a sphere between plane parallel boundaries. Part 1. Perpendicular motion. J. Fluid Mech. 99, 739.

GLUCKMAN, M.J., PFEFFER, R. & WEINBAUM, S. 1971 A new technique for treating multiparticle slow viscous flow: axisymmetric flow past spheres and spheroids. J. Fluid Mech. 50, 705.

GRADSHTEYN, I.S. & RYZHIK, I.M. (1980) Table of Integrals, Series and Products, 4th Edition Translated from the Russian by Scripta Technica Inc., New York.

GREEN, G. 1833 Researches on the vibration of pendulums in fluid media. Trans. Roy. Soc. Edin. reprinted 1970 in Mathematical Papers, Chelsea Publishing Co., New York.

HAPPEL, J. & BRENNER, H. 1965 Low Reynolds number hydrodynamics Prentice-Hall Inc. New Jersey.

HERNDON, J.R. 1961 A set of associate Legendre polynomials of the second kind. Comm. A.C.M. 4, Alg. 62.

HOCQUART, R. 1976 Régime instanté d'un liquide dans lequel un ellipsoïde de révolution tourne autour de son axe. C. R. Acad. Sci. Paris, Sér. A 283, 1119.

HOCQUART, R. 1977a Régime instanté d'un liquide dans lequel un ellipsoïde de révolution tourne autour d'un axe équatorial. C. R. Acad. Sci. Paris, Sér. A 284, 913.

HOCQUART, R. 1977b Mouvement brownien de rotation d'un ellipsoïde de révolution. Rotation autour de l'axe. C. R. Acad. Sci. Paris, Sér. A 284, 1421.

HOCQUART, R. & HINCH, E.J. 1983 The long-time tail of the angular velocity autocorrelation function for a rigid Brownian particle of arbitrary centrally symmetric shape. J. Fluid Mech. 137, 217.

HOMANN, F. 1936 Der Einfluss grosser zähigkeit bei der Strömung um den Zylinder und um die Kugel. Z. angew. Math. Mech. 16, 153

HSU, R. & GANATOS, P. 1986 The motion of a body of revolution near a plane wall at low Reynolds numbers. J. Fluid Mech. submitted.

JEFFREY, D.J. & CHEN, H.-S. 1977 The virtual mass of a sphere moving toward a plane wall. J. Appl. Mech. 44, 166

VON KARMAN, Th. 1921 Über laminare und turbulente Reibung. Z. angew. Math. Mech. 1, 233.

KIM, S. 1985 Sedimentation of two arbitrarily oriented spheroids in a viscous fluid. Int. J. Multiphase Flow 11, 699.

KUANG, Y. 1984 The inertial draining of a thin fluid layer between parallel plates with a constant normal force. M.E. THESIS, CITY COLLEGE OF C.U.N.Y.

LANDAU, L.D. & LIFSCHITZ, E.M. 1959 Fluid Mechanics, Pergamon Press, Addison Wesley.

LAWRENCE, C.J., KUANG, Y., & WEINBAUM, S. 1985 The inertial draining of a thin fluid layer between parallel plates with a constant normal force. Part 2. Boundary layer and exact numerical solutions. J. Fluid Mech. 156 , 479

LAWRENCE, C.J. & WEINBAUM, S. 1986a Hydrodynamic arrest of a flat body moving towards a parallel surface at arbitrary Reynolds number. J. Fluid Mech. under revision.

LAWRENCE, C.J. & WEINBAUM, S. 1986b The force on an axisymmetric body in linearized, time-dependent motion. J. Fluid Mech. under revision.

LEICHTBERG, S., WEINBAUM, S., PFEFFER, R. & GLUCKMAN, M.J. 1976 A study of unsteady forces at low Reynolds number: a strong interaction theory for coaxial settling of three or more spheres. Phil. Trans. Roy. Soc. Lond. A 282, 585

LIN, W.H. 1986 Hydrodynamic forces on multiple circular cylinders oscillating in a viscous incompressible fluid. J. Fluid Mech. submitted.

MAGNUS, W., OBERHETTINGER, F. & SONI, R.P. 1966 Formulas and Theorems for the Special Functions of Mathematical Physics, vol. 52, Springer-Verlag Inc., New York.

MAZUR, P. & BEDEAUX, D. 1974 A generalization of Faxén's Theorem to nonsteady motion of a sphere through an incompressible fluid in arbitrary flow. Physica 76, 235

MILOH, T. 1979 The virtual mass of a closed torus in axisymmetric motion. J. Eng. Math. 13, 1

MILOH, T., WAISMAN, G. & WEIHS, D. 1978 The added-mass coefficients of a torus. J. Eng. Math. 12, 1

OBERHETTINGER, F. & BADII, L. 1973 Tables of Laplace Transforms Springer-Verlag, Berlin.

PAYNE, L.E. & PELL, W.H. 1960 The Stokes flow problem for a class of axially symmetric bodies. J. Fluid Mech. 7, 529

PELL, W.H. & PAYNE, L.E. 1960 On Stokes flow about a torus. Mathematika 7, 78

SAMPSON, R.A. 1891 On Stokes's current function. Phil. Trans. Roy. Soc. Lond. A 182, 449.

SCHLICHTING, H. 1979 Boundary-Layer Theory, 7th Edition McGraw-Hill Book Company Inc., New York.

SECOMB. T.W. 1978 Flow in a channel with pulsating walls. J. Fluid Mech. 88, 273.

SMALL, R.D. & WEIHS, D. 1975 Axisymmetric potential flow over two spheres in contact. J. Appl. Mech. 42, 763.

STIMSON, M. & JEFFREY, G.B. 1926 The motion of two spheres in a viscous fluid. Proc. Roy. Soc. Lond. A 111, 110

STOKES, G.G. 1851 On the effect of the internal friction of fluids on the motion of pendulums. Trans. Camb. Phil. Soc. 9, 8.

STRATTON, J.A., MORSE, P.M., CHU, L.J. & HUTNER, R.A. 1941 Elliptic Cylinder and Spheroidal Wave Functions, John Wiley & Sons, Inc., New York. (also CHU, L.J. & STRATTON, J.A. 1941 Elliptic and spheroidal wave functions. J. Math. & Phys. 20, 259.)

TAYLOR, G.I. 1928 The energy of a body moving in an infinite fluid with an application to airships. Proc. Roy. Soc. Lond. A 120, 13.

TCHEN, C.M. 1947 Mean value and correlation problems connected with the motion of small particles suspended in a turbulent fluid. Ph.D. Thesis, Delft.

UCHIDA, S. & AOKI, H. 1977 Unsteady flows in a semi-infinite contracting or expanding pipe. J. Fluid Mech. 82, 371.

WAKIYA, S.J. 1961 Title unknown. Res. Rep. Fac. Eng. Niigata Univ. (Japan) 10, 15.

WEIHS, D. & SMALL, R.D. 1975 An exact solution of the motion of two adjacent spheres in axisymmetric potential flow. Israel J. Techn. 13, 1.

WEINBAUM, S. 1981 Strong interaction theory for particle motion through pores and near boundaries in biological flows at low Reynolds number. In: Some Mathematical Questions in Biology, ed. S. Childress, Amer. Math. Soc., Providence, Lectures on Mathematics in the Life Sciences 14, 119

WEINBAUM, S. LAWRENCE, C.J. & KUANG, Y. 1985 The inertial draining of a thin fluid layer between parallel plates with a constant normal force. Part 1. Analytic solutions; inviscid and small but finite Reynolds number limits. J. Fluid Mech. 156, 463.

YANG, K.-T. 1958 Unsteady laminar boundary layers in an incompressible stagnation flow. J. Appl. Mech. 25, 421 (A.S.M.E. Trans. 80).